Reconstruction of past variation in lake water balance at upstream Smoky and Wabasca watersheds to improve understanding of causes of lake drying in the Peace-Athabasca Delta

by

Hannah Thibault

A thesis

presented to the University of Waterloo

in fulfillment of the

thesis requirement for the degree of

Master of Science

in

Biology

Waterloo, Ontario, Canada, 2023

AUTHOR'S DECLARATION

I hereby declare that I am the sole author of this thesis. This is a true copy of the thesis, including any required final revisions, as accepted by my examiners.

I understand that my thesis may be made electronically available to the public.

ABSTRACT

Controversy persists regarding causes of recent lake-level drawdown within the internationally recognized Peace-Athabasca Delta (PAD), northern Alberta. Central to this debate are conflicting interpretations of causes of decline in Lower Peace River ice-jam flood frequency that has led to reduced flooding of lakes and water-level drawdown across the delta. On one hand, studies analyzing Peace River hydrometric data and Traditional Knowledge and historical records of ice-jam flood frequency have attributed lake drying to decreased ice-jam flood frequency caused by the W.A.C. Bennett Dam, which has regulated Peace River flow since 1968. Statistical analysis of these records has also been used to establish a hypothesis that ice-jam flood frequency was accelerating prior to construction of the dam and declined thereafter. In contrast, paleolimnological analyses of sediment cores from oxbow and perched lakes in the Peace sector of the PAD identified declining ice-jam flood frequency and lake drying since the late 1800s and attributed this to a shifting climate following the Little Ice Age. Further investigation is needed to delineate influences of climate versus Peace River flow regulation and reconcile contrasting interpretations of the timing and causes of declining ice-jam flood occurrence along the Lower Peace River and lake drying at the PAD. Reconstructing climate-driven hydrological change at the upstream unregulated Smoky and Wabasca watersheds, which provide substantial discharge to the Peace River when ice-jam floods occur at the PAD, may add critical insight into causes of hydrological change at the PAD. Recent analyses of sediment cores from oxbow lakes within the watersheds of these 'trigger tributaries' have revealed that flood influence began to decline decades before operation of the W.A.C. Bennett Dam, coincident with decline of ice-jam flood occurrence at the Lower Peace River and lake drying in the PAD (Girard, 2022; Stratton, 2022). Here, paleolimnological analyses of sediment cores from remote, upland lakes in the Smoky and Wabasca watersheds, whose water balance are controlled by climatic variations, are used to build on this newly generated paleohydrological knowledge and reconstruct variation in hydrological conditions from 1880 to 2019.

Sediment cores from two upland lakes within each of the Smoky and Wabasca watersheds were used to reconstruct temporal variation in water balance based on evaporation-to-inflow (E/I) ratios computed from cellulose-inferred lake water oxygen isotope records. Relative to

the pre-regulation averages (1880–1967), E/I ratios began to rise between ~1910 and 1940 at upland lakes in the Smoky River watershed and ~1960–1970 at upland lakes in the Wabasca River watershed. Use of linear regression for the pre-regulation (1880–1967) and post-regulation (1972–2019) intervals identified statistically significant rises in E/I ratios during the pre-regulation interval at both upland lakes in the Smoky watershed and at one upland lake in the Wabasca watershed, as well as at both upland lakes in the Wabasca watershed during the post-regulation interval. These results reveal that increasing importance of evaporation on water balance, associated with declining snowmelt runoff input, at upland lakes in the unregulated Smoky and Wabasca watersheds began before onset of Peace River flow regulation, and it intensified during the post-regulation interval. Periods of climate-driven increase in importance of evaporation on water balance of the upland lakes coincided with previously obtained paleolimnological evidence of decreasing flood occurrence at floodplain lakes in the Smoky and Wabasca river watersheds, and decreasing flood occurrence at an oxbow lake and increasing evaporation at a perched basin in the Peace sector of the PAD. Correspondence of hydrological change since the 1880s at upland and floodplain lakes located within unregulated and regulated portions of the Peace River watershed identifies a strong role of climate, not regulation of Peace River flow, on the flood regime and lake water balance at the PAD. This knowledge is critical for informing decisions regarding adaptive and mitigative conservation measures at the PAD, including those being contemplated by the federal Wood Buffalo National Park Action Plan.

ACKNOWLEDGEMENTS

DEDICATION

For Wallace, the light of my life, who has helped me more than he could ever know.

TABLE OF CONTENTS

LIST OF FIGURES

CHAPTER 1: INTRODUCTION

Understanding long-term natural variation in the conditions of aquatic ecosystems prior to anthropogenic disturbance is critical for detecting ecosystem changes and identifying their causes (Lindenmayer & Likens, 2010; Blais et al., 2015; Arciszewski et al., 2017). Without sufficient knowledge of an ecosystem's range of natural variation before onset of a potential disturbance, it is challenging to detect if a change has occurred (Smol, 2008; Roach & Walker, 2017). Inability to detect changes, and their cause(s), can stimulate conflict among stakeholders and reduce effectiveness of conservation measures. To improve ability to detect changes in aquatic ecosystems and their causes, monitoring programs are becoming more widely implemented. Monitoring records, however, are often too short or too sparse to adequately define the range of natural variation that existed prior to the human activity or are initiated only after an anthropogenic disturbance has occurred, which impedes an ability to determine if, when and why a change has occurred (Munkittrick et al., 2002; Kilgour et al., 2007; Blais et al., 2015). In these situations, paleolimnological analyses of lake sediment cores can be used to generate longer temporal data to define the range of natural variation in aquatic environments and identify when a change began and potential causes (Smol, 2010).

The Peace-Athabasca Delta (PAD) is a water-rich landscape in northern Alberta where concerns persist about degradation of aquatic ecosystems by multiple anthropogenic stressors, and where insufficient long-term monitoring has critically limited understanding of pre-disturbance baseline conditions necessary to attribute recent changes in the ice-jam flood regime and perched lake drawdown to regulation of Peace River flow by hydroelectric dams and shifts in climate (Timoney, 2002; MCFN, 2014; WBNP, 2019; ACFN, 2021). The PAD plays a prominent role in contributing to the UNESCO World Heritage status of Wood Buffalo National Park (WBNP), provides productive habitat for threatened wildlife (WBNP, 2019), and holds significance for local Indigenous communities (MCFN, 2014; ACFN, 2021). Reduced frequency of ice-jam floods along the Lower Peace River and drying of perched lakes in the PAD remains a primary concern and has been expressed in a petition by the Mikisew Cree First Nation (MCFN, 2014) to downgrade the status of WBNP to 'World Heritage in Danger'. Despite growing recognition of the influence of climate, the subsequent WBNP

Action Plan (WBNP, 2019) has proposed the installation of water control structures to mitigate effects of the W.A.C. Bennett Dam, which has regulated Peace River flow since 1968 and has been associated with drying at the PAD ever since (PADPG, 1973; Prowse & Lalonde, 1996; Prowse & Conly, 1998; Peters & Prowse, 2001; MCFN, 2014; Beltaos, 2014, 2018; Vannini & Vannini, 2019). Improved knowledge of the range of variation in hydrological conditions at the PAD before onset of potential stressors and the period thereafter is required to delineate relative influences of climate versus Peace River flow regulation. Such information is urgently needed to inform decisions on WBNP's UNESCO World Heritage status and conservation measures at the PAD.

Reconstructing Peace River flood frequency has long been a focus because of the recognition that pre-regulation data for this important hydrological process are key for identifying changes and their potential causes (Timoney et al., 1997, 2009; Wolfe et al., 2006, 2008; Beltaos, 2018; Lamontagne et al., 2021). Unresolved debate persists over the status and trends in ice-jam flood frequency at the PAD both before and after onset of Peace River flow regulation, which is a critical timeframe for understanding the timing and causes of lake drying in the PAD (Beltaos, 2018; Hall et al., 2019; Wolfe et al., 2020a; Beltaos & Peters, 2020ab). On one hand, recent statistical analysis of the Traditional Knowledge and historical record of ice-jam floods in the PAD was used to establish a hypothesis that ice-jam flood frequency was accelerating between 1880 and 1967, before installation of the W.A.C. Bennett Dam, and declined after onset of Peace River flow regulation (Beltaos, 2018). In contrast, paleolimnological records of flood frequency and lake water balance in the PAD identified that influence of ice-jam flood frequency declined, and perched lake evaporation increased since the late 1800s due to climate change following the Little Ice Age (Wolfe et al., 2005, 2006, 2008, 2020a). Beltaos and Peters (2020b) subsequently published a reanalysis of the flood frequency record shown in Wolfe et al. (2020a) based on magnetic susceptibility measurements in a sediment core from a river-proximal oxbow lake in the PAD (originally published in Wolfe et al., 2006) to reinforce the Beltaos (2018) hypothesis that declining flood frequency and increasing perched lake evaporation at the PAD has occurred since onset of Peace River regulation. However, Beltaos and Peters (2020b) did not account for confounding influence of rising water content and declining sediment compaction in the upper sediments on the magnetic susceptibility values

used to infer changes in the flood regime, which led to an underestimation of the frequency of floods during the post-dam era (Wolfe et al., 2006). Ongoing controversy and conflicting interpretations of hydrological conditions at the PAD during both the pre-regulation (1880–1967) and post-regulation (1972–present) intervals hampers effective decision making and prevents the identification of the timing and cause(s) of hydrological change at the PAD.

A new direction of inquiry is to generate long-term records of past variation in river discharge and lake water balance at key unregulated regions within the upper Peace River watershed, namely the Smoky and Wabasca watersheds. Here, opportunity exists to delineate the relative roles of climate versus river regulation at the PAD and address the Beltaos (2018) hypothesis that flood frequency was accelerating between 1880 and 1967 and declined thereafter due to Peace River flow regulation by characterizing the role of climate via paleolimnological analyses of sediment cores from upland and oxbow lakes in the Smoky River and Wabasca River watersheds. Long-term records from these watersheds are critical, as hydrographs spanning the past few decades demonstrate these rivers provide substantial discharge to the Peace River during the spring freshet when ice-jam flooding occurs at the Lower Peace River and the PAD (Prowse & Conly, 1998). Recent paleolimnological studies by Stratton (2022) and Girard (2022) have expanded temporal perspective of this hydrological link by reconstructing past variation in flood influence for portions of the Little Smoky River (a tributary of the Smoky River) and the Wabasca River. Their results reveal that snowmelt-driven influence of spring flood waters of these tributaries on floodplain lakes began to decline decades prior to Peace River regulation, which coincides with a decline of ice-jam flooding at the Lower Peace River and drying of perched lakes in the PAD identified in previously published paleolimnological records (Wolfe et al., 2005, 2006, 2008, 2012). There remains opportunity, however, to generate paleohydrological information from lake sediment records at hydrologically isolated upland lakes in the Smoky and Wabasca watersheds where, like other Prairie lakes, water balance is likely strongly influenced by input from snowmelt runoff (Pham et al., 2009). This knowledge would broaden understanding of pre-disturbance hydrological conditions in the 'trigger tributary' watersheds that influence spring ice-jam flooding downstream at the PAD via contributions of snowmelt runoff to the Peace River.

Here, paleolimnological analyses of sediment cores from upland lakes in the Smoky and Wabasca watersheds are used to characterize the role of past variations in climate on lake water balance and further address the Beltaos (2018) hypothesis that the frequency of ice-jam floods at the Lower Peace River was accelerating in the decades leading up to construction of the W.A.C. Bennett Dam (1880–1967) and decreased due to Peace River flow regulation (1972–present). Specifically, past variation in lake water balance (as evaporation-to-inflow (E/I) ratios) was reconstructed from measurements of cellulose oxygen isotope composition in sediment cores collected at four upland lakes (two per watershed) that are hydrologically isolated from nearby rivers and whose water balances are most likely controlled by hydroclimatic processes, including input from snowmelt runoff. Trends in reconstructed E/I ratios of the upland lakes in the Smoky and Wabasca watersheds were determined for the pre-regulation interval (1880–1967) and the post-regulation interval (1972–2019), and compared with flood influence records inferred from oxbow lake sediment cores in the same watersheds (Smoky 2 and Smoky 4 from Stratton, 2022; WAB 2 from Girard, 2022), and with previously published flood frequency (PAD 15 from Wolfe et al., 2006) and perched basin water balance (PAD 5 from Wolfe et al., 2005) records from analyses of sediment cores from lakes in the northern Peace sector of the PAD to delineate effects of climate versus river regulation at the PAD. If the timing and direction of past hydrological changes at the unregulated Smoky and Wabasca watersheds (influenced by climate, not hydroelectric regulation) are temporally coherent with those at the PAD (potentially influenced by climate and hydroelectric regulation), then climate, not the W.A.C. Bennett Dam, must be the main driver of reduced ice-jam flooding and perched lake drying at the PAD.

CHAPTER 2: METHODS

2.1 Study sites

Within the Smoky River and Wabasca River watersheds, four hydrologically isolated upland lakes (informally named: Smoky 5, Smoky 6, WAB 3 and WAB 4) were selected for sediment coring in September 2019 (Figure 2.1, 2.2). The upland lakes are shallow (average = 1.3 m, range = 0.7–2.0 m; Table A1, Appendix A), and aerial photos show little to no human modification of catchment vegetation (Figure 2.2). Vegetation zonation adjacent to the lake margins provides evidence of lake-level drawdown in recent decades, with trees showing former shorelines when water levels were higher, and wetland plants showing encroachment into the basins as water levels declined. The two upland lakes in the Smoky watershed possess a single outlet that was active at the time of sampling in September 2019, whereas the two upland lakes in the Wabasca watershed do not possess an outlet and are hydrologically closed basins. Water balance reconstructions from the upland lakes were compared to stratigraphic records from oxbow lakes in the Smoky (Smoky 2 and Smoky 4; Stratton, 2022) and Wabasca (WAB 2; Girard, 2022) watersheds, and to records from an oxbow lake (PAD 15; Wolfe et al., 2006) and a perched lake (PAD 5; Wolfe et al., 2005) in the northern Peace sector of the PAD (Figure 2.1).

2.2 Fieldwork

Sediment core collection

On September 9th and 11th of 2019, sediment cores were collected from Smoky 5, Smoky 6, WAB 3 and WAB 4. At the deepest and most central part of each lake, three cores were collected using a hammer-driven gravity corer deployed off the pontoon of a helicopter (Telford et al., 2021). Cores were sectioned into 0.5-cm intervals within 24 hours, stored in the dark and refrigerated (4°C) in Whirl-Pak® bags prior to further analyses. The primary core used for laboratory analyses was selected based on length and observed quality, where the longest core with minimal disturbance to the sediment-water interface was selected. For Smoky 6, a secondary core was used as the primary core did not have sufficient sediment mass for all analyses. For more information on collected sediment cores, refer to Table A2 (Appendix A).
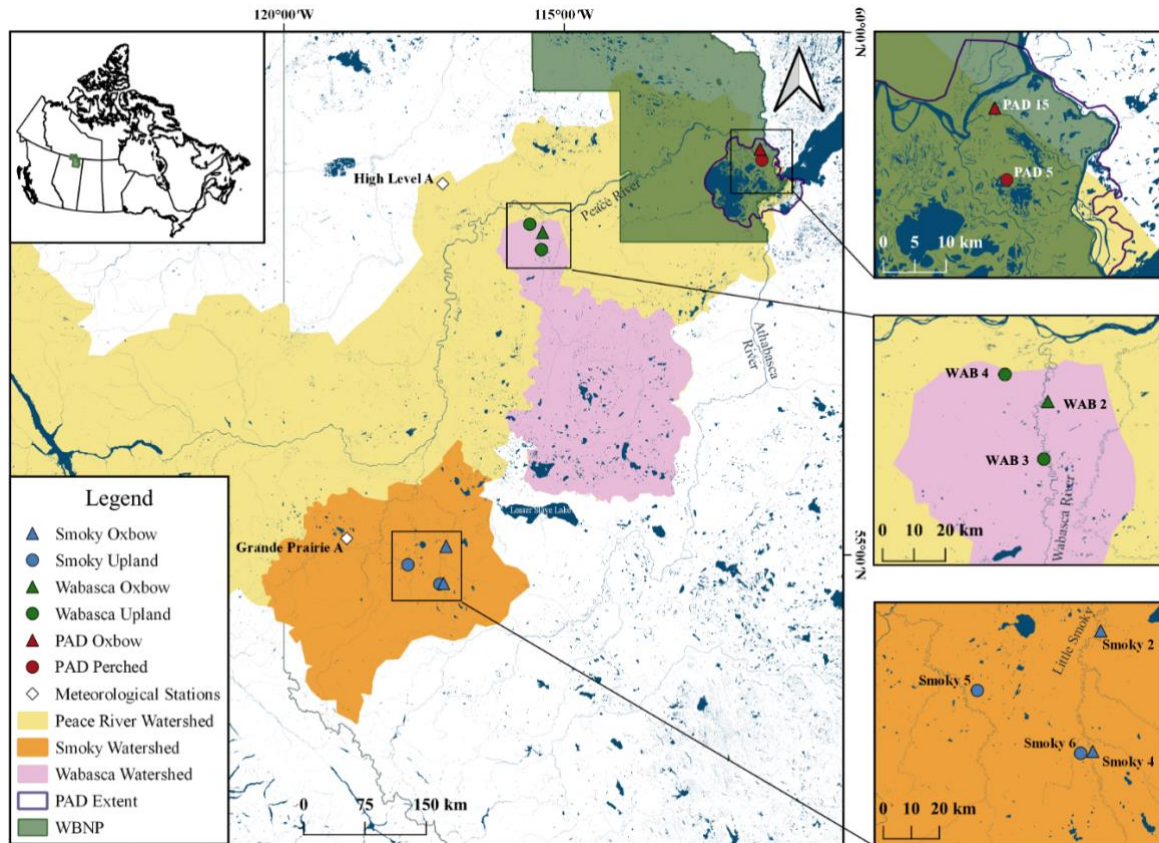
Figure 2.1. Map showing the lakes and watersheds studied in Alberta. The left panel shows the Peace River watershed (yellow) along with the Smoky River (orange) and Wabasca River (pink) watersheds, the extent of Wood Buffalo National Park (WBNP; green), and the outline of the Peace-Athabasca Delta (PAD) within and adjacent to WBNP. The upland and perched lakes are indicated by circles, oxbow lakes by triangles, and meteorological sites by white diamonds. Previously obtained paleohydrological records utilized in this study include oxbow lakes from the Smoky River watershed (Smoky 2 and Smoky 4; Stratton, 2022), the Wabasca River watershed (WAB 2; Girard, 2022), and the PAD (PAD 15; Wolfe et al., 2006), and a perched basin in the PAD (PAD 5; Wolfe et al., 2005). Panels along the right are magnified areas to show locations of the sites in the PAD (top), Wabasca River watershed (middle) and Smoky River watershed (bottom). Maps were created in QGIS version 3.10 (A Coruna).

Figure 2.2. Aerial views of Smoky (Smoky 5, 6) and Wabasca (WAB 3, 4) upland study sites. Photos taken in September 2019 by M. Stratton and C. Girard.

Water isotope and limnological measurements

Measurements of water isotope compositions and limnological variables (Table B1 and B2, Appendix B) contributed to understanding contemporary lake water balances and water quality at the time of sediment core collection and the isotope data were used to parameterize isotope-mass balance equations for determining E/I ratios from the lake sediment records. All upland lakes, along with the Little Smoky River, Smoky River, Peace River, and Wabasca River, were sampled for water isotope composition ($\delta^{18}O$ and δ^2H). Water samples were collected off the pontoon of a helicopter near the centre of the lake or river channel by submerging a 30 mL polyethylene Nalgene bottle approximately 10 cm below the water surface. To prevent evaporation prior to analyses, bottles were overfilled with water and capped tightly while submerged. Samples were analyzed at the University of Waterloo Environmental Isotope Laboratory. Results are reported as δ values in units per mil (‰) relative to the Vienna Standard Ocean Mean Water (VSMOW), with $\delta_{Sample} = [(R_{sample}/R_{standard}) -1] \times 10^3$ where R is the $^{18}O/^{16}O$

or ^{2}H/H ratio in sample and VSMOW (Table B1, Appendix B). Analytical uncertainties for the measurements are ±0.2‰ and ±0.8‰ for δ^{18}O and δ^{2}H, respectively. A YSI ProDSS multimeter was used to measure temperature, dissolved oxygen, specific conductivity, pH, and turbidity at 0.4 to 1.2 m (see Table B2, Appendix B).

2.3 Laboratory analyses

Loss-on-ignition

Loss-on-ignition (LOI) was used to obtain measurements of water, organic matter, mineral matter, and carbonate content following methods in Heiri et al. (2001). LOI results were used to assess variation in sediment composition and to align the two cores (one dated, the other undated) collected from Smoky 6. LOI measurements were obtained at every 0.5-cm interval by first weighing approximately 0.5 g of well-mixed wet sediment into pre-weighed dried crucibles. Next, sediments were dried for 24 hours at 90°C, cooled to room temperature in a desiccator for 2 hours and weighed to determine water content. Sediments were then heated in a muffle furnace for 2 hours at 550°C, cooled to 90°C, placed in a desiccator for 2 hours, and weighed to determine organic matter content. By subtracting the organic matter content from 100, mineral matter content was obtained. Finally, sediments were combusted at 950°C for 2 hours to remove carbonates, cooled to 90°C, placed in a desiccator for 2 hours and weighed. To calculate the carbonate content of the sample, the weight loss was multiplied by 1.36 (Dean, 1974). After all combustion steps, remaining material was carbonate-free mineral matter.

Radiometric dating

Age-depth profiles for working cores at each lake were constructed following methods presented by Appleby and Oldfield (1978) and Appleby (2001), where a gamma-ray spectrometer measured activities of ^{210}Pb, ^{226}Ra (via ^{214}Pb and ^{214}Bi), and ^{137}Cs. The ^{226}Ra content was used to determine the supported ^{210}Pb activity and then unsupported ^{210}Pb activity was estimated by subtracting supported ^{210}Pb activity from the total ^{210}Pb activity (Appleby and Oldfield, 1978). Sediment chronologies for the upper sediments were then estimated using unsupported ^{210}Pb activities and the Constant Rate of Supply (CRS) model (Sanchez-Cabeza & Ruiz-Fernandez, 2012). The background depth of supported ^{210}Pb activity was identified where total ^{210}Pb activity matched supported ^{210}Pb activity (which equaled the ^{226}Ra activity).

Below this background depth, the sediment chronology was linearly extrapolated based on the mean dry mass accumulation rate during the portion of the record dated from ^{210}Pb activities and the CRS model. Identification of a ^{137}Cs activity maximum associated with peak above-ground nuclear weapons testing in 1963, where possible, was used to corroborate the ^{210}Pb-based chronology (Appleby, 2001).

For radiometric dating, every 0.5-cm sediment interval was prepared for the top ~20-30 cm of the cores where rapid changes in ^{210}Pb activity and ^{137}Cs peaks typically occur. Alternating samples were then prepared until depths of ~40 cm where ^{210}Pb activities tended to reach constant low values. For each sample, wet sediments were frozen and freeze-dried. Freeze-dried sediments were then homogenized, compressed into pre-weighed polypropylene tubes to a height of 3.5 cm, and the mass was recorded. Compressed sediments were sealed with a silicon septum and 1 mL of epoxy resin. Samples were stored for at least 21 days to allow for equilibration of the parent and daughter radioisotopes prior to analyses on an Ortec HPGe Digital Gamma Ray Spectrometer with Maestro 32 software at the University of Waterloo.

Due to limited mass of dry sediment at each interval in cores from Smoky 6, the primary and secondary cores were both used for analyses. The primary core was used for radiometric dating and LOI, and the secondary core for measurement of LOI, organic carbon and nitrogen elemental and isotope composition, and oxygen isotope composition of cellulose. To accommodate this, a graphical 'wiggle-matching' depth-correction approach, using organic matter profiles, was used to account for discrepancies between sediment cores obtained at adjacent locations that may have captured the records at different angles of penetration by the corer, and thus present slightly different age-depth relationships (Thompson et al., 2012).

Oxygen isotope composition of cellulose

Sediment cores from each of the four upland lakes were prepared for measurement of oxygen isotope composition of cellulose to reconstruct past variation in lake water balances. Sample preparation followed Wolfe et al. (2001), where wet sediment was subsampled from every 0.5-cm interval and digested at 60°C for 2 hours using 10% HCl to remove inorganic carbon. Samples were then rinsed with deionized water, allowed to settle, then aspirated. This rinsing process was repeated until a neutral pH was reached, at which point sediments were frozen and

freeze-dried. Freeze-dried sediments were sieved (250 μm) to remove coarse organic debris which may be of terrestrial origin, and a pre-determined mass of the fine fraction (<250 μm) was submitted for organic carbon (%C_{org}) and nitrogen (%N) content and isotope analysis at the University of Waterloo Environmental Isotope Laboratory. Using %C_{org} and %N results, carbon-to-nitrogen ratios (C/N) were determined to assess the source of organic matter to the lakes, where values below 15 were interpreted as aquatically-derived autochthonous organic matter (Meyers & Teranes, 2001), a criterion needed to support reconstruction of cellulose-inferred lake water $\delta^{18}O$ (Wolfe et al., 2001). Carbon and nitrogen isotope data are not used here but can be found in Table F1-F4 (Appendix F) along with results of %C_{org}, %N and C/N ratios.

The remainder of the fine fraction (<250 μm) was sequentially treated for extraction and purification of cellulose from lake sediment. The treatments included a solvent extraction of 2:1 benzene to ethanol (to remove lipids, resins, and tannins), a glacial acetic acid and sodium chlorite bleaching solution (to remove lignin), alkaline hydrolysis using a 17% sodium hydroxide solution (to remove xylan, mannan, and other non-glucan polysaccharides), and oxyhydroxide leaching using a sodium dithionite, tri-ammonium citrate, and hydroxylamine hydrochloride solution (to remove iron and manganese hydroxides). After treatments, samples were frozen and freeze-dried. Using a microscope and tweezers, the white, fibrous cellulose was carefully identified and separated from the remaining dense minerogenic material prior to being weighed on a microbalance. Samples were analyzed using continuous flow-isotope ratio mass spectrometry at the University of Waterloo Environmental Isotope Laboratory. Results are reported as δ values, with units in per mil (‰) relative to the VSMOW. Analytical uncertainty for the measurements of cellulose $\delta^{18}O$ is ±0.3‰. The cellulose-water oxygen isotope fractionation factor ($\alpha^{18}O_{cell-lw}$ = 1.028) was then applied to measured cellulose $\delta^{18}O$ values to reconstruct lake water $\delta^{18}O$ (Wolfe et al., 2001; Savage et al., 2021).

2.4 Reconstruction of evaporation-to-inflow ratios

E/I ratios were estimated from cellulose-inferred lake water $\delta^{18}O$ values in the sediment cores to quantify changes in past lake water balance. Shifts towards higher E/I ratios are interpreted as increasing importance of evaporation on lake water balance associated with declining input

of snowmelt runoff to the upland lakes, while shifts towards lower E/I ratios are interpreted as decreasing importance of evaporation associated with increased snowmelt input. E/I ratios greater than 1 occur when the rate of water loss by evaporation exceeds the rate of water input to a lake.

E/I ratios were calculated using oxygen isotope values inserted into the equation described by Yi et al. (2008) and others:

$$(1)\ E/I = (\delta_I - \delta_L) / (\delta_E - \delta_L)$$

where δ_I is the isotope composition of the input water to the lake, δ_L is the isotope composition of lake water (inferred from the measured cellulose $\delta^{18}O$ value), and δ_E is the isotope composition of the evaporative flux.

Since δ^2H of lake water in the past is unknown, unique δ_I values could not be calculated for each 0.5-cm interval of the cores using the coupled-isotope tracer approach of Yi et al. (2008). To accommodate this, it was assumed that δ_I was approximately equal to δ_P, the amount-weighted mean annual isotope composition of precipitation. δ_E was calculated by the following equation presented in Yi et al. (2008) and based on the Craig and Gordon (1965) linear resistance model:

$$(2)\ \delta_E = [(\delta_L - \varepsilon^*) / (\alpha^* - h\delta_{AS} - \varepsilon_K)] / (1 - h + \varepsilon_K)$$

where ε^* is the equilibrium separation between liquid and vapor phases described by Horita and Wesolowski (1994):

$$(2.1)\ \varepsilon^* = (\alpha^* - 1)$$

α^* is the equilibrium liquid-vapor isotopic fractionation for $\delta^{18}O$ described by Horita and Wesolowski (1994):

$$(2.2)\ 1000\ln\alpha^* = -7.685 + 6.7123(10^3/T) - 1.6664(10^6/T^2) + 0.35041(10^9/T^3)$$

where T is the temperature in Kelvin.

δ_{AS} is the isotope composition of ambient atmospheric moisture (Gibson & Edwards, 2002):

$$(2.3)\ \delta_{AS} = (\delta_{PS} - \varepsilon^*) / \alpha^*$$

where δ_{PS} is the isotope composition of summer precipitation and ε_K is the kinetic separation for $\delta^{18}O$ (Gonfiantini, 1986):

$$(2.4)\ \varepsilon_K = 0.0142(1-h)$$

where h represents relative humidity.

Reconstructed E/I ratios were based on estimates of contemporary isotope and meteorological data, which were initially evaluated using lake-specific Local Evaporation Lines (LELs) derived from lake-specific estimates of δ_P and δ_{PS}, and watershed-specific estimates of temperature and relative humidity. The LELs were determined by identifying the equation of the line consisting of: δ_P, δ_{SSL} (isotope composition of a terminal basin at steady-state), and δ^* (isotope composition of a water body approaching desiccation). For each lake, estimates of δ_P (needed to solve equation 1 where $\delta_I \approx \delta_P$, and to calculate the LEL) and δ_{PS} (needed to solve equation 2.3 and constrained to May to September when average daily minimum temperatures are above 0 °C to represent the open-water season) were obtained from The Online Isotopes in Precipitation Calculator (OIPC; http://waterisotopes.org) (Bowen et al., 2005; IAEA/WMO, 2015; Bowen, 2022). For each lake, δ_{SSL} was calculated using the equation by Gonfiantini (1986):

$$(3)\ \delta_{SSL} = \alpha^*\delta_I(1 - h + \varepsilon_K) + \alpha^*h\delta_{AS} + \alpha^*\varepsilon_K + \varepsilon^*$$

where δ_I is assumed to be approximately equal to δ_P.

δ^* was calculated following the equation by Gonfiantini (1986):

$$(4)\ \delta^* = (h\delta_{AS} + \varepsilon_K + (\varepsilon^*/\alpha^*)) / (h - \varepsilon_K - (\varepsilon^*/\alpha^*)).$$

Temperature and relative humidity data needed for equations 2, 2.2., 2.4, 3 and 4 were obtained from meteorological stations Grande Prairie A (ID: 3072920) and High Level A (ID: 3073146) (obtained from: https://climate.weather.gc.ca) due to their proximity to the study lakes (Figure 2.1). Data from Grande Prairie A were used for the upland lakes in the Smoky watershed and data from High Level A were used for the upland lakes in the Wabasca watershed. For both stations, 1981–2010 climate normals of the daily average air temperature (Grande Prairie A: 13.20°C; High Level A: 12.54°C) and relative humidity (Grande Prairie A: 45.62%; High Level A: 48.28%) for the open-water season (May to September) were obtained. Measured lake and river water isotope compositions from September 2019 were used to evaluate the suitability of the lake-specific LELs, as well as a regionally-averaged LEL, for parameterization of the E/I equation.

2.5 Numerical analyses

Linear regression analysis was performed on the records of reconstructed E/I ratios for the pre-regulation (~1880–1967) and post-regulation (~1972–2019) intervals, following the approach advocated for by Beltaos (2018) to evaluate if reconstructed water balance at the upland lakes supported his postulation that flood frequency at the PAD was accelerating in the decades before installation of the W.A.C. Bennett Dam as a consequence of climatic trends, and declined thereafter as a consequence of Peace River flow regulation (Beltaos, 2018). Statistical significance of the linear regressions was determined based on alpha set to 0.05.

CHAPTER 3: RESULTS AND INTERPRETATION

3.1 Sediment core chronologies

Total ^{210}Pb activities increased with depth below the top of the core until ~4 cm and 8 cm at Smoky 5 and WAB 3, respectively, while they remained near constant until ~4 cm and 16 cm at Smoky 6 and WAB 4. Below these depths, total ^{210}Pb activities declined to supported ^{210}Pb levels (Smoky 5: 0.014 Bq/g, depth = 38 cm, year ~1889; Smoky 6: 0.024 Bq/g, depth = 17 cm, year ~1896; WAB 3: 0.005 Bq/g, depth = 36.5 cm, year ~1883; WAB 4: 0.026 Bq/g, depth = 30 cm, year ~1924). Linear extrapolation of the respective average sedimentation rate below the depth of supported ^{210}Pb activity was used to estimate the basal dates of the sediment cores (Smoky 5: ~1719; Smoky 6: ~1337; WAB 3: ~1277; WAB 4: ~1540). This study focuses on changes that have occurred since 1880, thus red dashed reference lines are included in Figure 3.1 to identify the depth corresponding to ~1880 in each core (Smoky 5: depth = 40.5 cm, year ~1880; Smoky 6: depth = 19 cm, year ~1881; WAB 3: depth = 37 cm, year ~1879; WAB 4: depth = 37 cm, year ~1880). This identifies that the post ~1880 period was largely captured by the CRS model, with relatively little extrapolation, which minimizes uncertainties in the age estimates.

^{137}Cs activities were not used to corroborate ^{210}Pb-based chronology results because the peaks were broad, poorly defined, and from before to after the age of peak nuclear fallout (1963) determined from ^{210}Pb dating (Figure 3.1). This indicated ^{137}Cs was upwardly and downwardly mobile in the sediment cores, which is typical of organic-rich sediments that tend to characterize hydrologically isolated lakes (Foster et al., 2006).

Wiggle-matching of the organic matter content profiles from the two cores obtained from Smoky 6 was achieved using a relatively small depth-correction factor of 1.17 (17%). The depth-correction factor was used to estimate the chronology of the non-dated core (Smoky 6 core 2) from the dated core (Smoky 6 core 1) (Figure D1 and Table D3, Appendix D). For the non-dated core, ~1881 was identified at a depth of ~16 cm, compared to the ~1881 estimation at a depth of 19 cm in the dated core.
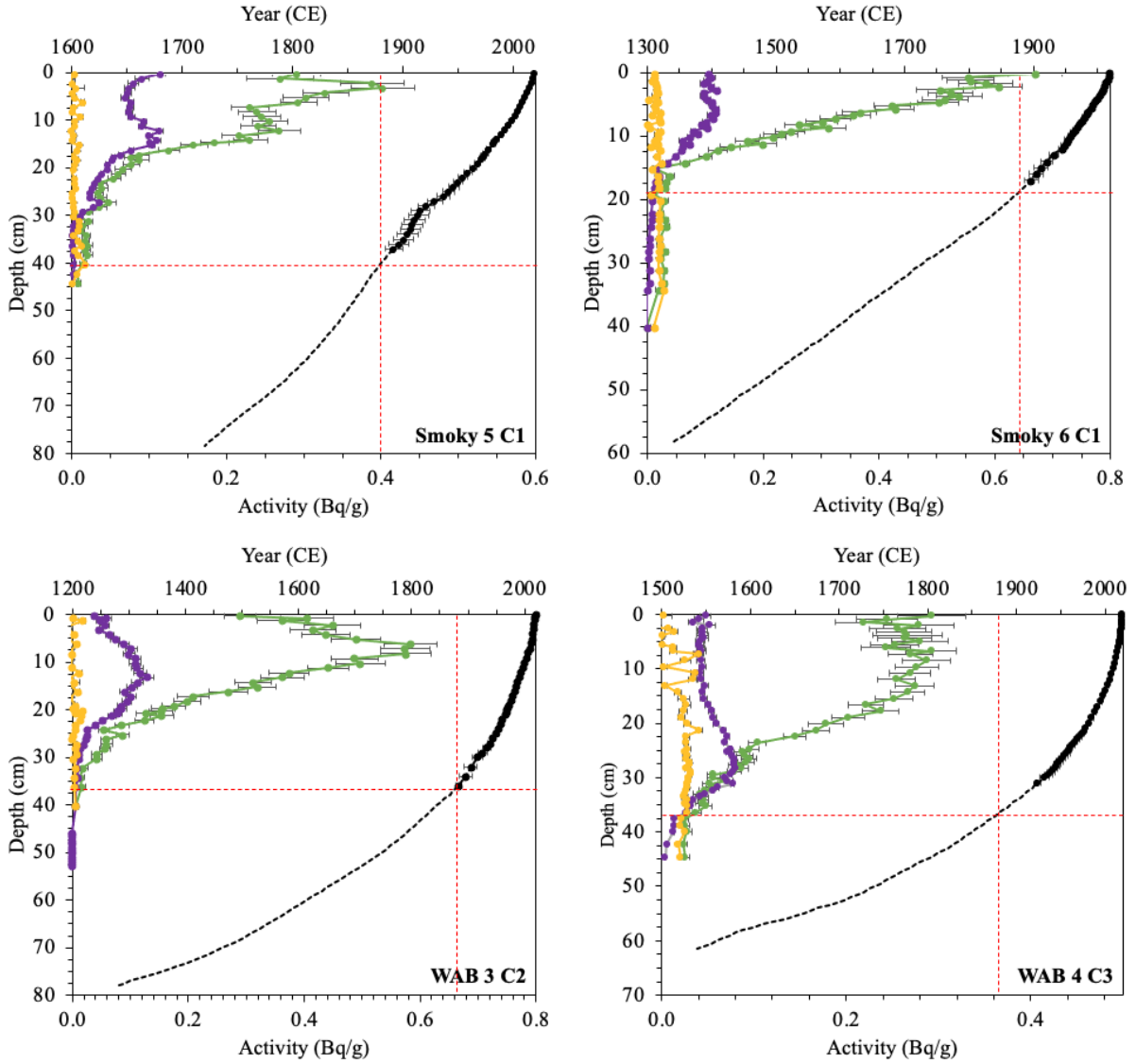
Figure 3.1. Radiometric dating results for Smoky 5 C1, Smoky 6 C1, WAB 3 C2, and WAB 4 C3. Activity profiles are shown for total [210]Pb (green), supported [210]Pb (as [226]Ra; yellow) and [137]Cs (purple). Also shown is the age-depth relation based on the CRS model with estimates based on measured samples (black) and estimates based on linear extrapolation below the depth where total and unsupported ^{210}Pb activity are equivalent (black dashed line). Error bars of ± 2 sigma are applied to CRS modelled ages, and error bars of ± 1 standard deviation are applied to radioisotope activities. The vertical and horizontal dashed red lines identify the depth horizon of ~1880, representing the stratigraphic interval of interest for this study.

15

3.2 Reconstruction of upland lake water balance using cellulose-inferred lake water δ^{18}O and modelled evaporation-to-inflow ratios

Evaluating the source of organic matter at upland lakes

At the four upland lakes, average C/N ratios since ~1880 were comparable and spanned mostly narrow ranges, with the largest range of values at WAB 3 (Smoky 5: average = 10.8, range = 10.4–11.4; Smoky 6: average = 11.7, range = 11.4–11.9; WAB 3: average = 12.4, range = 8.7–14.6; WAB 4: average = 11.3, range = 10.1–12.2; see Table F1-F4, Appendix F). Since C/N ratios at the upland study lakes were below a value of 15, the fine fraction of organic matter preserved in the upland lake sediments is likely to have formed mainly within the lake during primary production, as opposed to being washed in from terrestrial vegetation of the surrounding catchment (Meyers & Teranes, 2001). Thus, cellulose preserved within the lake sediments is reasonably assumed to be derived from within-lake aquatic processes, which is a primary assumption needed for the reconstruction of lake water oxygen isotope composition from cellulose oxygen isotope composition (Wolfe et al., 2001).

Water isotope composition of study lakes and rivers

Measured water isotope compositions of the upland lakes and major rivers in September 2019 (see Table B1, Appendix B) were plotted in δ^{18}O-δ^2H space and in relation to the Global Meteoric Water Line (GMWL; Craig, 1961) (Figure 3.2). For all upland lakes, isotope compositions showed varying offset, or enrichment, from the GMWL indicating varying importance of evaporation on individual lake water balances. The position of water isotope compositions in δ^{18}O-δ^2H space suggests that evaporation exerts greater influence on water balance of the upland lakes in the Wabasca watershed than those in the Smoky watershed. This is attributed to the absence of active outflow channels at the Wabasca lakes, which ensure most of the water loss occurs via evaporation, versus presence of active outflow channels at the Smoky lakes where substantial water loss may occur via outflow in addition to evaporation. These data support use of cellulose-inferred lake water δ^{18}O to reflect mainly changes in water balance, since the sediment record is reasonably assumed to be capturing changes in lake hydrology or water balance caused by shifting hydrological processes (i.e., precipitation, evaporation, outflow).

16
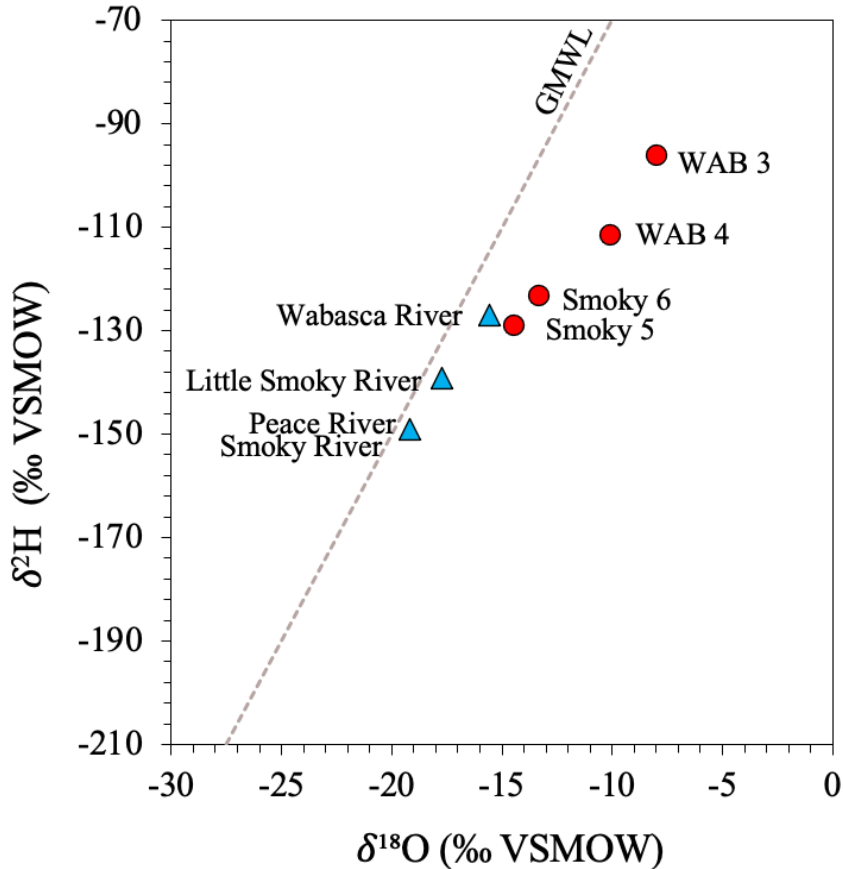
Figure 3.2. Isotope compositions of water samples collected in September 2019 from the upland lakes (red circles) and nearby river sites (blue triangles) in the Smoky and Wabasca watersheds in relation to the Global Meteoric Water Line (GMWL; Craig, 1961).

Cellulose-inferred lake water $\delta^{18}O$ records

Using the constant and well-established oxygen isotope fractionation factor of 1.028 between aquatic cellulose and lake water (Wolfe et al., 2001; Savage et al., 2021), temporal variation in lake water $\delta^{18}O$ was modelled from the cellulose $\delta^{18}O$ values (Figure 3.3; see Table F1-F4, Appendix F, for raw values). To generate confidence, modelled estimates of cellulose-inferred lake water $\delta^{18}O$ in a sediment core is often compared to contemporary lake water $\delta^{18}O$ measurements (e.g., Wolfe et al., 2005; Zabel et al., 2022). This approach is often most effective when water samples are systematically collected throughout one or more ice-free seasons to capture water isotope composition at the time of aquatic cellulose formation, and during the year of sediment core collection. For this study, the single water sample collected in September 2019 at the time of sediment core retrieval does not achieve this optimal characterization because it is unlikely that the aquatic cellulose preserved in the surface

17

sediment was produced in the fall. While some agreement is observed between the uppermost cellulose-inferred lake water $\delta^{18}O$ values and the contemporary lake water $\delta^{18}O$, there is observable offset. These offsets can be explained, however, by considering the hydrological settings of the upland lakes. Closest agreement exists at the upland lakes in the Smoky watershed, where contemporary lake water $\delta^{18}O$ is lower than cellulose-inferred lake water $\delta^{18}O$ at the top of the sediment cores (absolute difference = 3.6‰ at Smoky 5 and 0.42‰ at Smoky 6). This may be attributed to cellulose production likely occurring at these lakes at times when water levels were lower and the outlet channels were inactive (or discharge was very low), leading to more evaporative ^{18}O-enrichment compared to contemporary lake water $\delta^{18}O$ measurements in the fall when outflow channels were active. Contemporary lake water $\delta^{18}O$ for WAB 3 and WAB 4, on the other hand, are higher than cellulose-inferred lake water $\delta^{18}O$ values in the uppermost sediment sample (absolute difference = 1.58‰ at WAB 3 and 3.93‰ at WAB 4). These lakes are hydrologically closed (i.e., no outflow channels) and, thus, are subject to evaporative ^{18}O-enrichment throughout the summer, which would explain the higher contemporary lake water $\delta^{18}O$ relative to the uppermost cellulose-inferred lake water $\delta^{18}O$, which likely captures more isotopically depleted lake water earlier in the open-water season.

Stratigraphic records of cellulose-inferred lake water $\delta^{18}O$ from ~1880 to 2019 ranged from ~ -19 to -7‰ for the upland lakes and averaged -12.9‰, -11.5‰, -10.3‰, and -14.7‰ for Smoky 5, Smoky 6, WAB 3 and WAB 4, respectively (Figure 3.3). This range is very similar to the range of contemporary $\delta^{18}O$ measurements from 2019 for the upland lakes and rivers in the Smoky and Wabasca watersheds (~ -19 to -8‰; Table B1, Appendix B). This indicates that the cellulose-inferred lake water $\delta^{18}O$ of the upland lakes capture a range of hydrological conditions that span intervals when water balances of the lakes were more strongly influenced by input (low cellulose-inferred lake water $\delta^{18}O$ values) to intervals when importance of evaporation increased (identified by higher cellulose-inferred lake water $\delta^{18}O$ values). The cellulose-inferred lake water $\delta^{18}O$ results provide a basis to quantitatively describe changes in upland lake water balance using E/I ratios.

18
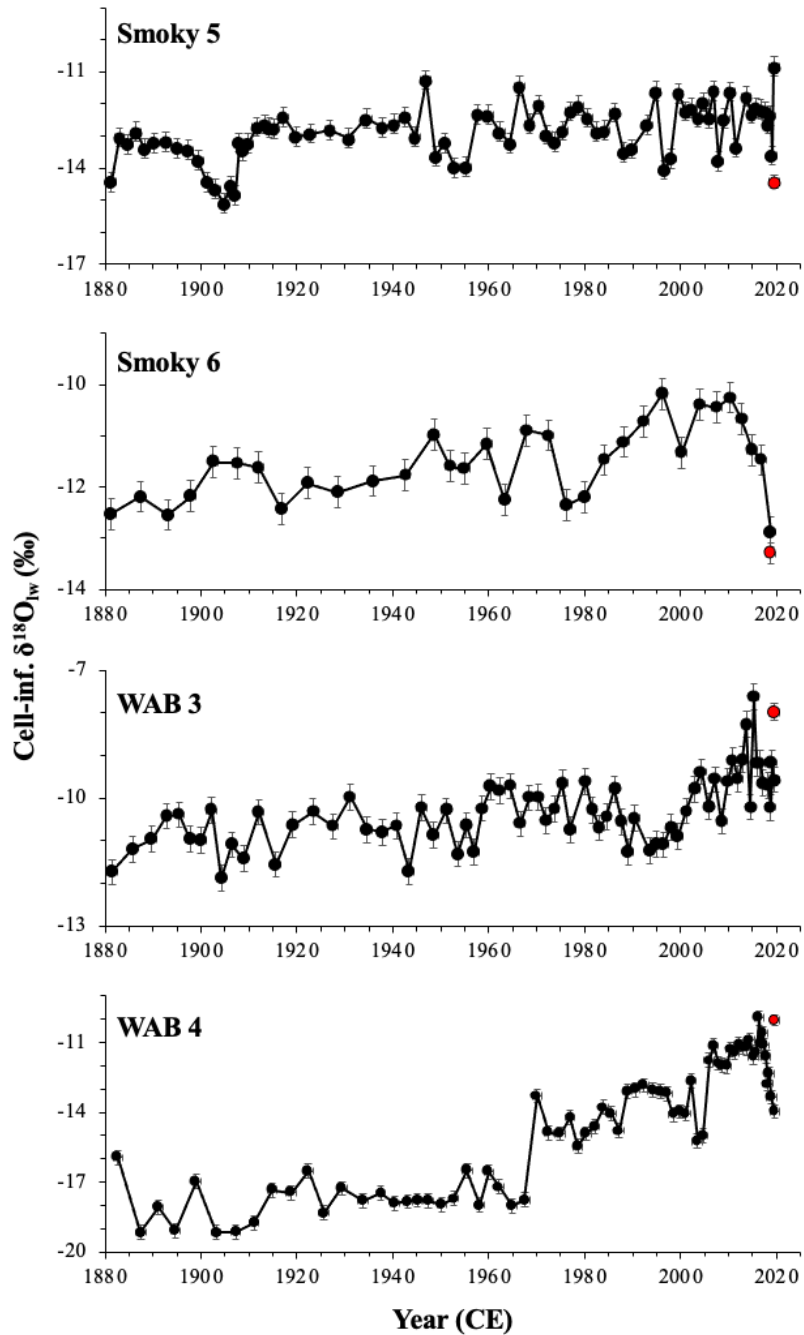
Figure 3.3. Graphs showing stratigraphic variation in cellulose-inferred lake water $\delta^{18}O$ (cell-inf. $\delta^{18}O_{lw}$) at the four study lakes. Error bars represent analytical uncertainty. Contemporary lake water $\delta^{18}O$, obtained in September of 2019, are coded in red, and error bars represent analytical uncertainty.

Using contemporary data to parameterize evaporation-to-inflow reconstructions

Contemporary lake and river isotope data were visualized alongside lake-specific Local Evaporation Lines (panels A-D, Figure 3.4) and a regionally-averaged Local Evaporation Line (panel E, Figure 3.4) to determine the most appropriate parameters for calculating E/I ratios from the stratigraphic records of cellulose-inferred lake water δ^{18}O (see equation 1). The LELs are anchored at δ_P, and the lake-specific δ_P values obtained from the OIPC ranged narrowly from -19.81 to -18.89‰ for δ^{18}O and -152.8 to -146.3‰ for δ^2H (δ^{18}O$_P$, δ^2H$_P$ of Smoky 5: -18.89‰, -146.3‰; Smoky 6: -19.09‰, -147.8‰; WAB 3: -19.76‰, -152.7‰; WAB 4: -19.81‰, -152.8‰) with an average value of -19.39‰ for δ^{18}O$_P$ and -149.9‰ for δ^2H$_P$. Similarly, lake-specific δ_{SSL} values (equation 3) differ minimally, ranging from -4.5 to -3.2‰ for δ^{18}O and -85.8 to -78.3‰ for δ^2H (δ^{18}O$_{SSL}$, δ^2H$_{SSL}$ of Smoky 5: -3.2‰, -78.3‰; Smoky 6: -3.4‰, -79.6‰; WAB 3: -4.5‰, -85.6‰; WAB 4: -4.5‰, -85.8‰) with an average value of -3.9‰ and -82.3 for δ^{18}O$_{SSL}$ and δ^2H$_{SSL}$, respectively. In contrast, δ^* (equation 4), the terminus of the LEL, ranged considerably: 12.4 to 16.4‰ for δ^{18}O and 3.9 to 24.5‰ for δ^2H (δ^{18}O*, δ^2H* of Smoky 5: 16.4‰, 24.5‰; Smoky 6: 16.3‰, 23.4‰; WAB 3: 12.4‰, 4.4‰; WAB 4: 12.7‰, 3.9‰) with an average value of 14.5‰ for δ^{18}O* and 13.8‰ for δ^2H*. Equations of the LELs were all quite similar, with a narrow range of slopes (between 4.83 and 4.85) and Y-intercepts (between -59.5 and -57.5). Given these results, the regionally-averaged LEL and associated isotope framework parameters were considered most appropriate for modelling E/I ratios from the cellulose-inferred lake water δ^{18}O records (Table C1, Appendix C). Contemporary lake and river water isotope data are also well described by the regionally-averaged LEL (Figure 3.4, panel E), supporting its use for parameterization of the E/I equation.
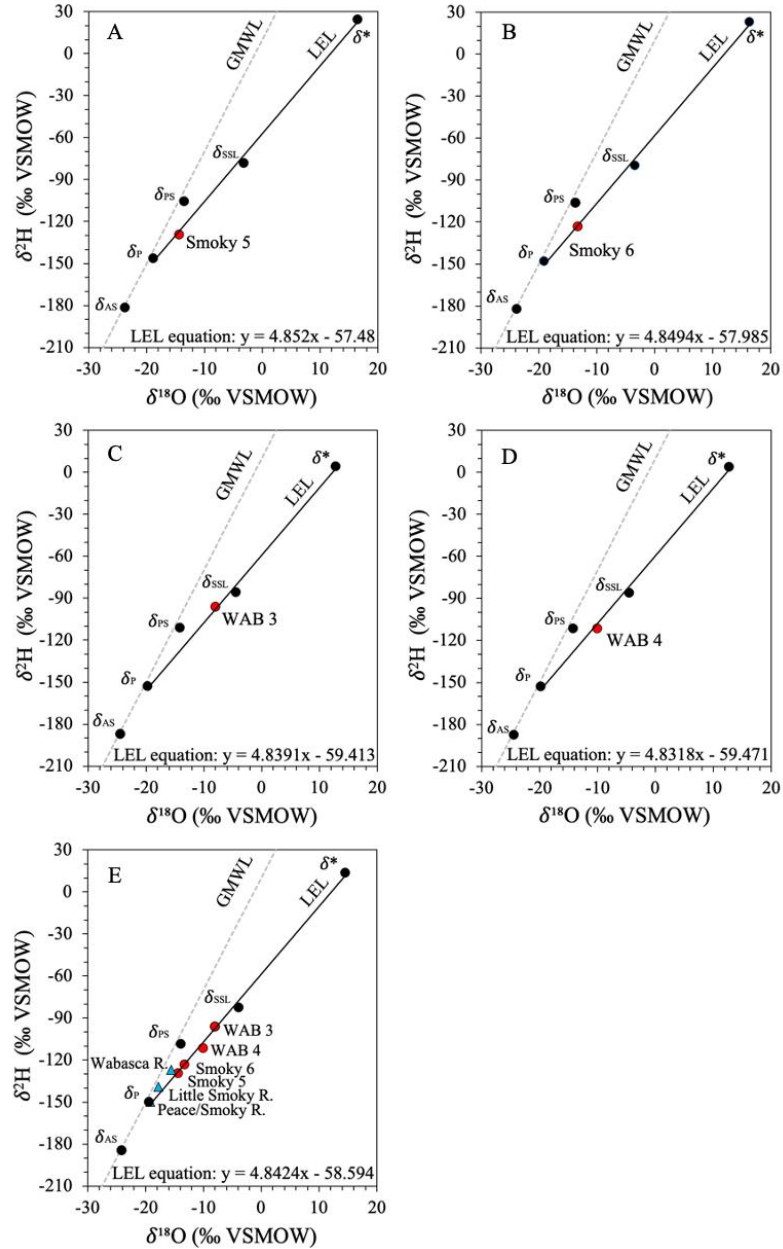
Figure 3.4. Lake-specific isotope frameworks (panels A-D) and a regionally-averaged isotope framework for the Smoky/Wabasca region (panel E) including Local Evaporation Lines (LELs). Isotope compositions of water samples collected from the upland lakes (red circles) and nearby river sites (blue triangles) in the Smoky and Wabasca watersheds are plotted in relation to the Global Meteoric Water Line (GMWL) and LELs. Isotope frameworks (black circles) include the isotope composition of a water body approaching desiccation ($\delta*$), the terminal basin steady-state isotope composition (δ_{SSL}), the amount-weighted mean annual isotope composition of precipitation (δ_P), the isotope composition of summer precipitation (δ_{PS}), and the isotope composition of summer atmospheric moisture (δ_{AS}). See Table C1 (Appendix C) for all values obtained from the OIPC (Bowen et al., 2005; IAEA/WMO, 2015; Bowen, 2022) and for all values calculated and used in the lake-specific and regionally-averaged isotope frameworks.

Reconstruction of evaporation-to-inflow ratios

Temporal variation of reconstructed E/I ratios was assessed by identifying samples with greater (coded as red symbols in Figure 3.5) and lesser (blue symbols) importance of evaporation than the mean of the pre-regulation interval (~1880–1967) at each of the four upland lakes. When analysed in this manner, E/I ratios generally increased over time (except at WAB 4 before the late 1960s), and they predominantly exceeded the pre-regulation average after ~1910 at Smoky 5, ~1940 at Smoky 6, ~1960 at WAB 3 and ~1968 at WAB 4. The greater importance of evaporation on water balance of the upland lakes in the Wabasca watershed since the 1960s can be attributed to the absence of active outflow channels which ensure water loss is mainly via evaporation. The sudden rise in inferred E/I ratios at WAB 4 after ~1968 may capture the point in time when water levels declined sufficiently to prevent water loss via outflow, leading to a 'step-shift' in importance of evaporation on the water balance. Comparatively, the upland lakes in the Smoky watershed continue to possess active outlet channels, which increase water loss by outflow. Relatively strong and rising importance of evaporation is also evident at all lakes since ~2000, based on highest values of inferred E/I ratios since ~1880 and aerial images of the lakes taken in 2019 that show marked lake drawdown during recent decades that has permitted encroachment of wetland plants from former treed shorelines (Figure 2.2). Despite this evidence of recent drying, however, E/I ratios remained below 1.0 throughout the sediment core records. Physical evidence of lake drawdown despite inferred E/I ratios below 1.0 likely reflects strong influence of snowmelt runoff on lake water balance at the time when the cellulose deposited and preserved in the sediment record was produced. Thus, aerial photos taken in September 2019 reflect lake level drawdown that most likely occurred during mid- to late summer, which is not fully captured by the aquatic cellulose preserved in the lake sediments because the preserved cellulose likely was produced in spring and early summer when isotope composition of lake water was lower due to the influence of isotopically depleted snowmelt. Additional support of recent drying at the upland lakes is evident when the water balance records presented here since 1880 are compared with the complete sediment core records of cellulose-inferred lake water $\delta^{18}O$, which extend back to ~1300-1700 and provide evidence that influence of evaporation during the past ~140 years was relatively high in context of longer-term natural variation (see Figure F1, Appendix F).

During the pre-regulation interval, linear regression analysis revealed significant rising trends in E/I ratios at three of the four lakes (Smoky 5, Smoky 6, WAB 3). The rise of E/I ratios at these lakes is interpreted as increasing importance of evaporation on lake water balance associated with declining input from snowmelt runoff in watersheds of these unregulated upstream 'trigger tributaries' during the decades before regulation of Peace River flow. In the post-regulation interval, inferred E/I ratios have continued to rise at all lakes, with statistically significant increases identified at WAB 3 and WAB 4. At the upland lakes in the Smoky watershed, the rate of increase in inferred E/I ratios was comparable during both the pre-regulation and post-regulation intervals (Smoky 5: rate of E/I ratio increase = 0.007/decade during both the pre- and post-regulation intervals; Smoky 6: rate of E/I ratio increase = 0.005/decade during both the pre- and post-regulation intervals). At the upland lakes in the Wabasca watershed, however, E/I ratios rose much more rapidly during the post-regulation interval (WAB 3: post-regulation rate of E/I ratio increase = 0.02/decade vs. pre-regulation rate of E/I ratio increase = 0.006/decade; WAB 4: post-regulation rate of E/I ratio increase = 0.04/decade vs pre-regulation rate of E/I ratio increase = 0.003/decade). The lack of active outlet channels at the upland lakes in the Wabasca watershed likely accounts for the more rapid rise in importance of evaporation compared to the upland lakes in the Smoky watershed.
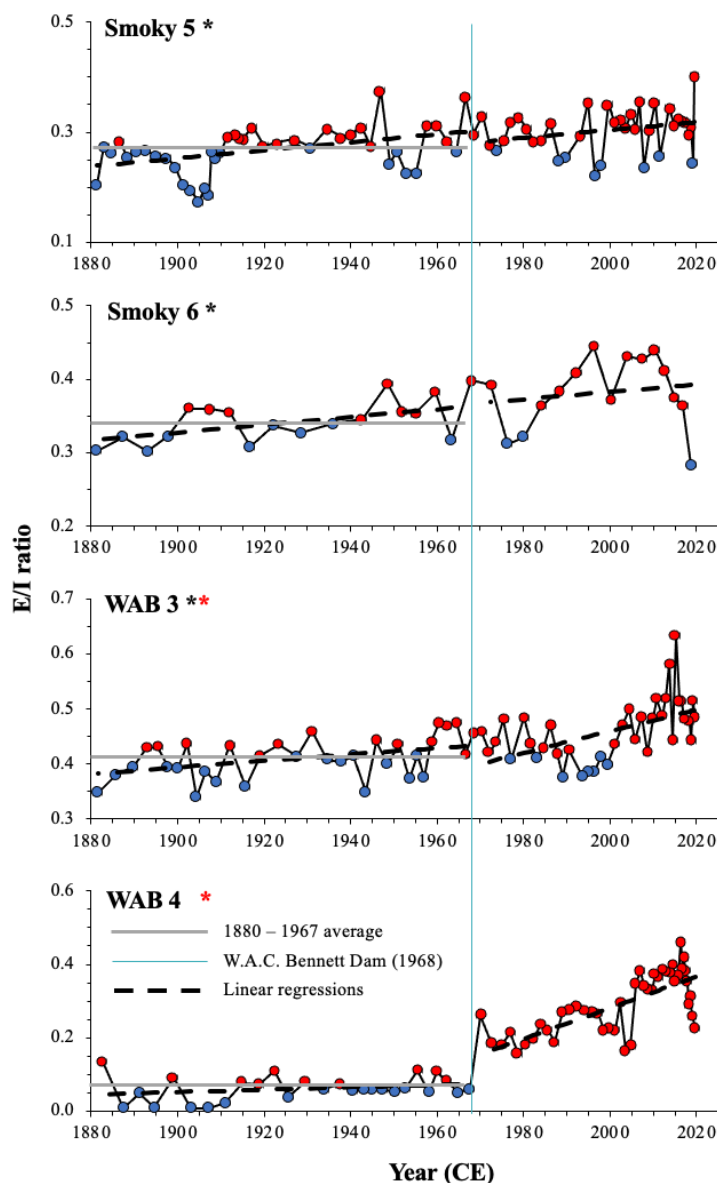
Figure 3.5. Temporal patterns of change in lake water balance expressed as E/I ratios, computed from cellulose-inferred lake water $\delta^{18}O$ results (Figure 3.4), from 1880 to 2019. Average E/I values for the pre-regulation interval (~1880–1967) are shown as grey lines. E/I values higher than the respective pre-regulation average were coded red, and values lower were coded blue for each upland lake. Records are shown with linear regressions for pre- (~1880–1967) and post-regulation (~1972–2019) intervals, where a black star next to the lake name indicates the pre-regulation regression is statistically significant and a red star indicates the post-regulation regression is statistically significant (Smoky 5 pre-regulation: y = 0.000731x – 1.1374, P = 3.7814x10^{-3}, df = 41; post regulation: y = 0.000713x – 1.1216, P = 0.1232, df = 34; Smoky 6 pre-regulation: y = 0.000532x – 0.6846 , P = 0.0280, df = 16; post-regulation: y = 0.000494x – 0.6046, P = 0.5739, df = 14; WAB 3 pre-regulation: y = 0.000584x – 0.7155, P = 0.0159, df = 31; post-regulation: y = 0.001973x – 3.4868, P = 6.9346x10^{-4}, df = 36; WAB 4 pre-regulation: y = 0.000328x – 0.5707, P = 0.2209, df = 25; post-regulation: y = 0.004238x – 8.1942, P = 1.6655x10^{-8}, df = 42).

24

3.3 Evaluating uncertainty and assumptions associated with lake water balance records

Assessment of timing and onset of climate-driven hydrological changes at the upland lakes in the Smoky and Wabasca watersheds hinges on the establishment of sediment core chronologies and lake water balance estimates that are sufficiently accurate and precise. Radiometric dating of the cores by ^{210}Pb and the Constant Rate of Supply model produced estimated errors of ± 2.5 to 3 years for ~1967, the year used to differentiate pre- and post-regulation intervals, indicating a high level of confidence in the chronologies. The cellulose-inferred lake water δ^{18}O records used to compute E/I ratios also showed good reproducibility, which provides confidence in the precision of the water balance records. For example, duplicates were taken every 5 cm at each lake and the average absolute differences between duplicates were small for measured cellulose δ^{18}O (0.48‰, 0.52‰, 0.43‰, and 0.33‰ at Smoky 5, Smoky 6, WAB 3 and WAB 4, respectively). Moreover, duplicate measurements on the fine fraction of sediment in subsamples taken every 5 cm revealed consistent C/N ratios that are typical of an autochthonous origin (i.e., aquatic primary production) for the organic matter analyzed for cellulose δ^{18}O (Meyers & Teranes, 2001) (e.g., average absolute differences = 0.08, 0.08, 0.18, and 0.12 for Smoky 5, Smoky 6, WAB 3 and WAB 4, respectively).

Knowledge of the hydrological settings of the study lakes was helpful to reconcile differences between one-time measurements of contemporary lake water δ^{18}O and the cellulose-inferred lake water δ^{18}O from the uppermost sediment samples, as well as to explain differences in patterns and trends in the inferred E/I ratio records among study lakes. For example, absence of active outflow channels at the upland lakes in the Wabasca watershed increased influence of evaporative ^{18}O-enrichment of the contemporary water samples relative to the upland lakes in the Smoky watershed where outflow channels are active. Consideration of the presence or absence of active outflow channels along with the seasonal timing of evaporative water loss and production of the cellulose preserved in the lake sediment likely accounts for different directions of the offset between contemporary measurements of lake water δ^{18}O and cellulose-inferred lake water δ^{18}O at the upland lakes in the two watersheds (Figure 3.3). Also, evidence of recent decline in surface area from former treed shorelines and encroachment of wetland vegetation is documented in aerial images taken in September 2019 at all four of the upland

lakes, which provides confidence in the accuracy of the rising trend in inferred E/I ratios since ~1968 to highest values of the ~140-year-long paleolimnological records.

Climatic conditions have not remained constant during the past 140 years, which imparts some uncertainty in the E/I records calculated from contemporary isotope data and climate normals. Estimates of air temperature and relative humidity derived from 30-year climate normal data were used to calculate E/I ratios, because the long-term means likely provide the most conservative approach to estimating E/I ratios. Nonetheless, the sensitivity of the calculated E/I ratios to variation in estimates of air temperature (± 2ºC) and relative humidity ($\pm 5\%$) were explored, with respect to climate normals used from the Grande Prairie A and High Level A meteorological stations. The sensitivity analysis revealed minimal changes in the average calculated E/I ratio from the records at each lake when temperature was varied by 2 ºC (maximum uncertainty of the average E/I ratio is ~0.008 among the four study lakes), with slightly larger differences observed when relative humidity was varied by 5% (maximum uncertainty of the average E/I ratio is ~0.028 among the four study lakes). Thus, there is considerable confidence in the accuracy of the estimates of E/I ratios and the interpretations drawn from the paleolimnological records.

CHAPTER 4: DISCUSSION

Characterizing the role of climate on the ice-jam flood regime at the Lower Peace River has long been recognized as critical for addressing the relative roles of Peace River flow regulation versus climatic changes on recent drying of lakes in the PAD (Prowse & Conly, 1998; Peters & Prowse, 2001; Wolfe et al., 2005, 2012, 2020a; Lamontagne et al., 2021). This includes hydrologic and hydraulic modelling of hydrometric data to quantify the 'naturalized' flow regime and determine the effect of regulation on the hydrograph of the Lower Peace River beyond effects attributable to changing climatic conditions (Peters & Prowse, 2001). This modelling exercise has demonstrated marked rise in discharge during winter months and reduction in summer months with little to no change during the spring freshet when ice-jam floods occur at the Lower Peace River and the PAD (Beltaos & Peters, 2020a) and is based on only 8 years of pre-regulation data (Wolfe et al., 2012, 2020a). Here, ~140-year-long records of past variation in water balance at upland lakes were developed to build upon newly generated paleohydrological information from oxbow lakes (Girard, 2022; Stratton, 2022) within watersheds of two 'trigger tributaries' known to contribute substantial discharge to the Peace River at the time of ice-jam flooding (Prowse & Conly, 1998). To improve understanding of the role of climate on hydrological changes at the Lower Peace River and PAD, paleolimnological records of past variation in reconstructed E/I ratios at the upland lakes in the Smoky and Wabasca watersheds are compared with records of flood influence at river-proximal oxbow lakes in the Smoky and Wabasca watersheds inferred from measurement of mineral matter content (Stratton, 2022; Girard, 2022), a record of flood influence at an oxbow lake adjacent to the Lower Peace River in the PAD inferred from measurement of magnetic susceptibility (Wolfe et al., 2006, 2012), and a record of water balance at a perched lake in the northern Peace sector of the PAD inferred from E/I ratios computed from measured cellulose $\delta^{18}O$ (Wolfe et al., 2005) (Figure 4.1). Variation in mineral matter content in cores from the oxbow lakes in the Smoky and Wabasca watersheds was selected here as a representative proxy of flood influence, which has been corroborated by strong correlation with temporal variation in Principal Component Analysis axis 1 scores of concentrations of several metals (e.g., Al, Si, Ti, Rb, Zr, K, Th; Girard, 2022; Stratton, 2022) indicative of allochthonous input to the lakes during flooding (Kylander et al., 2011; Peti & Augustinus, 2022). All lakes included in Figure 4.1 are strongly influenced by hydrological processes operating during the spring freshet, when

snowmelt runoff contributes important input to upland lake water balances and to discharge of the Smoky and Wabasca rivers and the Lower Peace River at the time of ice-jam formation. If intervals of increasing importance of evaporation on water balance associated with declining snowmelt input to the upland lakes in the Smoky and Wabasca watersheds correspond with intervals of declining flood influence at the oxbow lakes in those same watersheds, then a climate-driven decline in snowmelt runoff is likely the main factor promoting declines of discharge from the Smoky and Wabasca tributaries during the spring freshet. Similarly, if timing of increasing importance of evaporation on water balance at the upland lakes and declining flood influence at the oxbow lakes in the Smoky and Wabasca watershed coincides with intervals of declining influence of ice-jam flooding at the Lower Peace River and increased drying of perched lakes at the PAD, then a regional driver such as climate is implicated as an overwhelming cause of common hydrological changes across these locations, not Peace River flow regulation by the W.A.C. Bennett Dam. Information about the relative roles of Peace River flow regulation and climate on the Lower Peace River ice-jam flood regime and lake drying at the PAD is also provided by applying the compilation of paleohydrological records from sites in the Smoky and Wabasca watersheds and in the PAD to assess the hypothesis presented by Beltaos (2018) that flood frequency was accelerating between 1880 and 1967 and has declined coincident with onset of Peace River flow regulation.

Compilation of the paleohydrological records reveals that trends in reconstructed lake water balance at the upland lakes in the unregulated Smoky and Wabasca watersheds correspond well with trends in reconstructed flood influence at the oxbow lakes in the Smoky (Stratton, 2022) and Wabasca (Girard, 2022) watersheds (Figure 4.1, panels A-G). This includes during the pre-regulation interval (~1880–1967), when rising importance of evaporation relative to inflow, associated with decreased snowmelt input, at the upland lakes (Figure 4.1, panels A-D) corresponds with a decline in inferred flood influence at the oxbow lakes (panels E-G). It also includes during the post-regulation interval (~1972–2019) when rising evaporation relative to inflow at all four upland lakes coincides with low inferred flood influence at the oxbow lakes. The sole exception is the record from oxbow lake Smoky 4, where mineral matter content (and inferred flood influence) has been rising since ~1972, however, values have remained below the long-term average during most of the post-regulation interval (Figure 4.1,

28

panel F). Rising influence of evaporation at the upland lakes and decline of inferred flood influence at the oxbow lakes during the post-regulation interval are consistent with meteorological records at the nearby Grand Prairie, Alberta, station which document decline of precipitation and rise of air temperature during winter months between the late 1940s, when meteorological records began, and the late 1980s (Keller, 1997). Indeed, Keller (1997) identified that a climatic shift occurred in the mid-1970s, characterized by increased winter air temperatures and lower winter precipitation and (April 1) snowpack volume, which appears to be captured well in the paleolimnological records of the upland and oxbow lakes in the Smoky and Wabasca watersheds. In summary, compilation of the records from the upstream 'trigger tributaries' provides evidence of a long-term trend since the late 1800s towards rising importance of evaporation on upland lake water balance associated with declining input of snowmelt runoff and declining influence of river flooding caused by a shift in climatic conditions, with a more pronounced trend since the mid-1970s that began shortly after initiation of Peace River flow regulation by the W.A.C. Bennett Dam.

Rising importance of evaporation on water balance of the upland lakes and declining influence of floodwaters at the river proximal oxbow lakes in the Smoky and Wabasca watersheds also correspond with declining ice-jam flooding inferred from magnetic susceptibility measurements at an oxbow lake near the Lower Peace River and increasing evaporation of a perched lake in the northern Peace sector of the PAD (Figure 4.1, panels A-I). Linear regression analysis of magnetic susceptibility measurements on a sediment core from oxbow lake PAD 15 (Wolfe et al., 2006) reveals a significant decline in influence of ice-jam floods at the Lower Peace River during the pre-regulation interval. Values fall below the mean of the pre-regulation interval during ~1905–1930 and since ~1940 (Figure 4.1, panel H). Linear regression analysis for the post-regulation interval is not shown due to higher water content and lower sediment compaction towards the top of the sediment core that confounds interpretations of changes attributable to alteration of the flood regime. At perched lake PAD 5, reconstructed E/I ratios follow a rising trend during the pre- and post-regulation intervals (Wolfe et al., 2005; Figure 4.1, panel I) and E/I ratios consistently exceed 1.0 since ~1967 (indicative of water-level drawdown), except for four samples that capture ice-jam flood events including 1974 and 1996–1997 (Prowse & Conly 1998). Correspondence of increasing importance of evaporation

on water balance and declining flood influence at the upstream 'trigger tributaries' (associated with declining runoff during the spring freshet from thinner snowpack) with declining influence of ice-jam floods and drawdown of perched lake water levels in the PAD provides compelling evidence for a strong role of climate on the hydrological changes at the PAD.

Beltaos (2018) hypothesized that climatic forces were accelerating the frequency of ice-jam floods at the Lower Peace River between 1880 and 1967, prior to operation of the W.A.C. Bennett Dam, and declined thereafter because of Peace River flow regulation (Figure 4.1, panel J). Wolfe et al. (2020a) addressed, and countered, this testable hypothesis with paleohydrological records from the PAD. Here, additional paleohydrological data from the trigger tributaries provides further evidence that challenges the notion of accelerating ice-jam flood frequency during the decades prior to regulation of the Peace River. During the pre-regulation interval (1880–1967), acceleration of ice-jam flood frequency at the Lower Peace River would require rise over time in late-winter snowpack volume and decline of winter air temperatures to generate the river discharge and ice strength to accelerate the frequency of ice-jam floods (e.g., Lamontagne et al. 2021). If these hydroclimatic conditions were prevalent, this would have caused a *declining* trend in E/I ratios at the upland lakes in the upstream 'trigger tributaries' and a corresponding *increasing* trend in mineral matter content in sediments accumulated in the river-proximal oxbow lakes within the 'trigger tributaries' and the PAD. This is, however, the opposite of the paleolimnological evidence presented here, which identifies that climate-driven hydrological conditions have trended increasingly towards those that do not promote generation of ice-jam floods (Figure 4.1, panel A-H). This includes inferred decline of snowpack runoff since the late 1800s based on rising E/I ratios at the upland lakes in the Smoky and Wabasca watersheds, where snowmelt runoff provides important input to offset evaporative water losses in the Prairie region (Fang & Pomeroy, 2007; Pham et al., 2009) and inferred decline of discharge from the Smoky and Wabasca rivers during the spring freshet based on declining mineral matter content of the river-proximal oxbow lakes (Girard, 2022; Stratton, 2022). Strong influence of these climate-driven hydrological trends is evident at the PAD, where influence of ice-jam floods is inferred to have also declined based on magnetic susceptibility measurements at oxbow lake PAD 15 and resulted in increasing E/I ratios at perched lake PAD 5 due to decline in floodwater input and increase of evaporative

water loss (Wolfe et al. 2005, 2006, 2012; Remmer et al. 2018). These trends have continued during the post-regulation interval and have intensified since the mid-1970s when a shift in synoptic meteorological conditions fostered marked rise in winter air temperature and decline in winter precipitation and snowpack volume within the Smoky and Wabasca sub-watersheds of the Peace River (Moore & McKendry, 1996; Keller, 1997). Near-simultaneous timing of the onset of Peace River flow regulation by the W.A.C. Bennett Dam and the mid-1970s climatic shift has challenged scientists' ability to delineate effects of climate versus hydroelectric regulation. New evidence provided here from synthesis of analyses of sediment cores strategically collected from lakes affected and unaffected by Peace River flow regulation, however, reveals that aquatic ecosystems within both regulated and unregulated portions of the Peace River watershed downstream of the W.A.C. Bennett Dam have experienced similar hydrological changes, both before and since onset of Peace River flow regulation. This identifies climate as a main driver of the Lower Peace River ice-jam flood regime and perched lake water balance in the PAD, given the W.A.C. Bennett Dam has no influence on hydrological processes operating within the Smoky and Wabasca watersheds.
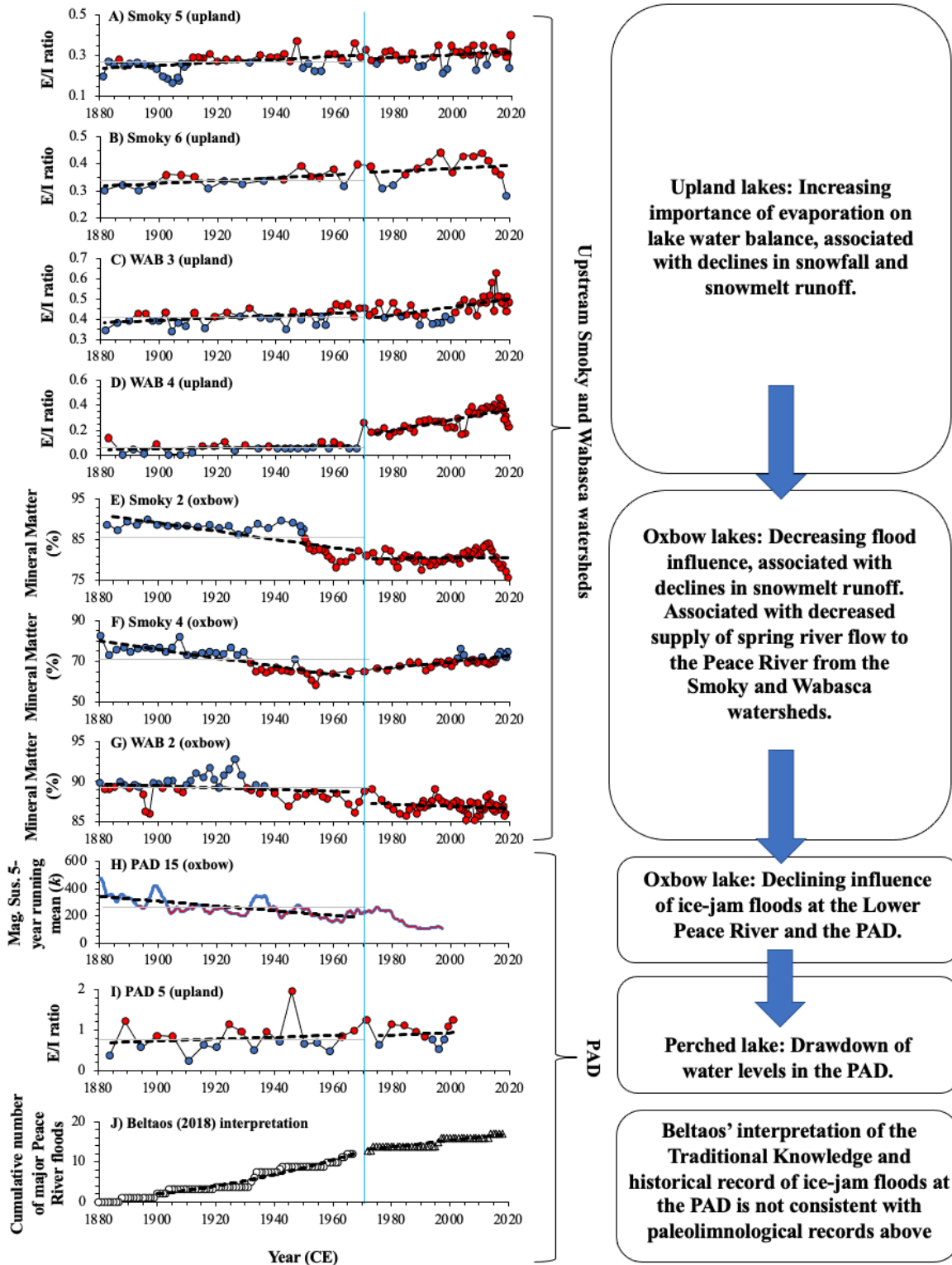
Figure 4.1. Comparison of paleolimnological reconstructions (A-I) and the Beltaos (2018; J) interpretation of hydrological change during the pre- ($y = 0.0009x^2 - 3.512x + 3254.6$) and post-regulation ($y = 0.0807x - 146.03$) intervals of the historical observation and traditional knowledge flood record of Peace River ice-jam floods. For paleolimnological reconstructions,

the grey line represents the respective pre-regulation (1880–1967) average, the dashed black lines the respective linear regressions of the dataset (1880–1967 and 1972–2019), blue dots/lines the measurements that indicate a wet interval relative to the pre-regulation average, and red dots/lines the measurements that indicate a dry interval relative to the pre-regulation average. E/I profiles generated in this study for Smoky 5 (A), Smoky 6 (B), WAB 3 (C), and WAB 4 (D) are shown with the same linear regressions as in Figure 3.5. Mineral matter records for oxbow lakes in the Smoky (Stratton, 2022) and Wabasca (Girard, 2022) watersheds are also shown (E) Smoky 2 pre- ($y = -0.101246x + 281.5770$, P = 2.8843×10^{-7}, df = 34) and post-regulation ($y = 0.005121x + 70.3588$, P = 0.7940, df = 48), (F) Smoky 4 pre- ($y = -0.210831x + 476.6011$, P = 1.8246×10^{-11}, df = 37) and post-regulation ($y = 0.142452 - 215.1237$, P = 1.0659×10^{-5}, df = 34), (G) WAB 2 pre- ($y = -0.011600x + 111.5284$, P = 0.1708, df = 43) and post-regulation ($y = -0.013595x + 114.1274$, P = 0.1527, df = 50). A record of PAD flood frequency is shown (H) as the PAD 15 (Wolfe et al., 2006), 5-year running mean of the magnetic susceptibility with just a pre-regulation linear regression ($y = -1.755285x + 3644.2106$, P = 6.1000×10^{-67}, df = 550) due to higher water content potentially impacting post-regulation interval results. A PAD perched basin water balance record (Wolfe et al., 2005) is also shown in (I) as an E/I ratio record with pre- ($y = 0.002297x - 3.6325$, P = 0.5626, df = 17) and post-regulation intervals ($y = 0.002928x - 4.9197$, P = 0.7781, df = 9).

CHAPTER 5: SYNTHESIS AND RECOMMENDATIONS

5.1 Key findings

Temporal variation in water balance since the 1880s, expressed as E/I ratios computed from cellulose-inferred lake water $\delta^{18}O$, was reconstructed at four hydrologically isolated upland lakes in the unregulated 'trigger tributary' Smoky and Wabasca watersheds, where water balance is strongly influenced by input of snowmelt runoff. The objective was to improve understanding of the processes responsible for past hydrological changes established previously from analysis of sediment cores from oxbow lakes in the Smoky and Wabasca watersheds (Stratton, 2022; Girard, 2022), and at an oxbow lake (Wolfe et al., 2006) and a perched lake (Wolfe et al., 2005) in the northern Peace sector of the PAD where hydrological processes are strongly influenced by ice-jam flooding at the regulated Lower Peace River. Results reveal that importance of evaporation on lake water balance, associated with declining input from snowmelt runoff, has increased over time at the upland lakes in the Smoky and Wabasca watersheds, both before and since onset of Peace River flow regulation by the W.A.C. Bennett Dam, and that this corresponds with inferred decline in flood influence at the oxbow lakes in the Smoky and Wabasca watersheds and at the PAD, and with drying of a perched lake in the PAD. Comparable hydrological changes over time at lakes within the unregulated upstream 'trigger tributaries' and the PAD support a prominent role of climate on the ice-jam flood regime and perched basin water balance at the PAD, where a long-term trend towards smaller snowpack volume and snowmelt runoff in the upstream 'trigger tributaries' has generated less discharge during the spring freshet upstream of the PAD leading to lower frequency and magnitude of ice-jam flooding at the PAD. Warming winter air temperatures likely also reduce resistive forces of river ice needed to generate dynamic breakup (Lamontagne et al., 2021).

A compilation of the paleolimnological records was used to further evaluate a hypothesis presented by Beltaos (2018), based on his interpretation of Traditional Knowledge and historical records of ice jam flood events at the PAD, suggesting that ice-jam flood frequency was accelerating at the PAD between 1880 and 1967, prior to construction of the W.A.C. Bennett Dam in 1968, and declined thereafter because of Peace River flow regulation. The paleolimnological results build upon those presented in Wolfe et al. (2020a) and reveal the

opposite pattern to that hypothesized by Beltaos (2018), where all records provide evidence to support declining Lower Peace River ice-jam flood frequency and magnitude between ~1880 and 1967. Increasing influence of evaporation on lake-water balance since 1972 also occurred at upland lakes in the Smoky and Wabasca watersheds, associated with a shift in synoptic meteorological conditions that reduced snowfall and raised winter air temperatures. These changes have had cascading effects downstream at the Lower Peace River, where declining discharge during the spring freshet from important upstream 'trigger tributaries' has led to reduced frequency of ice-jam flooding and increased drawdown of perched lakes at the PAD.

5.2 Significance and recommendations

Evidence for a strong role of climate on the Lower Peace River ice-jam flood regime and perched lake water balance at the PAD provides important knowledge to underpin decisions by stakeholders, and for local Indigenous communities that rely on the resources and waterways in the PAD for their traditional lifestyles and transportation routes. Reduced frequency and magnitude of ice-jam floods is clear from the paleolimnological records obtained at the PAD, which has degraded aquatic ecosystems and negatively affected the lived experience of Indigenous people who utilize the delta. Pronounced ecosystem alteration by climate change has also occurred outside of the PAD, which has incentivized Indigenous Peoples to adapt their traditional lifestyles to ensure sustainable transportation routes and continued food security (Macchi et al., 2008; Gauer et al., 2021). Recognition of climate effects is one critical step in supporting the local Indigenous communities at the PAD as they adapt and develop new sustainable strategies within their traditional lands. Further recognition of the role of climate on water-level drawdown in the PAD is also of immediate importance because a decision-making body at UNESCO is currently contemplating a downgrade in WBNP's status to 'World Heritage in Danger' based on widespread belief that Peace River flow regulation by the W. A. C. Bennett Dam is the main cause. Also, efforts to mitigate effects of Peace River flow regulation by the W.A.C. Bennett Dam have been initiated by stakeholders within the Action Plan for WBNP. These include installation of water control structures (dams) within the PAD to elevate water levels and inundate perched basins adjacent to the open-drainage network, and plans for intentional water releases from the W.A.C. Bennett Dam during the freshet of years when winter conditions produce a relatively high probability of ice-

jam flood occurrence. The results presented in this thesis suggest these strategies to mitigate the supposed effects of the W.A.C. Bennett will only be successful if they coincidentally happen to mitigate the effects of climate change.

Evidence generated here that has identified hydrological conditions and processes operating within the upstream Smoky and Wabasca watersheds are strongly associated with the ice-jam flood regime and perched lake drawdown at the PAD heightens a need to integrate effective watershed stewardship into future Action Plans for WBNP and the PAD. Effort should be placed to minimize human disturbances to these watersheds so as not to exacerbate effects of ongoing climate change on hydrological processes that alter the timing and volume of spring discharge from these 'trigger tributaries'. Monitoring of hydrological and meteorological conditions should be continued and expanded in the Smoky and Wabasca watersheds to track changes that influence Lower Peace River ice-jam flooding and water levels at the PAD.

To build upon this study, other statistical approaches could be explored to improve the detection and characterization of change in the water balance records reconstructed for the upland lakes in the Smoky and Wabasca watersheds. Linear regression analysis was used here to follow approaches taken by Beltaos (2018), Wolfe et al. (2020a), and Beltaos and Peters (2020b), but it may oversimplify long-term trends and variations in these systems. Use of breakpoint analysis and General Additive Models could be explored to identify significant points of change in the reconstructed E/I ratios and to describe onset of drying with increased statistical rigor (Simpson, 2018). Lakes within the Smoky and Wabasca watersheds have also been less studied from a paleolimnological perspective than at the PAD, thus, opportunity remains to spatially expand understanding of past changes in hydrological processes at these critical upstream watersheds. For example, lakes analyzed in this study for the Smoky watershed were situated along the Little Smoky River, near to the oxbow lakes that were sampled in 2019 (Stratton, 2022), and it may prove beneficial to study lakes directly along the Smoky River if suitable sites can be identified. Finally, contemporary hydrological studies could be conducted in future seasons and years at the four upland lakes to improve understanding of the influences of inputs from snowmelt and rainfall, and losses by outflow and evaporation on the lake water balances, as has been demonstrated for lakes at the PAD (e.g., Wolfe et al., 2005, 2012; Remmer et al. 2020).

REFERENCES

Appleby, P. G. (2001). Chronostratigraphic techniques in recent sediments. In: Last, W. M., & Smol, J. P. (Eds.), *Tracking Environmental Change Using Lake Sediments: Basin Analysis, Coring, and Chronological Techniques, Developments in Paleoenvironmental Research, Vol. 1* (pp. 171-203). Springer, Dordrecht.

Appleby, P. G., & Oldfield, F. (1978). The calculation of lead-210 dates assuming a constant rate of supply of unsupported ^{210}Pb to the sediment. *Catena*, *5*(1), 1-8.

Arciszewski, T. J., Munkittrick, K. R., Scrimgeour, G. J., Dubé, M. G., Wrona, F. J., & Hazewinkel, R. R. (2017). Using adaptive processes and adverse outcome pathways to develop meaningful, robust, and actionable environmental monitoring programs. *Integrated Environmental Assessment and Management, 13*(5), 877–891.

Athabasca Chipewyan First Nation (ACFN). (2021). A history of Wood Buffalo National Park's relations with the Denésuliné, Final Report, July 2021. Available from: https://www.theglobeandmail.com/files/editorial/politics/WBNP.pdf

Beltaos, S. (2014). Comparing the impacts of regulation and climate on ice-jam flooding of the Peace-Athabasca Delta. *Cold Regions Science and Technology, 108*, 49-58.

Beltaos, S. (2018). Frequency of ice-jam flooding of Peace-Athabasca Delta. *Canadian Journal of Civil Engineering*, *45*(1), 71-75.

Beltaos, S. & Peters, D. L. (2020a). Naturalized flow regime of the regulated Peace River, Canada, during the spring breakup of the ice cover. *Cold Regions Science and Technology. 172*, 103005.

Beltaos, S., & Peters, D. L. (2020b). Commentary on "Past variation in Lower Peace River ice-jam flood frequency" by Wolfe et al. (2020). *Environmental Reviews*, *28*(4), 560-566.

Blais, J. M., Rosen, M. R., & Smol, J. P. (2015). Using natural archives to track sources and long-term trends of pollution: An introduction. In: Blais, J. M., Rosen, M. R., & Smol, J. P.

(Eds.), *Developments in Paleoenvironmental Research Environmental Contaminants: Vol. 18* (pp. 1-3) Springer, Dordrecht.

Bowen, G. J., Wassenaar L. I., & Hobson K. A. (2005). Global application of stable hydrogen and oxygen isotopes to wildlife forensics. *Oecologia, 143*(3), 337-348.

Bowen, G. J. (2022). The online isotopes in precipitation calculator, version 3.1. http:///www.waterisotopes.org.

Craig, H. (1961). Isotopic variations in meteoric waters. *Science*, *133*(3465), 1702-1703.

Craig, H., & Gordon, L. I. (1965). Deuterium and oxygen 18 variations in the ocean and the marine atmosphere. In: Tongiorgi, E. (Ed.), *Stable Isotope in Oceanographic Studies and Paleotemperatures* (pp. 9-130). Laboratorio di Geologia Nucleare, Pisa, Italy.

Dean, W. E. (1974). Determination of carbonate and organic matter in calcareous sediments and sedimentary rocks by loss on ignition: Comparison with other methods. *Journal of Sedimentary Research*, *44*(1), 242-248.

Fang, X., & Pomeroy, J. W. (2007). Snowmelt runoff sensitivity analysis to drought on the Canadian prairies. *Hydrological Processes: An International Journal*, *21*(19), 2594-2609.

Foster, I. D. L., Mighall, T. M., Proffitt, H., Walling, D. E., & Owens, P. N. (2006). Post-depositional ^{137}Cs mobility in the sediments of three shallow coastal lagoons, SW England. *Journal of Paleolimnology, 35*(4), 881-895.

Gauer, V. H., Schaepe, D. M., & Welch, J. R. (2021). Supporting Indigenous adaptation in a changing climate: Insights from the Stó: Iō Research and Resource Management Centre (British Columbia) and the Fort Apache Heritage Foundation (Arizona). *Elementa: Science of the Anthropocene, 9*(1), 00164. https://doi.org/10.1525/elementa.2020.00164.

Gibson, J. J., & Edwards, T. W. D. (2002). Regional water balance trends and evaporation-transpiration partitioning from a stable isotope survey of lakes in northern Canada. *Global Biogeochemical Cycles*, *16*(2), 10-1.

Girard, C. (2022). *Paleohydrology of the Wabasca River and relations with past flood regimes at the downstream Peace-Athabasca Delta*. (Master's Thesis, University of Waterloo).

Gonfiantini, R. (1986). Environmental isotopes in lake studies. In: Fritz, P., & Fontes, J. – Ch. (Eds.), *Handbook of Environmental Isotope Geochemistry: The Terrestrial Environment, Vol. 2* (pp. 113-168). New York, Elsevier.

Hall, R. I., Wolfe, B. B., & Wiklund, J. A. (2019). Discussion of "Frequency of ice-jam flooding of Peace-Athabasca Delta". *Canadian Journal of Civil Engineering*, *46*(3), 236-238.

Heiri, O., Lotter, A. F., & Lemcke, G. (2001). Loss on ignition as a method for estimating organic and carbonate content in sediments: Reproducibility and compatibility of results. *Journal of Paleolimnology, 25*(1), 101-110.

Horita, J., & Wesolowski, D. J. (1994). Liquid-vapor fractionation of oxygen and hydrogen isotopes of water from the freezing to the critical temperature. *Geochimica et Cosmochimica Acta*, *58*(16), 3425-3437.

IAEA/WMO. (2015). Global network of isotopes in precipitation. The GNIP Database. Accessible at: https://nucleus.iaea.org/wiser.

Keller, R. A. (1997). *Variability in spring snowpack and winter atmospheric circulation pattern frequencies in the Peace River Basin* (Doctoral dissertation, University of Saskatchewan).

Kilgour, B. W., Dubé, M. G., Hedley, K., Portt, C. B., & Munkittrick, K. R. (2007). Aquatic environmental effects monitoring guidance for environmental assessment practitioners. *Environmental Monitoring and Assessment*, *130*(1), 423-436.

Kylander, M. E., Ampel, L., Wohlfarth, B., & Veres, D. (2011). High-resolution X-ray fluorescence core scanning analysis of Les Echets (France) sedimentary sequence: New insights from chemical proxies. *Journal of Quaternary Science*, *26*(1), 109-117.

Lamontagne, J. R., Jasek, M., & Smith, J. D. (2021). Coupling physical understanding and statistical modeling to estimate ice jam flood frequency in the northern Peace-Athabasca Delta under climate change. *Cold Regions Science and Technology*, *192*, 103383.

Lindenmayer, D. B., & Likens, G. E. (2010). The science and application of ecological monitoring. *Biological Conservation*, *143*(6), 1317-1328.

Macchi, M., Oviedo, G., Gotheil, S., Cross, K., Boedhihartono, A., Wolfangel, C., & Howell, M. (2008). Indigenous and traditional peoples and climate change: Issues paper IUCN. *International Journal for the Conservation of Nature,* Gland, Suiza. https://www2.ohchr.org/english/issues/climatechange/docs/iucn.pdf.

Meyers, P. A., & Teranes, J. L. (2001). Sediment organic matter. In: Last, W. M., & Smol, J. P. (Eds.), *Tracking Environmental Change Using Lake Sediments: Physical and Chemical Techniques, Developments in Paleoenvironmental Research, Vol. 2* (pp. 239–269). Kluwer Academic Publishers.

Mikisew Cree First Nation (MCFN). (2014). Petition to the World Heritage Committee requesting inclusion of Wood Buffalo National Park on the List of World Heritage in Danger, December 2014. Available from: https://cpawsnab.org/wp-content/uploads/2018/03/Mikisew_Petition_respecting_UNESCO_Site_256_-_December_8_2014.pdf

Moore, R. D., & McKendry, I. G. (1996). Spring snowpack anomaly patterns and winter climatic variability, British Columbia, Canada. *Water Resources Research, 32*(3), 623-632.

Munkittrick, K. R., McGeachy, S. A., McMaster, M. E., & Courtenay, S. C. (2002). Overview of freshwater fish studies from the pulp and paper environmental effects monitoring program. *Water Quality Research Journal Canada*, *37*(1), 49-77.

Peace-Athabasca Delta Project Group (PADPG). (1973). *Peace-Athabasca Delta Project, Technical Report and Appendices: Volume 1, Hydrological Investigations; Volume 2,*

Ecological Investigations. Peace–Athabasca Delta Project Group, Delta Implementation Committee, Governments of Alberta, Saskatchewan, and Canada.

Peters, D. L., & Prowse, T. D. (2001). Regulation effects on the lower Peace River, Canada. *Hydrological Processes*, *15*(16), 3181-3194.

Peti, L., & Augustinus, P. C. (2022). Micro-XRF-inferred depositional history of the Orakei maar lake sediment sequence, Auckland, New Zealand. *Journal of Paleolimnology*, *67*(4), 327-344.

Pham, S. V., Leavitt, P. R., McGowan, S., Wissel, B., & Wassenaar, L. I. (2009). Spatial and temporal variability of prairie lake hydrology as revealed using stable isotopes of hydrogen and oxygen. *Limnology and Oceanography*, *54*(1), 101-118.

Prowse, T. D., & Conly, F. M. (1998). Effects of climatic variability and flow regulation on ice-jam flooding of a northern delta. *Hydrological Processes*, *12*(10-11), 1589-1610.

Prowse, T. D., & Lalonde, V. (1996). Open-water and ice-jam flooding of a northern delta. *Nordic Hydrology, 27*(1-2), 85-100.

Remmer, C. R., Klemt, W. H., Wolfe, B. B., & Hall, R. I. (2018). Inconsequential effects of flooding in 2014 on lakes in the Peace-Athabasca Delta (Canada) due to long-term drying. *Limnology and Oceanography*, *63*(4), 1502-1518.

Remmer, C. R., Neary, L. K., Kay, M. L., Wolfe, B. B., & Hall, R. I. (2020). Multi-year isoscapes of lake water balances across a dynamic northern freshwater delta. *Environmental Research Letters*, *15*(10), 104066.

Roach, B., Walker, T. R. (2017). Aquatic monitoring programs conducted during environmental impact assessments in Canada: Preliminary assessment before and after weakened environmental regulation. *Environmental Monitoring and Assessment*, *189*(3), 1-11.

Sanchez-Cabeza, J. A., & Ruiz-Fernández, A. C. (2012). ^{210}Pb sediment radiochronology: An integrated formulation and classification of dating models. *Geochimica et Cosmochimica Acta*, *82*, 183-200.

Savage, C. A., Remmer, C. R., Telford, J. V., Kay, M. L., Mehler, E., Wolfe, B. B., & Hall, R. I. (2021). Field testing cellulose-water oxygen isotope relations in periphyton for paleohydrological reconstructions. *Journal of Paleolimnology*, *66*(3), 297-312.

Simpson, G. L. (2018). Modelling palaeoecological time series using generalized additive models. *Frontiers in Ecology and Evolution, 6*, 149.

Smol, J. P. (2008). Pollution of lakes and rivers: A paleoenvironmental perspective. *Blackwell Publishing*, Malden, MA, USA.

Smol, J. P. (2010). The power of the past: Using sediments to track the effects of multiple stressors on lake ecosystems. *Freshwater Biology*, *55*, 43-59.

Stratton, M. (2022). *Investigating the role of the Smoky River watershed on past ice-jam flood regimes at the Peace-Athabasca Delta via analysis of oxbow lake sediment cores*. (Master's Thesis, University of Waterloo).

Telford, J. V., Kay, M. L., Vander Heide, H., Wiklund, J. A., Owca, T. J., Faber, J. A., Wolfe, B. B., & Hall, R. I. (2021). Building upon open-barrel corer and sectioning systems to foster the continuing legacy of John Glew. *Journal of Paleolimnology*, *65*(2), 271-277.

Thompson, R., Clark, R. M, & Boulton, G. S. (2012). Core correlation. In: Birks, H. J. B., Lotter, A. F., Juggins, S., & Smol, J. P. (Eds.), *Tracking Environmental Change Using Lake Sediments: Data Handling and Numerical Techniques, Developments in Paleoenvironmental Research, Vol. 5* (415-430). Springer, Dordrecht.

Timoney, K., Peterson, G., Fargey, P., Peterson, M., McCanny, S., & Wein, R. (1997). Spring ice-jam flooding of the Peace-Athabasca Delta: Evidence of a climatic oscillation. *Climatic Change*, *35*(4), 463-483.

Timoney, K. (2002). A dying delta? A case study of a wetland paradigm. *Wetlands*, *22*(2), 282-300.

Timoney, K. (2009). Three centuries of change in the Peace–Athabasca Delta, Canada. *Climatic Change*, *93*(3), 485-515.

Vannini, P., & Vannini, A. 2019. The exhaustion of Wood Buffalo National Park: Mikisew Cree First Nation experiences and perspectives. *International Review of Qualitative Research*, *12*(3), 278-303.

Wolfe, B. B., Edwards, T. W. D., Elgood, R. J., & Beuning, K. R. (2001). Carbon and oxygen isotope analysis of lake sediment cellulose: Methods and applications. In: Last, W. M., & Smol, J. P. (Eds.), *Tracking Environmental Change Using Lake Sediments: Physical and Geochemical Methods, Developments in Paleoenvironmental Research, Vol. 2* (pp. 373-400). Springer.

Wolfe, B. B., Karst-Riddoch, T. L., Vardy, S. R., Falcone, M. D., Hall, R. I., & Edwards, T. W. D. (2005). Impacts of climate and river flooding on the hydro-ecology of a floodplain basin, Peace-Athabasca Delta, Canada since AD 1700. *Quaternary Research*, *64*(2), 147-162.

Wolfe, B. B., Hall, R. I., Last, W. M., Edwards, T. W. D., English, M. C., Karst-Riddoch, T. L., Paterson, A., & Palmini, R. (2006). Reconstruction of multi-century flood histories from oxbow lake sediments, Peace-Athabasca Delta, Canada. *Hydrological Processes*, *20*(19), 4131–4153.

Wolfe, B. B., Hall, R. I., Edwards, T. W., Jarvis, S. R., Sinnatamby, R. N., Yi, Y., & Johnston, J. W. (2008). Climate-driven shifts in quantity and seasonality of river discharge over the past 1000 years from the hydrographic apex of North America. *Geophysical Research Letters, 35*, L24402.

Wolfe, B. B., Hall, R. I., Edwards, T. W., & Johnston, J. W. (2012). Developing temporal hydroecological perspectives to inform stewardship of a northern floodplain landscape

subject to multiple stressors: Paleolimnological investigations of the Peace–Athabasca Delta. *Environmental Reviews*, *20*(3), 191-210.

Wolfe, B. B., Hall, R. I., Wiklund, J. A., & Kay, M. L. (2020a). Past variation in Lower Peace River ice-jam flood frequency. *Environmental Reviews*, *28*(3), 209-217.

Wolfe, B. B., Hall, R. I., Wiklund, J. A., & Kay, M. L. (2020b). Response to Commentary by Beltaos and Peters on: "Past variation in Lower Peace River ice-jam flood frequency" by Wolfe et al. (2020). *Environmental Reviews*, *28*(4), 567-568.

Wood Buffalo National Park (WBNP). (2019). World Heritage Site Action Plan. Parks Canada. Accessible at: https://www.pc.gc.ca/en/pn-np/nt/woodbuffalo/info/action.

Yi, Y., Brock, B. E., Falcone, M. D., Wolfe, B. B., & Edwards, T. W. D. (2008). A coupled isotope tracer method to characterize input water to lakes. *Journal of Hydrology*, *350*(1-2), 1-13.

Zabel, N. A., Soliguin, A. M., Wiklund, J. A., Birks, S. J., Gibson, J. J., Fan, X., Wolfe, B. B., & Hall, R. I. (2022). Paleolimnological assessment of past hydro-ecological variation at a shallow hardwater lake in the Athabasca Oil Sands Region before potential onset of industrial development. *Journal of Hydrology: Regional Studies*, *39*, 100977.

APPENDICES

Appendix A: Additional information for site locations and sediment cores.

Table A1. Additional information for study sites, comparison lakes (PAD sites and Smoky and Wabasca oxbows), and meteorological stations.

Name	Coordinates	Lake Surface Area (km^2)	Depth at Coring Site for this study (m)
Smoky 2	55°5'37.00"N 117°6'52.00"W	~114.1	N/A
Smoky 4	54°42'38.00"N 117°9'10.60"W	~65.3	N/A
Smoky 5	54°54'5.80"N 117°47'9.00"W	~241.8	1.2
Smoky 6	54°42'14.8"N 117°13'11.9"W	~338.6	2.0
WAB 2	58°10'21.70"N 115°23'28.70"W	~325.6	N/A
WAB 3	58°00'15.60"N 115°24'36.70"W	~74.3	0.7
WAB 4	58°14'42.70"N 115°36'58.20"W	~12.0	1.2
PAD 5	58°50'29.34"N 111°28'29.40"W	~128.2	N/A
PAD 15	58°56'34.32"N 111°30'24.30"W	~385.0	N/A
Grande Prairie A	55°10'47.000"N 118°53'06.000"W	N/A	N/A
High Level A	58°37'17.000"N 117°09'53.000"W	N/A	N/A

Table A2. Sediment core lengths for the primary, secondary, and archive cores with the core code denoted in brackets. Bolded sediment core lengths indicate cores that were used for laboratory analyses.

Lake Name	Sediment core length (cm) Primary/Secondary/Archive		
Smoky 5	**78.5** (C1)	54.5 (C2)	53.0 (C3)
Smoky 6	**59.0** (C1)	**46.0** (C2)	52.0 (C3)
WAB 3	**78.0** (C2)	68.5 (C3)	69.5 (C1)
WAB 4	**62.0** (C3)	63.5 (C1)	53.5 (C2)

Appendix B: Contemporary water isotope and water chemistry measurements.

Table B1. Summary of contemporary water isotope measurements (‰ VSMOW).

Sampling site	$\delta^{18}O$	δ^2H
Smoky 5	-14.42	-129.16
Smoky 6	-13.30	-123.22
WAB 3	-7.99	-96.22
WAB 4	-10.04	-111.49
Smoky River	-19.22	-149.79
Little Smoky River	-17.75	-139.10
Wabasca River	-15.58	-127.11
Peace River	-19.17	-149.04

Table B2. Summary of contemporary water chemistry measurements.

YSI Measurement	Smoky 5	Smoky 6	WAB 3	WAB 4
Temperature (°C)	13.8	14.3	13.1	12.9
Dissolved Oxygen (% saturation)	62.1	79.9	116.0	40.7
Specific Conductivity (µS/cm)	133.7	62.4	299.2	309.8
pH	7.01	7.24	8.41	7.5
Turbidity (FNU)	0.66	1.93	1.25	5.93
Depth of YSI device (m)	0.4	0.4	0.7	1.2

Appendix C: Summary of lake-specific and regionally-averaged isotope framework information for the upland study lakes.

Table C1. Values used for exploration of lake-specific and regionally-averaged isotope frameworks for the Smoky and Wabasca upland lakes. Temperature and relative humidity values are from the Grande Prairie A (Smoky lakes) and High Level A (Wabasca lakes) meteorological stations, and values are 1981-2010 climate normals for the open water (May-Sept) season. δ_P and δ_{PS} values are obtained from the OIPC (Bowen et al., 2005; IAEA/WMO, 2015; Bowen, 2022). All other values are calculated as described in the methods section.

	Smoky 5	Smoky 6	WAB 3	WAB 4	Values for regionally-averaged isotope framework
T (°C)	13.20	13.20	12.54	12.54	12.87
h (%)	45.62	45.62	48.28	48.28	46.95
α^*_{L-V} (^{18}O)	1.0104	1.0104	1.0105	1.0105	1.0104
α^*_{L-V} (^{2}H)	1.0927	1.0927	1.0936	1.0936	1.0931
ε^*_{L-V} (^{18}O) (‰)	10.41	10.41	10.48	10.48	10.44
ε^*_{L-V} (^{2}H) (‰)	92.71	92.71	93.57	93.57	93.14
$\varepsilon_{K\,L-V}$ (^{18}O) (‰)	7.72	7.72	7.34	7.34	7.53
$\varepsilon_{K\,L-V}$ (^{2}H) (‰)	6.80	6.80	6.47	6.47	6.635
$\delta^{18}O_{AS}$ (‰)	-23.72	-23.84	-24.40	-24.46	-24.11
δ^2H_{AS} (‰)	-181.3	-182.2	-187.1	-187.4	-184.5
$\delta^{18}O_P$ (‰)	-18.89	-19.09	-19.76	-19.81	-19.39
δ^2H_P (‰)	-146.3	-147.8	-152.7	-152.8	-149.9
$\delta^{18}O_{PS}$ (‰)	-13.56	-13.68	-14.18	-14.24	-13.92
δ^2H_{PS} (‰)	-105.4	-106.4	-111.0	-111.4	-108.6
$\delta^{18}O^*$ (‰)	16.4	16.3	12.4	12.7	14.50
δ^2H^* (‰)	24.5	23.4	4.4	3.9	13.80
$\delta^{18}O_{SSL}$ (‰)	-3.2	-3.4	-4.5	-4.5	-3.9
δ^2H_{SSL} (‰)	-78.3	-79.6	-85.6	-85.8	-82.3
Estimated elevation used for OIPC (m)	675	716	313	260	N/A

Appendix D: Radiometric dating raw data.

Table D1. Smoky 5 C1 CRS-based chronology derived from measured ^{210}Pb, ^{137}Cs, and ^{266}Ra (weighted mean of ^{214}Bi and ^{214}Pb) activities (dpm/g). Grey highlighted cells represent dates that were extrapolated using the CRS model, yellow highlighted cells represent interpolated values. BDL = below detection limit, where values should be treated as 0.

Top Depth (cm)	CRS Chronology (CE)	CRS Error (± 2 sigma)	^{210}Pb dpm/g	^{210}Pb Error (1 std. dev.) dpm/g	^{137}Cs dpm/g	^{137}Cs Error (1 std. dev.) dpm/g	^{226}Ra dpm/g	^{226}Ra Error (1 std. dev.) dpm/g
0.0	2019.29	0.09	17.4729	1.8782	6.9086	0.3222	0.2144	0.1467
0.5	2018.95	0.16	16.8202	3.2029				
1.0	2018.53	0.21	16.1839	2.5944	5.4359	0.5145	-0.1020	0.3041
1.5	2018.01	0.29	19.5354	3.5723				
2.0	2017.25	0.33	23.3203	2.4556	4.7882	0.4003	0.0141	0.2513
2.5	2016.23	0.44	23.7482	3.4840				
3.0	2015.36	0.49	24.1813	2.4715	4.4625	0.3991	0.3071	0.6362
3.5	2014.26	0.57	21.8695	3.0495				
4.0	2013.19	0.61	19.7099	1.7864	4.3667	0.2704	0.0493	0.0230
4.5	2012.12	0.68	18.9358	2.5099				
5.0	2010.91	0.73	18.1822	1.7630	4.1228	0.2863	0.2034	0.1340
5.5	2009.90	0.78	17.8955	2.2632				
6.0	2008.42	0.84	17.6118	1.4190	4.5986	0.2219	0.8552	0.1498
6.5	2007.36	0.89	15.6476	2.0170				
7.0	2006.42	0.92	13.8351	1.4334	4.5246	0.2438	0.1683	0.0572
7.5	2005.40	0.97	14.0899	2.0415				
8.0	2004.32	1.02	14.3478	1.4537	4.4718	0.2643	0.0342	0.0528
8.5	2002.90	1.09	14.5493	2.0837				
9.0	2001.68	1.14	14.7527	1.4928	4.6460	0.2645	0.6896	0.1752
9.5	2000.39	1.20	15.0670	2.0470				
10.0	1998.69	1.27	15.3858	1.4006	5.6002	0.2439	0.2444	0.1215
10.5	1997.33	1.33	14.9403	1.9670				
11.0	1995.75	1.40	14.5035	1.3811	5.4375	0.2483	0.1972	0.0676
11.5	1994.07	1.48	15.3123	2.1358				
12.0	1992.36	1.57	16.1506	1.6292	6.8108	0.2868	0.0029	0.0097
12.5	1990.59	1.65	14.5403	2.1513				
13.0	1989.07	1.73	13.0408	1.4050	6.0245	0.2614	0.1798	0.1081
13.5	1987.21	1.82	13.4443	1.9249				
14.0	1985.21	1.93	13.8560	1.3158	6.6534	0.2341	0.0548	0.1506
14.5	1983.29	2.05	11.1129	1.1134	6.1227	0.2105	-0.1153	0.0524
15.0	1981.53	2.16	9.4865	1.0354	6.2368	0.2188	0.6138	0.1247
15.5	1979.76	2.25	8.4654	1.3300				
16.0	1977.77	2.38	7.5202	0.8347	4.6413	0.1693	0.4539	0.0948
16.5	1976.24	2.47	6.3342	1.1198				

17.0	1974.73	2.57	5.2799	0.7465	3.7779	0.1730	-0.0298	0.0519
17.5	1973.03	2.69	4.6623	0.6097	3.2226	0.1433	0.2006	0.0801
18.0	1971.36	2.81	5.2822	0.7160	3.1811	0.1489	0.4306	0.0905
18.5	1969.48	2.93	4.9330	0.9504				
19.0	1967.56	3.09	4.5995	0.6249	2.7561	0.1316	0.2500	0.0605
19.5	1965.38	3.22	4.2766	0.9006				
20.0	1963.56	3.37	3.9692	0.6485	2.7641	0.1557	0.1812	0.0636
20.5	1961.08	3.51	3.7908	0.8477				
21.0	1958.87	3.73	3.6179	0.5460	2.3275	0.1194	-0.0137	0.0230
21.5	1956.43	3.89	3.4459	0.7472				
22.0	1954.15	4.13	3.2794	0.5101	2.0441	0.1141	0.1976	0.0937
22.5	1951.62	4.28	2.7220	0.6776				
23.0	1949.99	4.46	2.2317	0.4461	1.8071	0.1156	0.2068	0.0538
23.5	1948.00	4.60	2.2776	0.6160				
24.0	1945.77	4.85	2.3241	0.4249	1.6252	0.1067	0.3026	0.0673
24.5	1943.64	5.02	2.1789	0.5881				
25.0	1941.56	5.28	2.0399	0.4066	1.4583	0.1069	0.0941	0.0645
25.5	1939.12	5.50	2.1329	0.6189				
26.0	1936.61	5.86	2.2287	0.4666	1.4622	0.1286	0.0470	0.0285
26.5	1932.52	6.14	2.5222	0.7343				
27.0	1928.99	6.68	2.8403	0.5669	2.1935	0.1565	0.1765	0.0571
27.5	1924.75	7.11	2.5059	0.7331				
28.0	1921.20	7.73	2.1988	0.4648	1.7139	0.1325	0.1411	0.0715
28.5	1918.70	8.13	1.7186	0.5603				
29.0	1915.85	8.69	1.3140	0.3128	0.8547	0.0955	0.2232	0.0521
29.5	1914.61	8.89	0.7967	0.3475				
30.0	1913.92	9.02	0.4371	0.1512	0.6913	0.1081	0.1035	0.0493
30.5	1912.73	8.98	0.7936	0.3640				
31.0	1910.53	9.32	1.3053	0.3311	0.3385	0.1142	0.5609	0.0931
31.5	1909.11	9.37	1.1017	0.4320				
32.0	1908.27	9.42	0.9205	0.2774	BDL	BDL	0.5917	0.1005
32.5	1907.55	9.38	0.8115	0.3640				
33.0	1906.85	9.39	0.7114	0.2357	0.1613	0.1529	0.5275	0.1024
33.5	1905.69	9.25	0.8988	0.4050				
34.0	1903.88	9.49	1.1165	0.3294	BDL	BDL	0.1591	0.1279
34.5	1902.09	9.36	1.0897	0.4520				
35.0	1900.44	9.50	1.0634	0.3095	BDL	BDL	0.5408	0.1011
35.5	1898.46	9.26	1.1557	0.4680				
36.0	1896.27	9.32	1.2531	0.3511	BDL	BDL	0.8016	0.1597
36.5	1893.83	8.30	1.1723	0.4799				
37.0	1891.54	8.08	1.0951	0.3272	0.1085	0.1587	0.2329	0.1262
37.5	1889.13	7.25	1.1723	0.4782				
38.0	1887.47		1.2531	0.3487	0.1611	0.1421	0.5412	0.1114
38.5	1885.58		1.1418	0.5600				
39.0	1883.92		1.0373	0.4382				
39.5	1882.14		0.9394	0.5123				

40.0	1880.46	0.8478	0.2654	0.1902	0.1406	1.0593	0.1378
40.5	1879.04	0.7011	0.4013				
41.0	1877.31	0.5723	0.3010				
41.5	1875.55	0.4604	0.3329				
42.0	1874.01	0.3642	0.1420	BDL	BDL	0.4165	0.1021
42.5	1872.11	0.4030	0.2813				
43.0	1870.72	0.4446	0.2428				
43.5	1869.27	0.4889	0.3126				
44.0	1867.66	0.5361	0.1969	BDL	BDL	0.0974	0.0323
44.5	1866.31						
45.0	1864.62						
45.5	1863.06						
46.0	1861.50						
46.5	1859.90						
47.0	1858.27						
47.5	1856.61						
48.0	1855.14						
48.5	1853.44						
49.0	1852.20						
49.5	1850.53						
50.0	1849.30						
50.5	1847.45						
51.0	1845.80						
51.5	1844.38						
52.0	1842.98						
52.5	1841.40						
53.0	1839.63						
53.5	1837.88						
54.0	1836.10						
54.5	1834.17						
55.0	1832.37						
55.5	1830.51						
56.0	1828.64						
56.5	1826.82						
57.0	1824.92						
57.5	1823.25						
58.0	1821.42						
58.5	1819.58						
59.0	1817.57						
59.5	1815.57						
60.0	1813.61						
60.5	1811.51						
61.0	1809.43						
61.5	1807.07						
62.0	1805.09						
62.5	1803.14						

63.0	1800.67
63.5	1798.34
64.0	1796.49
64.5	1793.76
65.0	1790.98
65.5	1788.10
66.0	1785.28
66.5	1783.29
67.0	1780.89
67.5	1778.03
68.0	1775.59
68.5	1772.95
69.0	1770.10
69.5	1767.61
70.0	1764.34
70.5	1761.68
71.0	1758.78
71.5	1755.79
72.0	1753.03
72.5	1750.42
73.0	1747.98
73.5	1744.94
74.0	1742.39
74.5	1740.09
75.0	1737.57
75.5	1735.21
76.0	1732.71
76.5	1729.95
77.0	1727.60
77.5	1724.99
78.0	1722.44
78.5	1719.94

Table D2. Smoky 6 C1 CRS-based chronology derived from measured ^{210}Pb, ^{137}Cs, and ^{266}Ra (weighted mean of ^{214}Bi and ^{214}Pb) activities (dpm/g). Grey highlighted cells represent dates that were extrapolated using the CRS model, and yellow highlighted cells represent interpolated values. BDL = below detection limit, where values should be treated as 0.

Top Depth (cm)	CRS Chronology (CE)	CRS Error (± 2 sigma)	^{210}Pb dpm/g	^{210}Pb Error (1 std. dev.) dpm/g	^{137}Cs dpm/g	^{137}Cs Error (1 std. dev.) dpm/g	^{226}Ra dpm/g	^{226}Ra Error (1 std. dev.) dpm/g
0.0	2018.15	0.23	40.1835	2.8205	6.3828	0.3516	0.7941	0.1761
0.5	2016.65	0.35	33.2780	2.6684	6.6647	0.4031	0.7856	0.3407
1.0	2014.59	0.47	33.4543	2.4110	6.1583	0.3167	0.4653	0.1489
1.5	2013.21	0.54	35.0719	2.8049	5.9075	0.4175	0.8587	0.2009
2.0	2010.43	0.67	36.3844	2.4097	6.6468	0.2854	0.9933	0.1751
2.5	2008.58	0.76	30.2994	2.3970	7.1479	0.3314	0.9567	0.1964
3.0	2005.79	0.88	31.4221	2.2873	5.9320	0.3071	1.1401	0.2088
3.5	2002.58	1.03	32.2757	2.3800	5.8574	0.3472	0.9056	0.3886
4.0	1999.52	1.16	30.8585	2.3300	6.2357	0.3518	0.1382	0.1371
4.5	1995.97	1.32	30.1314	2.1327	6.6805	0.3009	1.0975	0.1912
5.0	1992.75	1.47	25.3486	1.9024	6.7704	0.2961	0.7399	0.1579
5.5	1989.26	1.64	25.6583	2.0006	7.0545	0.3369	0.9287	0.1823
6.0	1985.73	1.83	22.0116	1.7726	7.1028	0.2971	1.2848	0.2021
6.5	1982.11	2.04	21.3262	1.7683	6.5395	0.2985	0.5447	0.1326
7.0	1978.65	2.26	19.4772	1.6138	6.8340	0.2724	1.2463	0.1963
7.5	1975.61	2.47	18.1078	1.6771	6.0655	0.2953	1.3704	0.2645
8.0	1972.62	2.70	15.7219	1.4800	5.6068	0.2731	0.0525	0.0613
8.5	1968.82	3.01	18.7727	1.7966	6.1638	0.3294	0.1933	0.1463
9.0	1963.86	3.43	14.8206	1.4906	4.7386	0.2799	1.2862	0.2101
9.5	1961.13	3.71	13.8489	1.7715	5.2724	0.3589	1.0498	0.2567
10.0	1957.95	4.07	13.0402	1.3700	4.3714	0.2446	1.1170	0.1893
10.5	1953.25	4.59	10.3448	1.2643	3.5970	0.2517	0.7700	0.1640
11.0	1952.20	4.75	11.9079	1.4552	4.3420	0.2818	1.1145	0.2010
11.5	1947.54	5.36	8.5908	1.0813	3.6408	0.2182	0.3572	0.2448
12.0	1944.04	5.90	7.3176	0.9655	3.5626	0.2035	1.3169	0.1808
12.5	1938.18	6.60	6.6567	1.1934				
13.0	1931.42	7.82	6.0369	0.7014	2.8598	0.1414	0.9872	0.1257
13.5	1925.44	8.75	4.8990	0.8807				
14.0	1920.66	9.70	3.9141	0.5326	2.0920	0.1111	1.4339	0.1335
14.5	1916.05	10.24	1.9523	0.5736				
15.0	1912.21	10.75	0.7902	0.2129	0.8888	0.0817	0.5594	0.0751
15.5	1908.17	10.95	1.4368	0.4849				
16.0	1903.90	11.40	2.3658	0.4356	1.2465	0.1056	1.0876	0.1185
16.5	1899.74	11.08	2.1680	0.5889				
17.0	1896.20	10.89	1.9816	0.3962	0.8957	0.1008	1.0766	0.1151
17.5	1891.82		1.9246	0.5576				

18.0	1886.57	1.8688	0.3923	0.6974	0.1053	1.1904	0.1249
18.5	1881.60	1.1369	0.4391				
19.0	1876.00	0.6268	0.1973	0.4244	0.0961	0.4031	0.1158
19.5	1870.46	1.1073	0.4180				
20.0	1864.74	1.7866	0.3686	0.5160	0.0964	1.3781	0.1280
20.5	1859.10	1.6832	0.6239				
21.0	1853.89	1.5839	0.5034				
21.5	1848.46	1.4885	0.6091				
22.0	1842.04	1.3971	0.3429	0.4316	0.1075	1.2344	0.1290
22.5	1835.81	1.6076	0.5044				
23.0	1829.83	1.8382	0.3699	0.4833	0.0939	1.2142	0.1185
23.5	1822.31	1.8671	0.5280				
24.0	1816.49	1.8962	0.3768	0.3533	0.0945	1.2606	0.1220
24.5	1810.24						
25.0	1802.84						
25.5	1794.63						
26.0	1787.23	1.2552	0.2997	0.2306	0.0899	1.2189	0.1165
26.5	1780.83						
27.0	1773.38	1.3138	0.3099	0.2115	0.0957	1.3040	0.1241
27.5	1766.29						
28.0	1758.88	1.8614	0.3952	0.1409	0.1100	1.2591	0.1294
28.5	1751.33						
29.0	1743.73	1.4009	0.3000	0.1601	0.0811	1.1813	0.1079
29.5	1735.40						
30.0	1729.37						
30.5	1722.39						
31.0	1716.21	1.7504	0.3569	0.1739	0.0914	1.1880	0.1154
31.5	1709.46						
32.0	1703.53						
32.5	1695.91						
33.0	1690.28	1.7022	0.3348	0.1729	0.0824	1.5180	0.1249
33.5	1682.92						
34.0	1676.41	1.1842	0.3388	BDL	BDL	1.7224	0.1930
34.5	1669.10						
35.0	1662.07						
35.5	1654.50						
36.0	1647.78						
36.5	1641.23						
37.0	1634.59						
37.5	1628.25						
38.0	1621.29						
38.5	1614.61						
39.0	1609.22						
39.5	1603.68						
40.0	1596.38			BDL	BDL	0.6924	0.1097
40.5	1590.05						

41.0	1584.06
41.5	1577.62
42.0	1570.97
42.5	1563.83
43.0	1555.61
43.5	1549.16
44.0	1542.33
44.5	1535.84
45.0	1528.25
45.5	1521.50
46.0	1514.93
46.5	1508.48
47.0	1500.81
47.5	1494.13
48.0	1488.23
48.5	1480.76
49.0	1473.66
49.5	1466.50
50.0	1459.21
50.5	1451.42
51.0	1443.66
51.5	1438.03
52.0	1431.02
52.5	1425.20
53.0	1418.47
53.5	1411.96
54.0	1403.01
54.5	1395.77
55.0	1388.87
55.5	1381.70
56.0	1375.52
56.5	1367.83
57.0	1360.34
57.5	1352.35
58.0	1344.90
58.5	1337.95
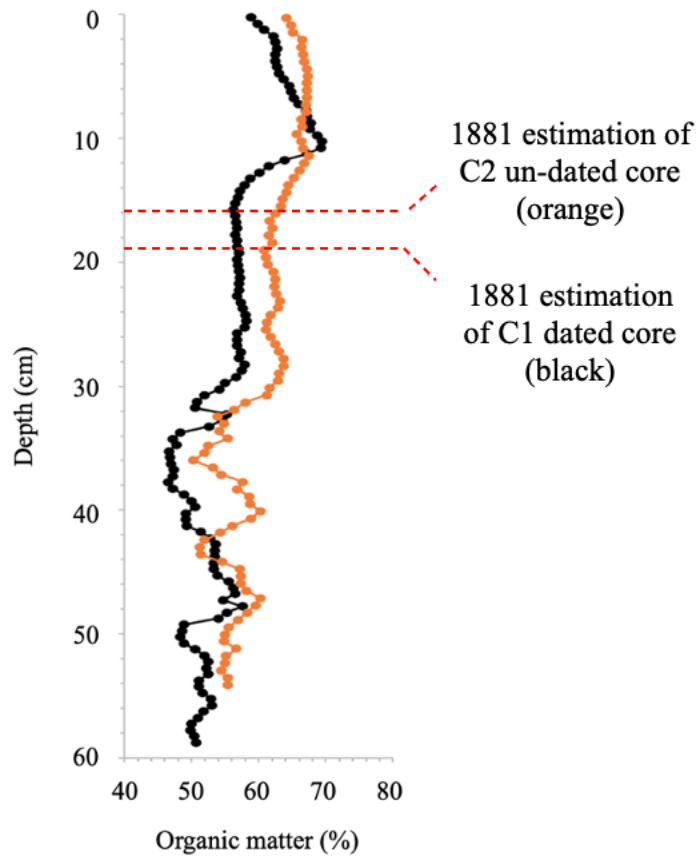
Figure D1. Cross-matching of Smoky 6 core 1 (black) with Smoky 6 core 2 (orange) using organic matter content profiles obtained via LOI. Cross-matching identified a 17% wiggle factor.

Table D3. Smoky 6 C1 CRS chronology dates compared to Smoky 6 C2 wiggle-matched dates that were obtained using a 1.17 depth correction factor (17% wiggle factor) as determined by differences amongst the C1 and C2 LOI profiles.

Top Depth (cm)	C1 CRS Chronology (CE)	C2 Wiggle-matched Chronology for plots (CE)
0.0	2018.15	2018.79
0.5	2016.65	2016.92
1.0	2014.59	2014.92
1.5	2013.21	2012.61
2.0	2010.43	2010.40
2.5	2008.58	2007.52
3.0	2005.79	2003.99
3.5	2002.58	2000.27
4.0	1999.52	1996.21
4.5	1995.97	1992.36
5.0	1992.75	1988.26
5.5	1989.26	1984.09
6.0	1985.73	1979.99
6.5	1982.11	1976.24
7.0	1978.65	1972.50
7.5	1975.61	1967.89
8.0	1972.62	1963.34
8.5	1968.82	1959.59
9.0	1963.86	1954.96
9.5	1961.13	1951.98
10.0	1957.95	1948.66
10.5	1953.25	1942.62
11.0	1952.20	1935.87
11.5	1947.54	1928.50
12.0	1944.04	1922.21
12.5	1938.18	1916.79
13.0	1931.42	1912.03
13.5	1925.44	1907.52
14.0	1920.66	1902.51
14.5	1916.05	1897.84
15.0	1912.21	1893.08
15.5	1908.17	1887.39
16.0	1903.90	1881.28
16.5	1899.74	1874.93
17.0	1896.20	1868.35
17.5	1891.82	1861.75
18.0	1886.57	1855.39
18.5	1881.60	1848.91
19.0	1876.00	1841.81
19.5	1870.46	1834.57

20.0	1864.74	1826.78
20.5	1859.10	1819.07
21.0	1853.89	1811.78
21.5	1848.46	1803.42
22.0	1842.04	1794.36
22.5	1835.81	1785.90
23.0	1829.83	1777.72
23.5	1822.31	1769.28
24.0	1816.49	1760.75
24.5	1810.24	1751.96
25.0	1802.84	1742.84
25.5	1794.63	1734.24
26.0	1787.23	1726.33
26.5	1780.83	1718.66
27.0	1773.38	1711.19
27.5	1766.29	1703.48
28.0	1758.88	1695.80
28.5	1751.33	1687.99
29.0	1743.73	1680.07
29.5	1735.40	1671.94
30.0	1729.37	1663.48
30.5	1722.39	1655.07
31.0	1716.21	1647.00
31.5	1709.46	1639.26
32.0	1703.53	1631.65
32.5	1695.91	1623.86
33.0	1690.28	1616.17
33.5	1682.92	1609.31
34.0	1676.41	1602.24
34.5	1669.10	1594.51
35.0	1662.07	1587.15
35.5	1654.50	1579.82
36.0	1647.78	1572.03
36.5	1641.23	1563.55
37.0	1634.59	1554.92
37.5	1628.25	1546.82
38.0	1621.29	1539.02
38.5	1614.61	1530.83
39.0	1609.22	1522.58
39.5	1603.68	1514.87
40.0	1596.38	1506.82
40.5	1590.05	1498.55
41.0	1584.06	1490.97
41.5	1577.62	1483.10
42.0	1570.97	1474.61
42.5	1563.83	1466.21

43.0	1555.61	1457.52
43.5	1549.16	1448.51
44.0	1542.33	1440.54
44.5	1535.84	1433.19
45.0	1528.25	1425.66
45.5	1521.50	1418.17
46.0	1514.93	1409.51
46.5	1508.48	
47.0	1500.81	
47.5	1494.13	
48.0	1488.23	
48.5	1480.76	
49.0	1473.66	
49.5	1466.50	
50.0	1459.21	
50.5	1451.42	
51.0	1443.66	
51.5	1438.03	
52.0	1431.02	
52.5	1425.20	
53.0	1418.47	
53.5	1411.96	
54.0	1403.01	
54.5	1395.77	
55.0	1388.87	
55.5	1381.70	
56.0	1375.52	
56.5	1367.83	
57.0	1360.34	
57.5	1352.35	
58.0	1344.90	
58.5	1337.95	

Table D4. WAB 3 C2 CRS-based chronology derived from measured ^{210}Pb, ^{137}Cs, and ^{266}Ra (weighted mean of ^{214}Bi and ^{214}Pb) activities (dpm/g). Grey highlighted cells represent dates that were extrapolated using the CRS model, yellow highlighted cells represent interpolated values. BDL = below detection limit, where values are treated as 0.

Top Depth (cm)	CRS Chronology (CE)	CRS Error (± 2 sigma)	^{210}Pb dpm/g	^{210}Pb Error (1 std. dev.) dpm/g	^{137}Cs dpm/g	^{137}Cs Error (1 std. dev.) dpm/g	^{226}Ra dpm/g	^{226}Ra Error (1 std. dev.) dpm/g
0.0	2019.30	0.08	17.3232	1.6487	2.2864	0.2907	-0.0089	0.0091
0.5	2018.95	0.11	24.3390	2.7179	3.5479	0.5037	0.0947	0.0727
1.0	2018.56	0.15	21.7980	2.6368	2.9135	0.4805	1.0414	0.3704
1.5	2018.06	0.22	24.2915	3.9235				
2.0	2017.53	0.25	26.9682	2.9053	3.3545	0.5071	-0.3354	0.4132
2.5	2016.87	0.32	25.9389	3.7513				
3.0	2016.26	0.34	24.9361	2.3731	2.8358	0.3978	-0.2608	0.1265
3.5	2015.62	0.38	25.5786	3.4177				
4.0	2014.85	0.42	26.2320	2.4594	3.8597	0.4629	0.2334	0.0740
4.5	2014.22	0.45	27.7708	3.5294				
5.0	2013.36	0.48	29.3687	2.5313	4.4226	0.4891	-0.4340	0.2075
5.5	2012.54	0.52	32.1094	3.6903				
6.0	2011.39	0.56	35.0156	2.6853	5.3686	0.5357	0.4424	0.1575
6.5	2010.36	0.61	34.7471	3.7254				
7.0	2009.32	0.65	34.4800	2.5823	6.0880	0.5773	-0.0562	0.0534
7.5	2007.98	0.71	34.5050	3.6941				
8.0	2006.57	0.77	34.5300	2.6416	5.8591	0.5704	0.0110	0.0048
8.5	2005.08	0.84	31.7893	3.5961				
9.0	2003.73	0.89	29.1976	2.4401	6.4648	0.6192	-0.0119	0.0110
9.5	2002.03	0.97	29.4987	3.5259				
10.0	2000.40	1.04	29.8019	2.5451	6.4908	0.6301	-0.1258	0.1949
10.5	1998.60	1.12	28.1247	3.3008				
11.0	1997.20	1.18	26.5116	2.1018	6.6780	0.6070	0.0077	0.0109
11.5	1995.71	1.24	24.4088	2.9395				
12.0	1994.22	1.31	22.4203	2.0550	7.0617	0.6506	0.7376	0.2499
12.5	1992.89	1.37	22.1105	3.0494				
13.0	1991.25	1.45	21.8036	2.2529	7.7515	0.7276	-0.1618	0.1461
13.5	1989.65	1.52	20.2060	2.9327				
14.0	1988.54	1.58	18.6884	1.8776	6.7189	0.6232	0.1665	0.5961
14.5	1987.05	1.65	18.9135	2.7169				
15.0	1985.35	1.74	19.1404	1.9637	6.1637	0.5931	-0.0530	0.1252
15.5	1983.84	1.82	17.6121	2.7911				
16.0	1982.32	1.90	16.1673	1.9834	5.4091	0.5551	0.5040	0.3131
16.5	1980.83	1.97	14.2653	2.5894				
17.0	1979.42	2.06	12.5186	1.6647	6.0227	0.5707	-0.0603	0.0619
17.5	1977.84	2.14	12.2246	2.1859				

18.0	1976.24	2.24	11.9353	1.4167	5.6037	0.5176	-0.0421	0.0281
18.5	1974.54	2.34	11.2022	1.8350				
19.0	1972.81	2.47	10.4999	1.1663	5.1335	0.4603	0.3716	0.0926
19.5	1971.25	2.59	9.3913	1.2462	5.1034	0.4727	0.1095	0.1602
20.0	1969.40	2.73	9.1428	1.2044	4.7031	0.4398	1.0442	0.1917
20.5	1967.52	2.88	7.6134	1.0211	4.6930	0.4250	0.3057	0.0806
21.0	1965.66	3.04	9.2711	1.2090	4.0817	0.3939	0.9269	0.2009
21.5	1963.37	3.20	8.3340	1.5644				
22.0	1961.33	3.39	7.4623	0.9927	3.1508	0.3089	0.8460	0.1614
22.5	1959.62	3.54	6.2244	1.2152				
23.0	1957.69	3.74	5.1315	0.7008	2.3524	0.2259	0.3838	0.0870
23.5	1956.22	3.88	4.1058	0.9041				
24.0	1954.62	4.05	3.2267	0.5712	1.5220	0.1607	0.3730	0.0766
24.5	1952.55	4.24	4.1466	0.8905				
25.0	1949.71	4.60	5.2266	0.6832	1.5534	0.1691	0.0194	0.0125
25.5	1947.29	4.87	4.3337	0.9131				
26.0	1944.68	5.21	3.5488	0.6058	1.3343	0.1522	0.0033	0.0026
26.5	1942.18	5.51	3.5553	0.8387				
27.0	1939.32	5.95	3.5617	0.5800	1.1413	0.1369	0.4491	0.0874
27.5	1936.34	6.37	3.4894	0.8069				
28.0	1932.85	7.00	3.4180	0.5610	0.8354	0.1186	0.3078	0.0710
28.5	1929.34	7.52	2.9323	0.7860				
29.0	1925.83	8.18	2.4949	0.5505	0.7199	0.1140	0.4770	0.1883
29.5	1920.90	8.83	2.5049	0.7654				
30.0	1917.32	9.70	2.5150	0.5318	0.7018	0.1111	0.1377	0.0492
30.5	1913.92	10.22	2.0901	0.8754				
31.0	1910.27	10.79	1.7160	0.6954				
31.5	1907.62	10.97	1.3896	0.8273				
32.0	1905.22	11.42	1.1074	0.4481	0.4513	0.0946	0.3325	0.0711
32.5	1903.27	11.45	1.0346	0.7589				
33.0	1901.14	11.54	0.9650	0.6125				
33.5	1898.90	11.09	0.8986	0.7414				
34.0	1896.56	11.15	0.8353	0.4176	0.5309	0.0948	0.1681	0.0653
34.5	1894.39	10.63	0.8618	0.7055				
35.0	1891.29	9.77	0.8889	0.5686				
35.5	1888.22	8.10	0.9165	0.6872				
36.0	1883.36	5.63	0.9448	0.3859	0.3726	0.0797	0.1556	0.0494
36.5	1879.57							
37.0	1875.48							
37.5	1871.90							
38.0	1868.19							
38.5	1858.62							
39.0	1853.62							
39.5	1849.12							
40.0	1844.86		0.3072	0.2748	0.3901	0.0736	0.2925	0.0573
40.5	1840.25							

41.0	1835.94
41.5	1831.32
42.0	1826.65
42.5	1822.08
43.0	1817.11
43.5	1812.64
44.0	1807.75
44.5	1803.39
45.0	1798.76
45.5	1794.46
46.0	1789.76
46.5	1785.29
47.0	1778.65
47.5	1774.22
48.0	1768.46
48.5	1763.41
49.0	1758.99
49.5	1753.56
50.0	1748.11
50.5	1742.69
51.0	1736.53
51.5	1729.72
52.0	1723.37
52.5	1717.38
53.0	1710.61
53.5	1704.30
54.0	1696.95
54.5	1690.39
55.0	1683.48
55.5	1677.35
56.0	1670.31
56.5	1663.13
57.0	1656.72
57.5	1649.36
58.0	1642.13
58.5	1633.67
59.0	1626.54
59.5	1620.06
60.0	1613.23
60.5	1606.22
61.0	1599.97
61.5	1592.90
62.0	1586.47
62.5	1579.70
63.0	1573.30
63.5	1566.49

64.0	1559.39
64.5	1552.78
65.0	1545.46
65.5	1538.27
66.0	1531.01
66.5	1523.98
67.0	1516.19
67.5	1508.82
68.0	1502.22
68.5	1494.03
69.0	1485.68
69.5	1476.22
70.0	1465.31
70.5	1456.96
71.0	1449.77
71.5	1439.73
72.0	1430.22
72.5	1419.02
73.0	1409.55
73.5	1398.40
74.0	1384.34
74.5	1374.68
75.0	1361.46
75.5	1348.35
76.0	1335.19
76.5	1320.35
77.0	1304.29
77.5	1291.32
78.0	1277.07

Table D5. WAB 4 C3 CRS-based chronology derived from measured ^{210}Pb, ^{137}Cs, and ^{266}Ra (weighted mean of ^{214}Bi and ^{214}Pb) activities (dpm/g). Grey highlighted cells represent dates that were extrapolated using the CRS model, yellow highlighted cells represent interpolated values. BDL = below detection limit, where values should be treated as 0.

Top Depth (cm)	CRS Chronology (CE)	CRS Error (± 2 sigma)	^{210}Pb dpm/g	^{210}Pb Error (1 std. dev.) dpm/g	^{137}Cs dpm/g	^{137}Cs Error (1 std. dev.) dpm/g	^{226}Ra dpm/g	^{226}Ra Error (1 std. dev.) dpm/g
0.0	2019.54	0.05	17.5631	2.1882	2.8640	0.3595	0.0989	0.5393
0.5	2019.30	0.09	14.6552	1.9569	2.4314	0.3321	-0.3347	0.1688
1.0	2019.11	0.11	13.1433	1.8374	2.0391	0.3130	-0.5482	0.5290
1.5	2018.85	0.13	16.7405	2.2935	3.1198	0.3885	-0.7954	0.4194
2.0	2018.66	0.14	15.3423	1.8553	2.6209	0.3150	0.4424	0.2326
2.5	2018.37	0.16	15.7905	1.8065	2.6849	0.3078	0.8452	0.2333
3.0	2018.05	0.19	15.9768	2.2555	2.6704	0.3876	0.0933	0.0817
3.5	2017.66	0.22	15.8049	1.7730	2.7495	0.2998	-0.0025	0.0013
4.0	2017.33	0.23	16.8110	1.8386	2.4976	0.3106	-0.2627	0.2287
4.5	2016.98	0.25	15.1686	1.5509	2.4591	0.2630	0.0689	0.0499
5.0	2016.60	0.27	14.5620	1.6014	2.5305	0.2741	0.7812	0.2289
5.5	2016.05	0.30	17.5225	1.6641	2.6031	0.2798	0.7813	0.2314
6.0	2015.50	0.32	16.1870	1.4791	2.3891	0.2459	2.4121	0.3470
6.5	2014.83	0.37	16.7031	2.1482				
7.0	2014.14	0.40	17.2301	1.5579	2.5494	0.2610	1.5442	0.3144
7.5	2013.32	0.46	16.9096	2.0980				
8.0	2012.58	0.49	16.5931	1.4051	2.6408	0.2306	0.1662	0.1999
8.5	2011.69	0.54	16.3697	1.9644				
9.0	2010.80	0.58	16.1483	1.3727	2.5358	0.2334	2.1952	0.3395
9.5	2010.04	0.62	15.7115	1.8433				
10.0	2009.23	0.65	15.2826	1.2301	2.5567	0.2068	2.0190	0.2940
10.5	2008.28	0.69	15.8705	1.7696				
11.0	2007.42	0.72	16.4732	1.2721	2.8130	0.2098	0.2369	0.1123
11.5	2006.46	0.76	16.2318	1.6922				
12.0	2005.40	0.80	15.9928	1.1160	2.6551	0.1857	1.0484	0.2180
12.5	2004.10	0.86	15.5532	1.6579				
13.0	2002.90	0.91	15.1218	1.2260	2.7272	0.2071	1.4256	0.3612
13.5	2001.67	0.96	14.1701	1.6729				
14.0	2000.57	1.01	13.2592	1.1382	3.0181	0.2020	1.6207	0.2458
14.5	1999.22	1.07	13.7448	1.6495				
15.0	1997.88	1.13	14.2421	1.1939	3.2374	0.2116	1.3976	0.2432
15.5	1996.51	1.18	13.1497	1.6151				
16.0	1995.16	1.24	12.1146	1.0877	3.3665	0.1957	1.3050	0.2230
16.5	1993.31	1.32	11.3908	1.5700				
17.0	1991.44	1.40	10.6963	1.1322	3.5438	0.2181	1.6539	0.2312
17.5	1989.80	1.46	10.3743	1.4363				

18.0	1988.16	1.54	10.0588	0.8837	4.0385	0.1778	2.4342	0.2194
18.5	1986.15	1.62	9.3540	1.1448				
19.0	1984.96	1.68	8.6828	0.7278	4.2467	0.1523	1.6130	0.1798
19.5	1983.04	1.75	7.3857	0.9216				
20.0	1981.32	1.84	6.2247	0.5654	4.1357	0.1228	1.5793	0.1366
20.5	1979.42	1.90	5.9566	0.8948				
21.0	1977.87	1.98	5.6963	0.6042	4.4704	0.1283	1.6777	0.1777
21.5	1976.06	2.08	5.2382	0.5075	4.2949	0.1134	1.5138	0.1278
22.0	1973.80	2.19	5.4062	0.5206	4.5350	0.1201	1.6802	0.1326
22.5	1971.33	2.34	5.6889	0.4720	4.7287	0.1069	1.5696	0.1827
23.0	1968.75	2.50	5.5003	0.5518	4.7373	0.1307	1.8383	0.1400
23.5	1966.30	2.65	4.8688	0.4974	4.6964	0.1188	1.7787	0.1310
24.0	1963.51	2.84	5.1456	0.4903	4.7903	0.1165	1.6128	0.1257
24.5	1960.80	3.05	4.7137	0.4505	4.6128	0.1091	1.8808	0.1196
25.0	1959.18	3.16	3.3754	0.4364	4.4710	0.1047	1.8681	0.1285
25.5	1957.07	3.31	3.3641	0.4106	4.1173	0.0947	1.7724	0.1202
26.0	1954.02	3.56	4.2270	0.4428	4.2297	0.1012	1.7205	0.1252
26.5	1951.53	3.66	3.1410	0.5025	4.6153	0.1209	1.6562	0.1382
27.0	1948.80	3.86	3.2706	0.4185	3.6397	0.0935	1.6920	0.1196
27.5	1945.92	4.02	2.8276	0.3857	3.3627	0.0839	1.5764	0.1124
28.0	1944.27	4.11	2.4690	0.3991	2.7792	0.0836	1.5298	0.1431
28.5	1941.98	4.22	2.6268	0.4154	2.4827	0.0840	1.4017	0.1158
29.0	1938.89	4.41	2.7029	0.3631	2.0118	0.0689	1.6342	0.1115
29.5	1936.05	4.54	2.6279	0.4060	1.7764	0.0758	1.5051	0.1142
30.0	1931.57	4.70	2.8523	0.4024	1.8796	0.0751	1.6307	0.1146
30.5	1927.20	3.78	2.5279	0.5560				
31.0	1924.06	3.27	2.2291	0.3838	1.5602	0.0708	1.6311	0.1120
31.5	1920.69		1.8390	0.4668				
32.0	1916.99		1.4973	0.2657	0.8113	0.0447	1.2518	0.0786
32.5	1912.82		1.5161	0.3749				
33.0	1909.33		1.5352	0.2645	0.7911	0.0445	1.2248	0.0787
33.5	1905.18		1.5895	0.3967				
34.0	1901.12		1.6451	0.2957	0.7820	0.0505	1.5318	0.0915
34.5	1896.92							
35.0	1892.41							
35.5	1889.86							
36.0	1885.03		1.4190	0.2534	0.3342	0.0387	1.0564	0.0821
36.5	1880.28							
37.0	1876.33							
37.5	1871.97							
38.0	1867.63		1.5172	0.2740	0.2428	0.0411	1.2236	0.0783
38.5	1863.17							
39.0	1859.04							
39.5	1854.39							
40.0	1850.10							
40.5	1845.26							

41.0	1840.77
41.5	1836.33
42.0	1831.87
42.5	1827.40
43.0	1822.58
43.5	1816.07
44.0	1810.13
44.5	1804.76
45.0	1798.82
45.5	1791.93
46.0	1786.75
46.5	1780.74
47.0	1774.31
47.5	1769.23
48.0	1763.22
48.5	1757.65
49.0	1751.92
49.5	1746.23
50.0	1740.69
50.5	1733.73
51.0	1727.93
51.5	1721.36
52.0	1713.45
52.5	1705.77
53.0	1698.12
53.5	1690.34
54.0	1677.10
54.5	1667.76
55.0	1660.44
55.5	1650.82
56.0	1639.99
56.5	1626.74
57.0	1613.56
57.5	1604.23
58.0	1591.26
58.5	1583.37
59.0	1577.31
59.5	1569.55
60.0	1562.17
60.5	1556.01
61.0	1548.27
61.5	1540.14

Appendix E: Loss-on-ignition raw data

Table E1. Smoky 5 C1 LOI data (% dry weight) including water (% H_2O), organic matter (% OM), mineral matter excluding carbonates (%MM), and carbonate content (%$CaCO_3$).

Top Depth (cm)	% H_2O	% OM	% MM	%$CaCO_3$
0.0	98.84	74.81	18.13	7.05
0.5	96.90	75.00	20.38	4.62
1.0	95.93	75.43	20.24	4.32
1.5	96.91	74.17	20.11	5.72
2.0	95.92	74.71	20.49	4.80
2.5	96.47	76.47	19.97	3.56
3.0	95.83	75.94	20.12	3.94
3.5	94.87	75.16	20.39	4.44
4.0	95.00	76.40	18.63	4.97
4.5	94.92	75.67	20.36	3.97
5.0	94.05	75.84	20.32	3.85
5.5	93.88	75.40	19.57	5.04
6.0	94.15	75.92	20.61	3.47
6.5	94.48	74.19	20.25	5.56
7.0	94.25	73.97	22.30	3.73
7.5	94.77	75.85	20.21	3.94
8.0	94.31	76.90	20.29	2.81
8.5	93.25	74.52	19.52	5.96
9.0	93.87	74.55	20.51	4.95
9.5	94.16	76.22	19.35	4.43
10.0	93.53	75.37	20.25	4.39
10.5	94.47	74.39	20.36	5.25
11.0	93.87	74.32	20.75	4.93
11.5	94.30	75.24	20.93	3.84
12.0	94.54	76.12	21.34	2.54
12.5	94.39	75.69	21.47	2.83
13.0	94.18	74.77	20.21	5.02
13.5	93.82	74.85	19.73	5.42
14.0	93.99	75.24	20.33	4.43
14.5	93.36	75.30	20.25	4.45
15.0	93.15	74.02	19.90	6.08
15.5	92.79	75.13	19.83	5.04
16.0	91.40	75.29	19.73	4.98
16.5	92.33	75.56	20.71	3.73
17.0	90.60	72.86	22.03	5.11
17.5	90.75	74.53	20.03	5.44
18.0	90.83	76.57	19.59	3.84
18.5	90.56	75.15	20.73	4.12
19.0	89.33	76.32	19.96	3.72

19.5	90.06	74.67	21.45	3.89
20.0	89.50	75.64	19.38	4.98
20.5	88.60	76.29	17.85	5.86
21.0	89.23	74.18	21.12	4.70
21.5	88.82	73.57	19.39	7.04
22.0	88.56	74.53	19.43	6.04
22.5	87.37	75.91	19.76	4.33
23.0	88.17	74.56	20.12	5.32
23.5	88.21	75.37	20.42	4.22
24.0	88.40	75.08	20.62	4.29
24.5	88.84	75.23	19.61	5.16
25.0	88.66	75.00	20.08	4.92
25.5	89.17	75.39	20.84	3.77
26.0	88.87	75.50	19.07	5.43
26.5	89.37	75.63	19.59	4.77
27.0	89.83	74.85	20.26	4.89
27.5	89.53	76.11	18.55	5.33
28.0	89.77	76.37	19.39	4.23
28.5	90.19	75.26	19.41	5.33
29.0	90.27	77.31	17.23	5.46
29.5	91.47	77.22	16.88	5.90
30.0	92.19	76.12	18.89	5.00
30.5	90.60	71.05	23.93	5.03
31.0	89.42	70.05	25.58	4.36
31.5	90.58	68.26	27.01	4.73
32.0	91.65	66.92	26.90	6.18
32.5	92.06	66.50	27.98	5.52
33.0	91.28	66.95	28.22	4.84
33.5	92.14	68.61	27.75	3.64
34.0	91.81	69.85	26.39	3.76
34.5	91.52	70.63	24.62	4.76
35.0	91.87	70.50	24.74	4.76
35.5	91.54	69.54	26.66	3.80
36.0	92.31	68.06	27.31	4.63
36.5	91.46	71.67	24.45	3.89
37.0	91.87	69.80	26.50	3.70
37.5	92.32	72.31	21.76	5.93
38.0	92.75	73.10	22.76	4.14
38.5	91.34	71.69	23.96	4.35
39.0	92.42	73.07	22.52	4.41
39.5	92.32	72.75	22.83	4.42
40.0	92.46	72.85	22.40	4.75
40.5	93.70	74.92	21.33	3.74
41.0	92.32	72.01	23.84	4.15
41.5	91.99	72.52	23.44	4.04
42.0	92.62	72.43	21.69	5.88

42.5	91.94	74.16	20.96	4.88
43.0	93.17	74.64	19.93	5.42
43.5	92.63	74.41	21.68	3.91
44.0	93.12	78.49		
44.5	94.02	77.27		
45.0	92.14	76.47	18.66	4.87
45.5	92.83	75.14	20.30	4.56
46.0	92.95	76.02	20.27	3.71
46.5	92.19	74.41	20.57	5.02
47.0	92.55	76.34	19.86	3.81
47.5	92.52	76.23	18.85	4.92
48.0	92.66	73.57	21.61	4.82
48.5	92.61	74.87	21.17	3.96
49.0	93.56	74.17	21.74	4.08
49.5	93.12	77.39	17.09	5.52
50.0	93.59	74.45	20.04	5.51
50.5	92.84	74.66	21.20	4.14
51.0	92.35	72.13	22.30	5.57
51.5	93.61	75.08	20.79	4.13
52.0	93.46	73.93	20.23	5.84
52.5	92.75	72.80	21.03	6.17
53.0	91.49	69.06	27.02	3.91
53.5	92.48	70.80	23.93	5.27
54.0	91.97	69.49	24.91	5.60
54.5	91.63	71.27	23.50	5.23
55.0	92.15	70.12	25.51	4.37
55.5	91.85	68.42	26.05	5.53
56.0	91.59	69.17	23.56	7.26
56.5	91.82	68.65	25.54	5.81
57.0	92.15	69.25	25.48	5.27
57.5	91.96	68.21	27.26	4.53
58.0	91.51	66.75	28.09	5.17
58.5	91.16	66.89	27.59	5.51
59.0	91.13	70.14	24.51	5.35
59.5	91.04	68.64	27.18	4.18
60.0	91.02	65.38	29.09	5.52
60.5	90.88	65.38	29.09	5.52
61.0	90.57	64.39	30.26	5.35
61.5	90.34	67.07	25.51	7.42
62.0	91.01	64.47	28.07	7.46
62.5	91.07	64.92	28.88	6.20
63.0	88.88	62.72	31.67	5.61
63.5	89.66	66.10	28.29	5.60
64.0	90.13	65.38	29.11	5.51
64.5	88.42	62.72	31.51	5.77
65.0	88.13	63.33	32.59	4.08

65.5	87.10	60.57	33.00	6.44
66.0	87.60	61.78	32.49	5.73
66.5	90.79	65.28	28.48	6.24
67.0	89.45	65.54	29.36	5.09
67.5	87.58	58.97	36.15	4.88
68.0	89.74	63.98	30.00	6.02
68.5	87.99	58.58	35.36	6.06
69.0	87.60	58.82	35.62	5.56
69.5	88.51	58.07	35.49	6.44
70.0	86.74	59.12	35.30	5.58
70.5	88.09	59.54	35.28	5.19
71.0	86.66	59.94	35.07	4.99
71.5	87.47	60.12	34.08	5.80
72.0	87.14	59.43	35.65	4.92
72.5	88.13	55.18	38.90	5.91
73.0	88.88	55.42	38.30	6.28
73.5	87.26	60.27	34.55	5.18
74.0	89.27	54.61	39.50	5.89
74.5	89.17	56.95	37.09	5.96
75.0	88.54	50.25	45.36	4.39
75.5	89.59	53.08	40.65	6.28
76.0	88.70	53.31	42.53	4.16
76.5	88.30	53.10	42.12	4.78
77.0	89.58	56.43	38.09	5.48
77.5	89.12	57.17	37.70	5.13
78.0	88.58	59.52	34.69	5.78
78.5	88.14	61.06	34.04	4.90

Table E2. Smoky 6 C1 (C2) LOI data (% dry weight) including water (% H_2O), organic matter (% OM), mineral matter excluding carbonates (%MM), and carbonate content (%$CaCO_3$).

Top Depth (cm)	% H_2O C1	(C2)	% OM C1	(C2)	% MM C1	(C2)	%$CaCO_3$ C1	(C2)
0.0	97.70	(97.39)	58.11	(65.76)	34.08	(27.59)	7.81	(6.65)
0.5	95.69	(95.09)	59.64	(62.55)	32.96	(30.95)	7.40	(6.50)
1.0	95.01	(95.07)	61.62	(66.32)	32.34	(28.44)	6.04	(5.25)
1.5	95.07	(94.78)	61.13	(66.55)	30.68	(28.07)	8.19	(5.38)
2.0	94.85	(95.16)	63.60	(66.67)	31.34	(27.94)	5.06	(5.40)
2.5	94.63	(94.80)	62.47	(65.75)	30.80	(27.29)	6.73	(6.96)
3.0	94.15	(94.58)	62.02	(67.29)	30.44	(26.06)	7.54	(6.65)
3.5	94.22	(94.47)	62.86	(67.19)	31.31	(30.69)	5.83	
4.0	94.49	(94.53)	62.64	(67.19)	30.67	(26.36)	6.69	(6.45)
4.5	94.45	(94.18)	62.86	(67.63)	30.20	(25.53)	6.94	(6.85)
5.0	94.28	(93.97)	63.62	(66.88)	29.75	(26.19)	6.63	(6.93)
5.5	94.68	(94.85)	64.84	(67.15)	28.29	(25.98)	6.87	(6.87)
6.0	94.08	(94.20)	65.08	(67.33)	28.71	(26.39)	6.21	(6.28)
6.5	94.38	(94.48)	64.56	(66.67)	28.83	(26.32)	6.60	(7.02)
7.0	94.94	(94.49)	66.15	(67.14)	27.23	(26.06)	6.62	(6.80)
7.5	94.83	(93.98)	66.96	(65.22)	25.25	(25.91)	7.79	(8.87)
8.0	95.85	(94.63)	68.03	(67.07)	25.43	(25.19)	6.54	(7.74)
8.5	94.67	(93.88)	66.51	(64.59)	27.16	(26.05)	6.33	(9.36)
9.0	94.34	(93.98)	68.55	(67.48)	25.29	(27.51)	6.15	(5.01)
9.5	95.37	(94.28)	67.89	(67.92)	25.72	(26.98)	6.39	(5.11)
10.0	96.05	(94.18)	69.73	(66.99)	23.81	(28.22)	6.46	(4.79)
10.5	95.24	(93.61)	70.44	(65.34)	22.19	(29.24)	7.37	(5.42)
11.0		(92.84)		(65.78)		(28.81)		(5.41)
11.5	93.69	(93.03)	63.10	(64.64)	29.62	(29.35)	7.29	(6.01)
12.0	93.27	(92.01)	60.78	(62.85)	31.55	(31.27)	7.67	(5.88)
12.5	91.05	(92.71)	60.58	(64.91)	32.76	(29.63)	6.66	(5.45)
13.0	91.30	(92.52)	59.03	(62.76)	32.79	(32.04)	8.19	(5.20)
13.5	90.79	(91.12)	56.55	(62.40)	35.43	(32.26)	8.02	(5.34)
14.0	90.56	(90.76)	58.06	(62.16)	34.97	(32.05)	6.97	(5.79)
14.5	89.94	(90.27)	56.80	(60.32)	35.86	(33.96)	7.34	(5.72)
15.0	90.05	(91.35)	55.95	(63.84)	36.22	(31.61)	7.83	(4.55)
15.5	90.48	(89.63)	56.55	(60.32)	34.97	(34.11)	8.48	(5.57)
16.0	90.65	(89.51)	56.05	(61.95)	35.58	(33.89)	8.37	(4.16)
16.5	90.49	(89.34)	56.88	(60.14)	34.18	(35.02)	8.94	(4.84)
17.0	91.37	(88.51)	57.05	(61.00)	33.99	(34.69)	8.96	(4.31)
17.5	90.79	(87.56)	56.51	(63.06)	35.08	(32.61)	8.41	(4.33)
18.0	91.45	(87.31)	55.85	(62.37)	34.09	(33.65)	10.06	(3.98)
18.5	91.51	(87.88)	57.76	(61.85)	34.78	(34.18)	7.47	(3.98)
19.0	91.06	(87.19)	56.63	(62.86)	34.20	(33.03)	9.17	(4.11)
19.5	90.91	(88.42)	56.73	(62.92)	33.66	(32.28)	9.61	(4.80)
20.0	90.18	(87.54)	57.09	(63.64)	35.86	(32.24)	7.06	(4.12)

20.5	90.67	(87.11)	57.11	(62.13)	34.68	(33.69)	8.21	(4.18)
21.0	91.08	(87.30)	56.76	(59.53)	35.10	(37.07)	8.14	(3.40)
21.5	90.84	(87.04)	57.51	(61.82)	35.02	(33.53)	7.48	(4.65)
22.0	89.61	(86.97)	56.81	(62.01)	34.57	(33.74)	8.61	(4.25)
22.5	89.68	(86.03)	56.89	(61.55)	34.54	(33.83)	8.57	(4.62)
23.0	90.03	(87.64)	56.61	(63.99)	34.00	(32.08)	9.39	(3.94)
23.5	87.84	(86.40)	58.28	(63.64)	33.91	(31.90)	7.81	(4.46)
24.0	88.86	(86.68)	57.73	(63.58)	34.79	(29.83)	7.49	
24.5	89.23	(86.98)	58.14	(63.76)	34.16	(31.58)	7.71	(4.65)
25.0	87.94	(87.15)	58.54	(61.82)	33.11	(33.68)	8.34	(4.51)
25.5	86.51	(86.32)	56.96	(63.12)	35.36	(32.67)	7.69	(4.21)
26.0	87.25	(87.43)	54.95	(59.90)	36.94	(36.22)	8.11	(3.88)
26.5	88.95	(87.21)	58.29	(60.52)	33.54	(34.64)	8.17	(4.84)
27.0	87.27	(88.05)	57.14	(53.59)	35.13	(41.21)	7.73	(5.21)
27.5	87.72	(87.68)	56.72	(55.11)	35.48	(39.59)	7.80	(5.31)
28.0	87.81	(88.22)	57.33	(52.88)	34.51	(41.42)	8.16	(5.70)
28.5	86.76	(86.14)	59.59	(56.57)	33.59	(38.01)	6.82	(5.42)
29.0	87.59	(88.74)	55.68	(52.85)	37.46	(41.82)	6.86	(5.32)
29.5	86.60	(89.66)	54.64	(56.60)	38.32	(38.20)	7.04	(5.20)
30.0	87.61	(87.59)	54.72	(48.01)	37.23	(46.58)	8.05	(5.41)
30.5	90.26	(88.34)	53.12	(51.02)	37.81	(44.21)	9.07	(4.78)
31.0	88.16	(88.10)	47.84	(51.82)	43.80	(43.21)	8.36	(4.96)
31.5	89.42	(88.88)	51.51	(56.51)	41.31	(38.70)	7.18	(4.79)
32.0	88.92	(89.12)	52.10	(54.98)	39.44	(40.11)	8.45	(4.91)
32.5		(89.82)		(61.45)		(34.24)		(4.31)
33.0	89.51	(89.28)	49.35	(53.96)	43.28	(40.91)	7.37	(5.13)
33.5	87.73	(90.15)	46.20	(60.27)	45.01	(34.25)	8.79	(5.48)
34.0	88.30	(90.37)	49.24	(61.87)	42.73	(32.50)	8.03	(5.63)
34.5	88.63	(89.37)	46.15	(58.47)	43.62	(37.15)	10.22	(4.39)
35.0	88.43	(89.35)	47.83	(56.26)	44.62	(37.97)	7.54	(5.76)
35.5	88.31	(89.12)	45.76	(53.58)	46.63	(41.54)	7.61	(4.87)
36.0	87.88	(88.83)	46.84	(52.92)	45.70	(41.70)	7.46	(5.37)
36.5	89.39	(88.28)	48.24	(49.41)	42.93	(45.53)	8.83	(5.06)
37.0	88.04	(87.06)	47.08	(51.14)	46.34	(43.82)	6.58	(5.04)
37.5	89.53	(88.42)	46.30	(53.59)	45.70	(42.41)	8.00	(4.00)
38.0	88.49	(88.91)	46.15	(58.79)	45.05	(36.05)	8.80	(5.16)
38.5	88.91	(89.79)	49.02	(59.21)	42.04	(36.44)	8.94	(4.35)
39.0	90.13	(88.49)	51.59	(53.95)	40.32	(39.50)	8.10	(6.55)
39.5	90.21	(89.49)	49.49	(58.96)	42.26	(35.62)	8.24	(5.42)
40.0	88.00	(88.91)	50.59	(61.49)	40.73	(33.30)	8.69	(5.21)
40.5	90.03	(89.58)	47.29	(60.08)	43.71	(34.60)	8.99	(5.32)
41.0	89.24	(88.71)	49.43	(57.01)	41.07	(37.33)	9.49	(5.67)
41.5	88.97	(88.12)	51.02	(57.69)	40.18	(36.90)	8.80	(5.42)
42.0	88.16	(88.45)	53.72	(56.12)	37.74	(37.70)	8.54	(6.18)
42.5	88.32	(85.96)	53.58	(52.77)	38.59	(41.77)	7.83	(5.46)
43.0	87.70	(87.51)	53.42	(56.07)	40.82	(38.27)	5.76	(5.66)

43.5	88.88	(87.75)	53.26	(55.78)	38.61	(38.53)	8.13	(5.70)
44.0	88.14	(87.84)	53.59	(58.08)	38.46	(36.58)	7.95	(5.34)
44.5	88.68	(86.13)	53.21	(51.59)	36.89	(43.43)	9.90	(4.98)
45.0	88.09	(87.23)	53.26	(55.31)	37.89	(39.34)	8.85	(5.34)
45.5	88.01	(87.12)	55.03	(56.39)	37.66	(38.51)	7.30	(5.10)
46.0	88.83	(85.93)	58.26	(54.43)	31.84	(39.74)	9.90	(5.83)
46.5	89.22		55.26		36.05		8.69	
47.0	87.89		55.82		37.30		6.88	
47.5	88.98		52.81		38.30		8.89	
48.0								
48.5	87.36		48.82		42.59		8.59	
49.0	87.83		49.02		42.34		8.64	
49.5	87.82		48.73		42.61		8.66	
50.0	86.84		48.13		43.74		8.13	
50.5	87.82		48.08		42.61		9.31	
51.0	87.16		50.46		43.95		5.60	
51.5	90.11		52.98		37.92		9.10	
52.0	88.44		52.31		39.09		8.60	
52.5	90.11		51.92		38.46		9.62	
53.0	88.56		52.51		39.24		8.25	
53.5	88.92		52.84		37.92		9.23	
54.0	85.64		48.00		43.75		8.25	
54.5	87.94		52.30		39.82		7.88	
55.0	88.29		54.76		34.83		10.41	
55.5	88.20		51.68		40.11		8.21	
56.0	89.20		52.84		38.92		8.23	
56.5	87.53		50.64		41.27		8.09	
57.0	87.56		49.37		41.81		8.82	
57.5	86.92		49.84		41.82		8.34	
58.0	87.12		50.23		40.84		8.93	
58.5	88.57		51.11		39.36		9.53	

Table E3. WAB 3 C2 LOI data (% dry weight) including water (% H_2O), organic matter (% OM), mineral matter excluding carbonates (%MM), and carbonate content (%$CaCO_3$).

Top Depth (cm)	% H_2O	% OM	% MM	%$CaCO_3$
0.0	99.43	72.73	12.85	14.42
0.5	98.97	75.00	22.17	2.83
1.0	98.14	65.79	24.37	9.84
1.5	97.65	61.65	25.05	13.29
2.0	98.10	75.98	24.02	0.00
2.5	97.19	74.27		
3.0	97.73	70.64	23.00	6.37
3.5	97.69	74.47	21.91	3.62
4.0	97.39	73.89	20.08	6.03
4.5	97.77	81.34	13.45	5.21
5.0	97.55	84.12	12.96	2.92
5.5	97.51	83.40	11.97	4.63
6.0	97.41	81.52	13.30	5.17
6.5	97.70	86.86	11.41	1.73
7.0	97.48	85.84	12.96	1.20
7.5	97.15	86.88	9.43	3.69
8.0	96.89	87.14	11.56	1.30
8.5	96.76	81.39	12.66	5.96
9.0	97.15	86.50	11.21	2.30
9.5	96.31	78.55	17.44	4.01
10.0	96.67	71.25	15.72	13.03
10.5	96.38	83.94	15.43	0.62
11.0	97.34	86.67	12.77	0.57
11.5	96.97	85.02	13.45	1.53
12.0	96.56	80.19	10.97	8.83
12.5	97.05	86.28	8.30	5.42
13.0	96.51	84.44	7.70	7.86
13.5	96.90	81.43	9.96	8.61
14.0	97.48	85.49	10.98	3.52
14.5	96.72	85.50	10.42	4.08
15.0	96.91	85.06	10.79	4.15
15.5	96.95	85.17	9.07	5.76
16.0	96.83	84.08	12.50	3.42
16.5	96.76	82.01	16.52	1.47
17.0	96.10	85.06	9.96	4.98
17.5	96.36	87.50	6.13	6.37
18.0	95.95	84.96	12.24	2.81
18.5	96.09	85.11	11.59	3.31
19.0	96.05	86.57	11.40	2.03
19.5	95.81	84.75	9.76	5.49
20.0	95.50	85.53	10.60	3.88

20.5	95.32	84.29	11.34	4.37
21.0	95.19	84.05	11.61	4.34
21.5	95.25	84.68	12.03	3.29
22.0	94.94	85.43	12.86	1.71
22.5	95.29	83.37	12.64	3.99
23.0	94.52	85.80	11.33	2.87
23.5	94.10	85.59	10.33	4.08
24.0	93.14	85.92	11.66	2.42
24.5	93.06	84.03	12.93	3.04
25.0	93.49	85.90	11.66	2.44
25.5	93.43	85.03	10.49	4.49
26.0	92.49	85.40	11.62	2.98
26.5	92.90	86.19	11.93	1.88
27.0	92.67	87.12	11.57	1.31
27.5	93.16	85.66	12.43	1.90
28.0	92.34	86.52	10.73	2.75
28.5	92.17	85.42	12.51	2.08
29.0	90.95	85.76	11.60	2.64
29.5				
30.0	92.70	86.68	11.49	1.83
30.5	91.71	82.61	13.67	3.72
31.0	92.32	83.30	13.50	3.20
31.5	92.59	85.68	10.75	3.57
32.0	91.96	86.61	11.53	1.86
32.5	92.52	86.21	11.66	2.13
33.0	91.86	85.67	13.60	0.73
33.5	92.58	87.48	11.74	0.79
34.0	91.79	86.81	11.49	1.70
34.5	92.47	87.03	9.72	3.26
35.0	91.28	85.74	12.85	1.40
35.5	91.68	86.89	11.15	1.95
36.0	90.40	84.74	11.80	3.46
36.5	90.73	85.43	12.99	1.57
37.0	90.19	85.17	12.79	2.04
37.5	90.48	86.35	11.62	2.03
38.0	90.50	85.71	12.89	1.40
38.5				
39.0	88.01	85.44	11.93	2.63
39.5	88.65	85.63	12.46	1.91
40.0	88.29	85.27	10.47	4.27
40.5	89.20	84.75	12.24	3.01
41.0	88.43	85.37	12.49	2.15
41.5	88.82	85.13	11.76	3.11
42.0	88.15	84.54	11.08	4.38
42.5	88.89	85.81	11.73	2.46
43.0	87.45	83.53	14.39	2.08

43.5	89.51	85.28	11.43	3.29
44.0	88.19	84.71	12.49	2.81
44.5	88.52	85.57	12.13	2.30
45.0	88.51	82.77	12.86	4.37
45.5	89.13	82.83	14.36	2.81
46.0	88.59	81.46	13.85	4.70
46.5	88.24	83.07	13.71	3.22
47.0				
47.5	88.54	80.66	15.21	4.14
48.0	87.23	73.69	19.60	6.71
48.5	87.35	71.70	16.90	11.40
49.0	89.27	66.11	22.47	11.42
49.5	86.71	64.71	22.76	12.52
50.0	86.14	61.30	24.42	14.28
50.5	87.41	56.85	26.28	16.87
51.0	84.92	61.59	24.12	14.29
51.5	83.93	50.62	26.54	22.84
52.0	84.84	60.66	26.16	13.18
52.5	85.32	57.95	25.61	16.44
53.0	84.16	48.47	28.85	22.68
53.5	84.27	45.28	30.33	24.38
54.0	83.82	52.74	27.44	19.83
54.5	83.96	49.17	29.16	21.67
55.0	83.56	42.59	31.31	26.10
55.5	85.37	54.28	27.12	18.60
56.0	84.18	48.00	29.44	22.56
56.5	83.05	45.18	30.61	24.21
57.0	83.45	53.21	25.74	21.05
57.5	84.20	56.13	25.79	18.08
58.0	84.09	40.96	30.75	28.29
58.5	82.34	43.24	30.40	26.36
59.0	83.77	51.57	28.32	20.11
59.5	83.91	52.28	28.97	18.75
60.0	83.87	49.72	30.11	20.16
60.5	83.70	53.12	27.23	19.65
61.0	85.38	60.68	24.90	14.42
61.5	83.90	56.63	26.99	16.38
62.0	85.25	65.53	24.69	9.78
62.5	84.06	60.44	25.31	14.25
63.0	84.45	62.34	25.81	11.86
63.5	84.69	56.04	26.57	17.39
64.0	84.25	59.32	25.85	14.83
64.5	84.11	61.80	24.61	13.59
65.0	83.78	57.77	26.27	15.96
65.5	83.51	57.98	25.94	16.08
66.0	83.75	61.38	24.60	14.03

66.5	83.15	55.34	27.12	17.55
67.0	82.71	56.37	27.75	15.88
67.5	82.59	56.96	26.27	16.78
68.0	83.67	59.74	24.98	15.28
68.5	81.38	53.39	27.40	19.21
69.0	81.95	51.37	27.65	20.98
69.5	81.01	53.80	27.59	18.61
70.0	80.43	52.36	28.04	19.60
70.5	79.98	49.35	29.18	21.47
71.0	79.90	48.67	29.16	22.17
71.5	76.91	46.71	29.71	23.58
72.0	78.40	48.65	29.21	22.14
72.5	78.50	50.49	28.25	21.26
73.0	77.01	41.26	31.11	27.63
73.5	77.41	46.98	29.24	23.78
74.0	75.62	44.04	30.54	25.43
74.5	74.76	40.78	31.40	27.82
75.0	73.58	40.40	31.46	28.14
75.5	69.41	33.12	34.54	32.34
76.0	70.80	34.87	34.07	31.07
76.5	68.56	30.28	35.87	33.84
77.0	68.83	32.36	35.10	32.54
77.5	68.73	31.03	36.00	32.97
78.0	68.55	28.18	36.67	35.14

Table E4. WAB 4 C3 LOI data (% dry weight) including water (% H_2O), organic matter (% OM), mineral matter excluding carbonates (%MM), and carbonate content (%$CaCO_3$).

Top Depth (cm)	% H_2O	% OM	% MM	%$CaCO_3$
0.0	99.59	66.67		
0.5	98.09	57.61	37.96	4.43
1.0	98.25	62.64	32.88	4.48
1.5	98.04	57.45	39.66	2.89
2.0	98.47	58.97	37.54	3.49
2.5	98.09	58.59		
3.0	97.57	61.67	37.20	1.13
3.5	97.04	59.59	36.68	3.73
4.0	97.58	57.72	35.64	6.63
4.5	97.63	60.00	34.33	5.67
5.0	97.40	57.14	35.70	7.16
5.5	96.25	60.73	36.42	2.85
6.0	96.57	57.14	41.24	1.62
6.5	96.16	56.19	38.91	4.91
7.0	95.77	55.87	39.66	4.47
7.5	94.77	56.06	40.33	3.61
8.0	95.71	54.67	39.61	5.72
8.5	95.04	55.33	40.21	4.46
9.0	94.66	54.09	42.21	3.70
9.5	95.72	57.01	39.29	3.69
10.0	95.35	53.78	42.22	4.00
10.5	95.18	55.33	41.89	2.79
11.0	95.57	54.34	42.56	3.11
11.5	95.51	54.75	40.94	4.31
12.0	94.18	53.10	44.08	2.81
12.5	94.50	51.47	44.53	4.00
13.0	94.25	51.86	43.53	4.61
13.5				
14.0	94.41	49.48	45.31	5.21
14.5	93.55	49.06	44.53	6.42
15.0	93.76	49.53	44.96	5.51
15.5	93.74	49.19	45.97	4.84
16.0	93.07	49.28	47.19	3.53
16.5	92.65	46.40	47.80	5.80
17.0	91.55	45.68	49.06	5.25
17.5	92.05	47.52	48.44	4.04
18.0	92.07	47.09	47.40	5.51
18.5	90.62	46.42	47.68	5.90
19.0	94.15	48.26	48.90	2.83
19.5	88.26	48.03	47.08	4.88
20.0	89.15	47.87	47.59	4.54

20.5	88.85	48.63	45.16	6.22
21.0	87.89	49.34	44.84	5.82
21.5	88.12	48.89	45.32	5.79
22.0	87.17	46.17	47.09	6.75
22.5	86.63	46.20	49.25	4.55
23.0	87.12	47.56	47.51	4.93
23.5	86.86	46.70	47.38	5.92
24.0	86.06	49.35	45.56	5.09
24.5	87.40	46.38	47.75	5.87
25.0	86.80	50.98	43.71	5.32
25.5	86.20	49.42	44.06	6.52
26.0	86.70	49.47	43.98	6.54
26.5	83.15	50.18	44.50	5.31
27.0	84.76	51.27	43.21	5.52
27.5	83.58	50.06	44.20	5.74
28.0	86.48	51.19	42.94	5.87
28.5	85.55	50.72	43.54	5.73
29.0				
29.5	84.07	50.25	44.25	5.50
30.0	82.80	50.23	44.27	5.50
30.5	81.92	49.62	45.04	5.34
31.0	83.17	50.90	43.40	5.70
31.5	81.88	52.75	44.94	2.31
32.0	80.72	50.00	44.36	5.64
32.5	78.89	48.91	45.56	5.53
33.0	79.76	48.45	46.11	5.45
33.5	79.52	49.90	44.72	5.37
34.0	80.12	49.59	45.29	5.11
34.5	78.07	50.27	44.51	5.22
35.0	79.32	49.48	44.74	5.78
35.5	85.24	55.51	39.79	4.70
36.0	76.86	46.94	47.51	5.55
36.5	74.63	44.77	49.62	5.61
37.0	77.90	48.76	45.13	6.11
37.5	77.14	52.24	42.47	5.29
38.0	77.29	45.43	48.96	5.61
38.5	76.41	44.71	49.72	5.57
39.0	76.80	46.69	48.63	4.68
39.5	76.09	46.94	48.11	4.95
40.0	75.85	45.18	48.32	6.50
40.5	76.83	47.52	46.85	5.63
41.0	75.70	44.97	48.89	6.14
41.5	76.12	43.31	50.92	5.77
42.0	75.60	45.01	49.78	5.21
42.5	75.91	45.61	48.76	5.63
43.0	75.84	43.68	50.55	5.76

43.5	71.97	43.79	50.61	5.60
44.0	75.37	43.64	50.52	5.84
44.5	73.49	42.86	51.82	5.33
45.0	73.40	39.85	54.03	6.13
45.5	68.02	41.98	52.33	5.69
46.0	73.96	41.79	52.45	5.75
46.5	71.44	38.92	55.58	5.51
47.0	73.54	40.96	52.62	6.42
47.5	74.17	40.28	53.32	6.40
48.0	71.72	37.48	55.83	6.69
48.5	72.73	39.42	54.96	5.62
49.0	72.11	37.90	56.02	6.08
49.5	71.47	37.94	56.15	5.91
50.0	72.63	39.50	54.37	6.14
50.5	71.08	35.56	58.44	6.00
51.0	68.39	33.55	59.56	6.89
51.5	68.65	37.24	56.36	6.39
52.0	65.22	27.62	65.72	6.66
52.5	62.99	23.83	67.66	8.51
53.0	68.88	34.10	59.27	6.63
53.5	66.43	31.36	62.12	6.52
54.0	49.07	14.90	78.44	6.67
54.5	62.56	27.51	65.53	6.96
55.0	64.43	33.56	60.42	6.02
55.5	55.00	15.33	77.14	7.53
56.0	49.24	7.37	84.36	8.26
56.5	59.44	19.01	73.13	7.86
57.0	49.97	4.34	90.79	4.87
57.5	50.32	4.78	88.49	6.73
58.0	51.49	9.14	85.31	5.55
58.5	68.30	40.01	53.98	6.01
59.0	56.30	28.25	67.33	4.42
59.5	68.87	54.47	41.10	4.44
60.0	68.04	59.14	36.39	4.47
60.5	65.20	51.97	42.84	5.19
61.0	61.79	45.26	50.12	4.61
61.5	64.14	50.62	44.25	5.13

Appendix F: Organic carbon and nitrogen elemental and isotope data and cellulose oxygen isotope data, and reconstructed cellulose-inferred lake water oxygen isotope composition and evaporation-to-inflow ratios.

Table F1. Smoky 5 C1.

Top Depth (cm)	% C$_{org}$ (%)	%N (%)	C/N ratio	$\delta^{13}C$ (‰)	$\delta^{15}N$ (‰)	%O (%)	$\delta^{18}O_{cell}$ (‰)	$\delta^{18}O_{lw}$ (‰)	E/I ratio
0.0	42.87	4.10	10.46	-27.47	2.61	32.28	16.83	-10.82	0.40
0.5	43.06	4.13	10.43	-27.55	2.77	30.19	13.96	-13.61	0.24
1.0	42.86	4.08	10.51	-27.50	2.79	27.71	15.24	-12.37	0.31
1.5	43.00	4.08	10.54	-27.47	2.76	32.39	14.98	-12.62	0.30
2.0	43.08	4.12	10.45	-27.67	2.58	31.69	15.39	-12.22	0.32
2.5	42.92	4.12	10.42	-27.58	2.93	29.75	15.45	-12.16	0.32
3.0	43.10	4.09	10.53	-27.59	2.76	29.43	15.50	-12.11	0.33
3.5	43.32	4.14	10.47	-27.51	2.75	30.50	15.30	-12.31	0.31
4.0	42.93	4.04	10.63	-27.40	2.55	30.95	15.86	-11.77	0.35
4.5	43.57	4.08	10.67	-27.35	2.44				
5.0	43.88	4.15	10.57	-27.31	2.81	26.91	14.21	-13.37	0.26
5.5	43.12	4.02	10.72	-27.23	3.03	30.38	16.02	-11.61	0.35
6.0	43.73	4.06	10.78	-27.14	2.67	30.54	15.15	-12.46	0.31
6.5	43.40	4.07	10.67	-27.20	2.47	35.40	13.78	-13.79	0.24
7.0	43.25	4.05	10.68	-27.18	2.49	34.37	16.05	-11.59	0.36
7.5	42.72	4.01	10.66	-27.18	2.41	30.71	15.16	-12.45	0.31
8.0	43.35	4.04	10.73	-27.17	2.86	22.47	15.68	-11.94	0.34
8.5	43.04	4.03	10.67	-27.11	2.83	31.60	15.19	-12.42	0.31
9.0	42.84	4.05	10.57	-27.15	2.63	28.57	15.48	-12.13	0.32
9.5	43.44	4.08	10.65	-27.21	2.61	29.65	15.39	-12.23	0.32
10.0	43.76	4.16	10.52	-27.27	2.61	28.26	15.96	-11.67	0.35
10.5	42.59	4.05	10.51	-27.31	2.71	29.20	13.87	-13.71	0.24
11.0	43.22	4.12	10.49	-27.24	2.75	23.31	13.50	-14.06	0.22
11.5	43.63	4.14	10.55	-27.31	2.62	25.99	16.03	-11.60	0.36
12.0	42.82	4.14	10.35	-27.37	2.74	23.90	14.95	-12.65	0.30
12.5	42.82	4.05	10.56	-27.43	2.35				
13.0	42.81	4.06	10.55	-27.47	2.43	29.20	14.17	-13.41	0.26
13.5	42.87	4.09	10.49	-27.54	2.37	26.94	14.06	-13.52	0.25
14.0	42.95	4.02	10.69	-27.55	2.86	28.37	15.35	-12.26	0.32
14.5	42.76	4.02	10.62	-27.52	3.01	25.89	14.78	-12.82	0.29
15.0	42.85	4.04	10.61	-27.53	2.90	27.45	14.74	-12.86	0.28
15.5	43.34	4.09	10.60	-27.51	3.13	26.49	15.18	-12.43	0.31
16.0	43.44	4.06	10.71	-27.23	3.00	28.50	15.57	-12.05	0.33
16.5	43.43	4.07	10.68	-27.30	2.95	34.06	15.39	-12.23	0.32
17.0	43.87	4.10	10.69	-27.17	2.99	27.54	14.76	-12.83	0.29
17.5	44.16	4.06	10.87			26.01	14.40	-13.19	0.27
18.0	43.66	4.08	10.71	-27.31	2.78	26.13	14.64	-12.95	0.28

18.5	43.81	4.09	10.70	-27.17	2.81	29.62	15.60	-12.03	0.33
19.0	44.19	4.09	10.80	-27.23	3.19	24.30	14.98	-12.63	0.30
19.5	43.80	4.11	10.65	-27.12	3.29	26.93	16.20	-11.44	0.37
20.0	44.24	4.20	10.53	-27.05	3.17	29.71	14.36	-13.23	0.26
20.5	44.44	4.23	10.51	-27.08	2.94	28.03	14.74	-12.86	0.28
21.0	44.03	4.18	10.53	-27.05	3.24	28.33	15.27	-12.34	0.31
21.5	44.35	4.25	10.44	-27.07	3.07	29.63	15.29	-12.32	0.31
22.0	44.04	4.14	10.64	-27.23	2.90	23.11	13.60	-13.97	0.23
22.5	43.92	4.13	10.62	-27.20	2.99	21.44	13.58	-13.98	0.23
23.0	44.28	4.13	10.71	-27.18	3.26	26.08	14.38	-13.21	0.27
23.5	44.14	4.11	10.73	-27.21	3.19	25.09	13.94	-13.64	0.24
24.0	44.61	4.09	10.91	-27.17	3.07	30.53	16.40	-11.25	0.38
24.5	44.78	4.07	11.02	-27.13	2.74	27.79	14.57	-13.02	0.28
25.0	44.65	4.05	11.02	-27.12	2.92	25.05	15.21	-12.40	0.31
25.5	43.88	3.95	11.11	-27.15	3.28	32.17	14.98	-12.62	0.30
26.0	45.30	4.11	11.03	-27.26	3.10	31.02	14.88	-12.72	0.29
26.5	44.86	4.06	11.06	-27.39	3.21	32.81	15.16	-12.45	0.31
27.0	45.05	4.08	11.05	-27.54	2.67	29.63	14.52	-13.07	0.27
27.5	45.05	4.15	10.86	-27.50	3.32	29.57	14.80	-12.80	0.29
28.0	44.46	4.03	11.04	-27.65	3.33	29.45	14.68	-12.92	0.28
28.5	44.97	4.07	11.04	-27.58	3.27	27.78	14.58	-13.01	0.28
29.0	45.86	4.21	10.88	-27.24	2.92	29.57	15.21	-12.40	0.31
29.5	45.71	4.21	10.86	-26.97	2.69	30.55	14.83	-12.77	0.29
30.0	44.93	4.16	10.80	-26.67	2.89	28.16	14.86	-12.74	0.29
30.5	42.82	3.91	10.96	-26.24	3.16	28.61	14.97	-12.64	0.30
31.0	41.01	3.67	11.16	-26.68	3.63	22.45	14.89	-12.72	0.29
31.5	39.78	3.55	11.21	-26.58	3.49	28.30	14.35	-13.24	0.26
32.0	39.71	3.49	11.38	-26.81	3.11	23.66	14.12	-13.46	0.25
32.5	39.95	3.52	11.33	-26.84	3.17	29.75	14.38	-13.21	0.27
33.0	40.54	3.60	11.25	-26.85	3.34	22.61	12.70	-14.85	0.18
33.5	40.77	3.61	11.30	-26.90	3.69	21.13	12.98	-14.57	0.20
34.0	40.86	3.69	11.08	-26.90	3.54	19.59	12.43	-15.11	0.17
34.5	41.19	3.67	11.21	-26.79	3.31	16.86	12.89	-14.66	0.19
35.0	41.51	3.75	11.07	-26.89	3.46	22.41	13.12	-14.44	0.20
35.5	41.53	3.78	10.98	-26.84	3.83	21.37	13.82	-13.76	0.24
36.0	41.23	3.74	11.02	-26.75	3.57	26.18	14.14	-13.44	0.25
36.5	41.63	3.82	10.90	-26.64	3.62	24.77	14.21	-13.37	0.26
37.0	42.61	3.90	10.93	-26.68	3.53	26.54	14.41	-13.18	0.27
37.5	42.49	3.88	10.94	-26.44	3.19	28.49	14.37	-13.22	0.27
38.0	42.37	3.90	10.85	-26.50	3.33	22.88	14.19	-13.40	0.26
38.5	42.79	3.93	10.88	-26.23	3.31	24.85	14.73	-12.87	0.28
39.0	43.15	4.00	10.78	-26.07	3.13	26.23	14.32	-13.26	0.26
39.5	42.42	3.92	10.82	-26.06	3.10	24.55	14.55	-13.04	0.27
40.0	43.61	4.03	10.83	-25.97	3.12	21.80	13.12	-14.43	0.20
40.5	42.71	3.96	10.78	-26.12	3.45	24.84	15.40	-12.22	0.32
41.0	43.00	4.03	10.68	-25.93	3.65	25.33	15.06	-12.55	0.30

41.5	41.38	3.92	10.57	-25.77	3.54	26.66	14.98	-12.62	0.30
42.0	43.34	4.01	10.80	-25.79	3.34	27.29	15.57	-12.05	0.33
42.5	43.42	4.18	10.39	-25.24	2.90	23.57	14.71	-12.88	0.28
43.0	42.70	4.19	10.20	-24.88	3.01	29.15	15.69	-11.93	0.34
43.5	43.91	4.35	10.11	-24.58	2.97	26.04	15.55	-12.07	0.33
44.0	43.64	4.31	10.13	-24.79	2.66	26.56	15.45	-12.17	0.32
44.5	44.84	4.46	10.05	-24.04	2.60	26.54	15.36	-12.25	0.32
45.0	45.13	4.57	9.88	-23.95	2.12	25.66	15.91	-11.72	0.35
45.5	44.70	4.45	10.04	-24.28	2.40	28.00	15.57	-12.05	0.33
46.0	44.37	4.44	10.00	-24.35	2.47	25.48	15.47	-12.15	0.32
46.5	44.69	4.47	10.00	-24.30	2.59	30.90	15.23	-12.38	0.31
47.0	44.98	4.45	10.11	-24.42	2.58	25.54	15.07	-12.54	0.30
47.5	44.41	4.39	10.12	-24.40	2.48	25.35	15.16	-12.45	0.31
48.0	44.59	4.39	10.16	-24.55	2.59	22.27	14.55	-13.04	0.27
48.5	44.37	4.34	10.23	-24.65	2.42	25.63	14.33	-13.26	0.26
49.0	43.70	4.37	10.00	-24.46	2.68	28.87	14.66	-12.94	0.28
49.5	44.54	4.42	10.07	-24.26	2.42	23.83	14.91	-12.69	0.29
50.0	44.34	4.33	10.24	-24.23	2.43	27.36	13.76	-13.81	0.23
50.5	44.46	4.39	10.14	-24.21	2.35	29.18	15.56	-12.06	0.33
51.0	43.39	4.34	10.00	-24.75	2.26	18.21	14.32	-13.27	0.26
51.5	43.92	4.38	10.03	-24.72	2.58	26.60	15.95	-11.68	0.35
52.0	42.14	4.18	10.09	-24.58	2.81	21.71	14.60	-13.00	0.28
52.5	43.99	4.42	9.96	-24.64	2.43	25.11	15.78	-11.85	0.34
53.0	42.98	4.26	10.08	-25.20	2.54	22.91	14.56	-13.03	0.28
53.5	42.50	4.19	10.14	-25.18	2.77	29.87	15.02	-12.58	0.30
54.0	42.16	4.15	10.16	-25.42	2.96	26.27	13.81	-13.77	0.24
54.5	42.12	4.10	10.26	-25.58	2.92	25.03	13.97	-13.61	0.24
55.0	40.43	3.89	10.39	-25.71	2.88	20.22	14.88	-12.72	0.29
55.5	39.94	3.89	10.28	-25.71	2.66	21.76	14.57	-13.03	0.28
56.0	40.77	3.94	10.35	-25.48	2.77	22.88	14.59	-13.00	0.28
56.5	40.69	3.97	10.25	-25.47	2.70	24.51	14.51	-13.08	0.27
57.0	40.20	3.94	10.21	-25.97	3.00	24.24	15.19	-12.42	0.31
57.5	40.54	3.96	10.24	-26.12	3.07	23.89	14.77	-12.83	0.29
58.0	40.74	3.94	10.34	-26.06	3.13	23.65	14.98	-12.63	0.30
58.5	39.55	3.74	10.57	-26.54	3.07	22.40	15.14	-12.47	0.31
59.0	39.59	3.78	10.49	-26.60	3.11	22.98	14.81	-12.79	0.29
59.5	40.43	3.87	10.46	-26.13	3.23	22.46	11.5	-16.01	0.13
60.0	38.33	3.66	10.47	-26.39	3.22	25.38	14.21	-13.37	0.26
60.5	38.69	3.63	10.66	-26.45	3.05	21.14	14.59	-13.01	0.28
61.0	38.88	3.72	10.45	-26.15	2.88	24.36	14.89	-12.71	0.29
61.5	38.20	3.66	10.43	-25.95	2.92	21.72	14.49	-13.10	0.27
62.0	37.76	3.61	10.47	-25.80	2.97	23.51	14.50	-13.09	0.27
62.5	38.47	3.67	10.47	-25.93	3.05	23.18	15.05	-12.56	0.30
63.0	37.59	3.61	10.41	-25.80	2.54	22.39	12.84	-14.71	0.19
63.5	37.23	3.60	10.33	-25.72	2.89	27.56	14.07	-13.51	0.25
64.0	38.34	3.72	10.31	-25.82	3.33	20.18	13.38	-14.18	0.22

64.5	37.51	3.63	10.33	-25.77	3.18	22.79	12.75	-14.79	0.19
65.0	35.75	3.43	10.42	-25.72	2.92	24.47	11.62	-15.89	0.14
65.5	36.38	3.51	10.38	-25.69	2.63	17.73	10.48	-17.00	0.09
66.0	36.45	3.49	10.43	-25.75	3.10	18.17	11.25	-16.25	0.12
66.5	36.74	3.53	10.42	-25.78	3.23	25.69	11.91	-15.61	0.15
67.0	37.63	3.63	10.36	-25.73	3.20	24.26	11.39	-16.12	0.13
67.5	34.75	3.29	10.55	-25.82	3.00	20.16	11.52	-15.99	0.13
68.0	36.09	3.47	10.39	-25.72	2.84	23.12	12.59	-14.95	0.18
68.5	33.94	3.25	10.44	-25.87	3.43	21.78	10.74	-16.75	0.10
69.0	34.02	3.28	10.38	-25.88	3.38	24.93	11.97	-15.56	0.15
69.5	34.36	3.30	10.42	-25.93	3.16	21.22	11.38	-16.13	0.13
70.0	33.44	3.19	10.48	-25.91	3.37	15.33	10.12	-17.36	0.08
70.5	34.08	3.26	10.44	-25.88	2.80	19.00	10.95	-16.55	0.11
71.0	34.44	3.30	10.42	-25.93	3.21	20.13	11.04	-16.46	0.11
71.5	34.17	3.30	10.35	-25.96	3.27	19.76	12.49	-15.05	0.17
72.0	33.55	3.18	10.55	-26.01	3.45	18.50	11.80	-15.72	0.14
72.5	33.39	3.11	10.72	-26.16	3.31	20.24	11.18	-16.32	0.12
73.0	32.83	3.12	10.53	-26.16	3.43	18.27	11.26	-16.25	0.12
73.5	32.52	3.10	10.49	-25.75	3.62	19.68	10.42	-17.06	0.09
74.0	31.69	3.01	10.54	-25.87	3.45	21.22	12.36	-15.18	0.17
74.5	31.86	3.05	10.44	-25.68	3.54	16.57	10.9	-16.59	0.11
75.0	31.41	3.01	10.44	-25.38	3.65	17.19	10.72	-16.77	0.10
75.5	31.31	3.01	10.39	-25.26	3.27	17.44	10.60	-16.88	0.10
76.0	31.19	3.01	10.35	-25.40	3.63	17.75	10.97	-16.53	0.11
76.5	31.36	3.05	10.28	-25.27	3.44	17.76	11.13	-16.37	0.12
77.0	31.94	3.14	10.16	-24.87	3.06	17.42	11.14	-16.36	0.12
77.5	32.56	3.22	10.13	-24.80	3.23	18.18	11.54	-15.97	0.13
78.0	33.13	3.26	10.17	-24.87	2.90	19.20	11.53	-15.98	0.13
78.5	32.90	3.24	10.16	-24.80	3.39	20.59	11.81	-15.70	0.15

Table F2. Smoky 6 C2.

Top Depth (cm)	% C$_{org}$ (%)	%N (%)	C/N ratio	δ^{13}C (‰)	δ^{15}N (‰)	%O (%)	δ^{18}O$_{cell}$ (‰)	δ^{18}O$_{lw}$ (‰)	E/I ratio
0.0	35.36	3.03	11.68	-30.15	2.69	24.42	14.72	-12.88	0.28
0.5	36.65	3.16	11.61	-30.17	2.75	32.66	16.17	-11.47	0.36
1.0	37.06	3.19	11.60	-29.90	2.84	32.79	16.36	-11.28	0.37
1.5	37.42	3.22	11.63	-29.92	2.82	43.50	16.99	-10.67	0.41
2.0	37.47	3.23	11.61	-29.88	2.68	43.59	17.42	-10.25	0.44
2.5	38.32	3.27	11.70	-29.71	2.82	37.24	17.22	-10.44	0.43
3.0	37.37	3.16	11.81	-29.74	2.66	38.90	17.28	-10.39	0.43
3.5	38.52	3.30	11.69	-29.63	2.24	37.66	16.31	-11.33	0.37
4.0	38.56	3.30	11.68	-29.71	2.64	38.60	17.49	-10.18	0.44
4.5	39.41	3.34	11.81	-29.67	2.32	30.74	16.94	-10.72	0.41
5.0	38.89	3.31	11.75	-29.68	2.61	35.31	16.53	-11.12	0.38
5.5	38.67	3.33	11.60	-29.61	2.49	36.49	16.17	-11.47	0.36
6.0	39.26	3.36	11.68	-29.63	2.62	31.48	15.42	-12.20	0.32
6.5	39.19	3.37	11.64	-29.60	2.75	38.85	15.26	-12.35	0.31
7.0	38.66	3.31	11.69	-29.70	2.52	37.79	16.66	-10.99	0.39
7.5	39.27	3.37	11.66	-29.60	2.46				
8.0	39.09	3.33	11.75	-29.60	2.12	26.45	15.36	-12.25	0.32
8.5	34.88	2.97	11.76	-29.74	2.13	38.21	16.49	-11.16	0.38
9.0	39.22	3.36	11.67	-29.56	2.44	35.08	15.99	-11.64	0.35
9.5	39.32	3.35	11.74	-29.43	2.24	35.81	16.04	-11.59	0.36
10.0	37.49	3.23	11.59	-29.22	2.92	36.75	16.68	-10.97	0.39
10.5	38.56	3.30	11.68	-29.18	2.50	30.61	15.86	-11.77	0.35
11.0	36.57	3.14	11.65	-29.18	2.44	26.11	15.74	-11.88	0.34
11.5	37.52	3.24	11.59	-29.00	2.66	26.66	15.52	-12.10	0.33
12.0	37.09	3.22	11.52	-29.00	2.75	31.24	15.70	-11.92	0.34
12.5	37.66	3.31	11.37	-29.11	2.71	26.92	15.18	-12.43	0.31
13.0	36.92	3.22	11.45	-28.88	3.00	23.90	16.02	-11.61	0.35
13.5	36.50	3.17	11.50	-28.85	2.86	26.34	16.10	-11.53	0.36
14.0	36.16	3.13	11.55	-28.81	2.68	28.69	16.12	-11.52	0.36
14.5	35.15	3.02	11.64	-28.75	2.95	30.01	15.44	-12.18	0.32
15.0	34.06	2.86	11.90	-28.46	3.13	31.00	15.06	-12.55	0.30
15.5	36.13	3.08	11.74	-28.42	2.28	21.44	15.43	-12.19	0.32
16.0	36.20	3.10	11.67	-28.31	2.80	25.92	15.08	-12.53	0.30
16.5	37.09	3.17	11.71	-28.24	2.75	38.07	15.64	-11.98	0.33
17.0	36.87	3.16	11.68	-28.14	2.62	35.94	15.46	-12.16	0.32
17.5	36.48	3.13	11.67	-28.29	2.64	35.33	16.09	-11.54	0.36
18.0	36.71	3.14	11.67	-28.25	2.89	24.28	15.35	-12.26	0.32
18.5	36.99	3.20	11.54	-28.28	3.17	33.08	15.55	-12.07	0.33
19.0	36.78	3.13	11.75	-28.18	2.63	33.83	15.04	-12.57	0.30
19.5	36.72	3.14	11.69	-28.27	2.87	30.44	14.97	-12.63	0.30
20.0	37.17	3.19	11.66	-28.29	3.02	27.64	14.48	-13.11	0.27

20.5	37.20	3.17	11.75	-28.22	2.65	30.76	14.62	-12.97	0.28
21.0	37.09	3.20	11.58	-28.25	2.92	33.41	13.92	-13.66	0.24
21.5	37.53	3.23	11.61	-28.31	2.98	34.23	14.58	-13.01	0.28
22.0	36.64	3.13	11.70	-28.31	2.80	25.38	14.28	-13.31	0.26
22.5	37.44	3.20	11.70	-28.21	2.90	35.40	14.82	-12.78	0.29
23.0	36.31	3.10	11.72	-28.29	2.79	33.37	13.95	-13.63	0.24
23.5	36.96	3.16	11.70	-28.35	2.87	30.67	13.98	-13.60	0.25
24.0	36.57	3.15	11.61	-28.25	2.93	29.14	14.00	-13.58	0.25
24.5	34.71	2.91	11.91	-28.27	2.43	22.20	14.87	-12.73	0.29
25.0	36.14	3.11	11.63	-28.41	3.01	28.87	14.54	-13.05	0.27
25.5	35.48	2.97	11.94	-28.28	2.53	31.00	14.46	-13.13	0.27
26.0	33.71	2.84	11.87	-28.56	2.97	20.66	15.03	-12.58	0.30
26.5	33.33	2.82	11.82	-28.44	2.96	32.14	14.07	-13.51	0.25
27.0	34.55	2.89	11.93	-28.47	2.69	25.87	14.98	-12.62	0.30
27.5	32.80	2.75	11.93	-28.47	3.43	25.98	14.41	-13.18	0.27
28.0	32.46	2.70	12.01	-28.49	3.18	25.66	14.26	-13.33	0.26
28.5	32.23	2.70	11.93	-28.42	2.91	25.58	14.66	-12.94	0.28
29.0	31.97	2.65	12.06	-28.31	3.14	33.21	14.70	-12.90	0.28
29.5	31.91	2.67	11.97	-28.34	3.25	25.45	15.01	-12.60	0.30
30.0	30.50	2.60	11.75	-28.62	3.88	26.47	14.79	-12.81	0.29
30.5	30.87	2.55	12.10	-28.77	3.31	25.37	14.09	-13.49	0.25
31.0	30.81	2.49	12.35	-28.85	3.43	24.81	14.62	-12.97	0.28
31.5	33.92	2.72	12.46	-29.08	3.03	28.33	13.51	-14.05	0.22
32.0	33.67	2.72	12.37	-29.17	3.59	25.46	14.72	-12.88	0.28
32.5	30.76	2.49	12.37	-28.86	3.64	26.82	14.94	-12.66	0.29
33.0	32.55	2.66	12.22	-28.57	3.23	24.44	12.56	-14.98	0.18
33.5	35.31	2.86	12.35	-29.07	3.69	26.66	13.74	-13.83	0.23
34.0	34.52	2.83	12.20	-28.99	3.49	27.44	13.64	-13.93	0.23
34.5	33.87	2.77	12.21	-28.86	3.33	28.40	14.56	-13.03	0.27
35.0	33.30	2.72	12.23	-29.07	3.37	23.14	13.91	-13.67	0.24
35.5	32.73	2.73	12.01	-28.83	3.63	22.75	13.47	-14.09	0.22
36.0	31.74	2.66	11.91	-28.73	3.40	17.82	13.95	-13.63	0.24
36.5	33.42	2.73	12.23	-29.01	3.74	22.16	13.28	-14.28	0.21
37.0	31.87	2.62	12.15	-29.02	3.76	26.75	12.98	-14.57	0.20
37.5	34.14	2.78	12.28	-29.02	3.33	29.97	12.47	-15.07	0.17
38.0	34.01	2.79	12.18	-29.00	3.44	30.13	12.78	-14.77	0.19
38.5	35.46	2.87	12.38	-28.97	3.35	29.53	12.90	-14.65	0.19
39.0	34.98	2.87	12.19	-28.95	3.53	29.51	12.58	-14.96	0.18
39.5	34.90	2.92	11.97	-28.93	4.11	27.83	13.43	-14.13	0.22
40.0	35.45	2.96	11.99	-28.91	3.97	25.50	13.24	-14.32	0.21
40.5	35.39	2.90	12.21	-28.89	3.93	28.25	13.43	-14.13	0.22
41.0	34.77	2.92	11.92	-28.85	3.85	21.50	13.70	-13.87	0.23
41.5	34.25	2.87	11.95	-28.67	3.82	24.28	13.05	-14.50	0.20
42.0	34.77	2.95	11.78	-28.70	3.98	25.55	12.91	-14.64	0.19
42.5	30.36	2.51	12.12	-28.68	3.95	26.81	11.46	-16.05	0.13
43.0	34.34	2.88	11.92	-28.56	4.14	19.62	12.73	-14.81	0.19

43.5	33.31	2.74	12.16	-28.74	3.55	25.05	11.75	-15.77	0.14
44.0	33.34	2.75	12.12	-28.71	3.91	27.00	12.77	-14.78	0.19
44.5	32.90	2.70	12.16	-28.74	3.41	26.71	11.39	-16.12	0.13
45.0	31.89	2.59	12.30	-28.69	3.97	19.21	13.71	-13.86	0.23
45.5	33.54	2.78	12.05	-28.55	3.66	27.16	13.91	-13.67	0.24
46.0	33.52	2.78	12.05	-28.70	3.79	25.74	11.96	-15.56	0.15

Table F3. WAB 3 C2.

Top Depth (cm)	% C_{org} (%)	%N (%)	C/N ratio	$\delta^{13}C$ (‰)	$\delta^{15}N$ (‰)	%O (%)	$\delta^{18}O_{cell}$ (‰)	$\delta^{18}O_{lw}$ (‰)	E/I ratio
0.0	39.92	4.51	8.85	-22.14	0.49	36.53	18.12	-9.57	0.49
0.5	38.98	4.46	8.74	-22.82	1.29	44.93	18.54	-9.16	0.51
1.0	38.24	4.29	8.92	-22.60	1.01	48.89	17.46	-10.21	0.44
1.5	36.94	3.92	9.41	-22.86	1.85	39.18	17.98	-9.71	0.48
2.0									
2.5	36.70	3.99	9.19	-22.68	1.36	43.50	18.05	-9.64	0.48
3.0	37.81	4.27	8.85	-22.85	0.92	42.86	18.52	-9.18	0.51
3.5	36.69	3.84	9.57	-23.11	1.28	32.46	18.52	-9.18	0.51
4.0	49.65	4.78	10.39	-23.32	1.20	45.08	20.12	-7.63	0.63
4.5	49.19	4.45	11.06	-23.67	1.70	36.06	17.46	-10.21	0.44
5.0	50.35	4.61	10.92	-23.97	0.97	40.44	19.45	-8.28	0.58
5.5	50.36	4.36	11.55	-24.20	1.52	37.69	18.60	-9.10	0.52
6.0	51.74	4.56	11.34	-24.47	1.08	41.49	18.14	-9.55	0.49
6.5	47.90	4.07	11.78	-24.68	1.31	40.93	18.58	-9.12	0.52
7.0	51.41	4.38	11.73	-25.06	0.85	38.68	18.08	-9.61	0.48
7.5	51.18	4.27	12.00	-25.22	1.78	33.66	17.12	-10.54	0.42
8.0	52.13	4.39	11.87	-25.17	1.01	36.26	18.12	-9.57	0.49
8.5	51.42	4.23	12.16	-25.15	1.58	33.64	17.48	-10.19	0.44
9.0	52.55	4.44	11.83	-25.18	1.45	37.39	18.31	-9.39	0.50
9.5	50.50	4.21	11.99	-24.83	1.33	35.53	17.89	-9.79	0.47
10.0	52.03	4.49	11.59	-24.86	1.42	37.26	17.37	-10.30	0.44
10.5	49.22	4.21	11.68	-24.63	1.86	33.18	16.76	-10.89	0.40
11.0	51.16	4.41	11.59	-24.66	1.00	39.03	16.99	-10.67	0.41
11.5	49.73	4.19	11.86	-24.40	1.58	33.02	16.56	-11.09	0.39
12.0	50.72	4.39	11.55	-24.59	1.15	34.61	16.56	-11.08	0.39
12.5	50.14	4.23	11.85	-24.64	1.87	30.75	16.41	-11.23	0.38
13.0	51.34	4.33	11.84	-24.66	1.57				
13.5	50.21	4.23	11.86	-24.43	1.67	36.58	17.19	-10.47	0.43
14.0	50.93	4.34	11.74	-24.34	1.57	35.09	16.38	-11.26	0.38
14.5	49.74	4.19	11.87	-24.19	1.11	35.73	17.10	-10.57	0.42
15.0	50.49	4.36	11.58	-24.12	1.49	39.27	17.89	-9.79	0.47
15.5	49.53	4.35	11.38	-24.03	1.62	39.38	17.24	-10.43	0.43
16.0	50.43	4.35	11.58	-24.21	1.52	35.83	16.96	-10.69	0.41
16.5	50.02	4.28	11.68	-24.00	1.74	36.23	17.39	-10.28	0.44
17.0	50.96	4.33	11.76	-23.92	1.79	40.21	18.08	-9.60	0.48
17.5									
18.0	50.88	4.22	12.06	-23.94	1.56	37.12	16.92	-10.74	0.41
18.5	51.18	4.20	12.18	-23.89	1.60	39.94	18.04	-9.64	0.48
19.0	51.86	4.16	12.47	-23.84	1.49	34.48	17.41	-10.26	0.44
19.5	51.52	4.10	12.55	-23.72	1.65	36.36	17.14	-10.52	0.42
20.0	51.11	4.10	12.47	-23.52	1.59	35.61	17.69	-9.98	0.46

20.5	51.51	4.23	12.17	-23.48	1.86	40.44	17.69	-9.99	0.46
21.0	51.22	4.07	12.57	-23.58	1.91	32.20	17.06	-10.60	0.42
21.5	50.65	4.01	12.63	-23.37	1.64	29.46	17.97	-9.72	0.48
22.0	50.92	3.92	13.00	-23.31	1.58	38.06	17.85	-9.83	0.47
22.5	51.00	3.80	13.41	-23.54	1.69	28.97	17.95	-9.73	0.47
23.0	51.68	3.78	13.67	-23.48	1.73	33.60	17.43	-10.24	0.44
23.5	50.31	3.77	13.35	-23.56	1.96	28.19	16.38	-11.26	0.38
24.0	51.12	3.73	13.72	-23.53	1.91	33.25	17.02	-10.63	0.41
24.5	50.40	3.65	13.82	-23.58	2.03	28.95	16.33	-11.31	0.37
25.0	51.45	3.78	13.61	-23.78	1.78	37.14	17.37	-10.30	0.44
25.5	51.03	3.70	13.80	-23.76	1.52	31.35	16.78	-10.87	0.40
26.0	51.11	3.71	13.76	-23.75	1.89	38.25	17.45	-10.22	0.44
26.5	50.54	3.62	13.95	-23.59	1.90	34.18	15.91	-11.72	0.35
27.0	51.00	3.72	13.72	-23.97	2.02	34.50	17.02	-10.64	0.41
27.5	50.81	3.71	13.70	-23.89	1.88	32.83	16.85	-10.80	0.40
28.0	51.35	3.69	13.93	-24.08	1.52	32.17	16.92	-10.74	0.41
28.5	50.93	3.61	14.09	-23.94	2.01	33.98	17.71	-9.97	0.46
29.0	51.14	3.59	14.25	-24.11	1.86	33.07	17.00	-10.66	0.41
29.5	50.39	3.59	14.03	-24.13	2.18	34.97	17.35	-10.32	0.44
30.0	51.38	3.61	14.23	-24.30	1.91	38.50	17.03	-10.63	0.42
30.5	50.96	3.62	14.06	-24.39	2.18	29.26	16.08	-11.55	0.36
31.0	51.27	3.61	14.19	-24.37	2.12	23.37	17.33	-10.33	0.43
31.5	51.05	3.56	14.33	-24.40	1.91	30.60	16.22	-11.42	0.37
32.0	51.81	3.68	14.09	-24.46	1.59	31.54	16.56	-11.09	0.39
32.5	51.25	3.68	13.93	-24.46	1.53	28.10	15.75	-11.88	0.34
33.0	51.09	3.69	13.83	-24.30	2.15	21.94	17.38	-10.29	0.44
33.5	50.76	3.65	13.90	-24.16	1.64	32.78	16.67	-10.98	0.39
34.0	51.42	3.70	13.89	-24.03	2.00	28.66	16.69	-10.96	0.39
34.5	50.77	3.67	13.83	-24.01	1.72	29.77	17.28	-10.39	0.43
35.0	51.18	3.52	14.54	-23.45	2.15	28.68	17.25	-10.42	0.43
35.5	51.02	3.54	14.41	-23.56	2.21	32.62	16.69	-10.96	0.39
36.0	50.88	3.49	14.59	-23.38	1.94	23.39	16.45	-11.19	0.38
36.5	51.06	3.55	14.39	-23.52	1.96	20.97	15.90	-11.73	0.35
37.0	51.44	3.38	15.21	-23.00	2.13	21.00	17.46	-10.21	0.44
37.5	49.77	3.32	14.97	-23.38	1.69	26.84	16.44	-11.20	0.38
38.0	50.60	3.27	15.48	-22.70	2.33	35.61	17.88	-9.81	0.47
38.5	50.61	3.31	15.29	-22.69	2.46	30.35	17.57	-10.10	0.45
39.0	50.69	3.33	15.22	-22.50	2.19	36.76	17.73	-9.94	0.46
39.5	50.85	3.26	15.60	-22.23	2.18	34.10	17.54	-10.13	0.45
40.0	51.47	3.22	16.00	-22.33	1.55	30.56	16.60	-11.05	0.39
40.5	50.69	3.26	15.54	-22.60	1.80	31.11	17.47	-10.20	0.44
41.0	50.96	3.27	15.59	-22.46	2.21	29.33	16.32	-11.32	0.37
41.5	50.97	3.18	16.02	-22.34	1.75	33.89	17.34	-10.33	0.43
42.0	51.75	3.18	16.27	-22.33	2.08	21.04	17.52	-10.15	0.45
42.5	51.44	3.20	16.10	-22.21	1.69	33.91	17.14	-10.52	0.42
43.0	51.21	3.16	16.21	-22.21	1.77	26.63	17.42	-10.25	0.44

43.5	51.14	3.11	16.46	-22.48	1.05	30.92	16.67	-10.98	0.39
44.0	51.26	3.16	16.20	-22.36	1.65	29.75	16.97	-10.69	0.41
44.5	50.62	3.08	16.43	-22.02	1.21	34.59	17.31	-10.36	0.43
45.0	50.29	2.99	16.82	-21.82	1.17	28.64	16.99	-10.66	0.41
45.5	47.48	3.32	14.31	-21.98	1.75	27.42	16.81	-10.84	0.40
46.0	52.23	3.73	14.01	-21.99	1.99	31.00	17.87	-9.81	0.47
46.5	50.88	3.62	14.06	-21.79	1.75	31.99	17.50	-10.17	0.44
47.0	51.58	3.73	13.83	-21.63	1.58	32.63	17.59	-10.08	0.45
47.5	50.17	3.58	14.03	-21.46	1.44	30.96	16.97	-10.69	0.41
48.0	50.69	3.59	14.13	-21.60	1.97	30.14	17.24	-10.43	0.43
48.5	50.37	3.68	13.69	-21.37	1.63	30.38	17.49	-10.18	0.44
49.0	49.74	3.67	13.56	-21.33	1.45	33.21	18.20	-9.49	0.49
49.5	49.19	3.63	13.53	-21.44	1.95	26.91	16.93	-10.73	0.41
50.0	48.49	3.63	13.35	-21.30	1.76	29.59	16.11	-11.52	0.36
50.5	48.19	3.60	13.37	-21.29	1.58	34.48	16.79	-10.86	0.40
51.0	48.43	3.64	13.32	-21.65	1.65	32.96	17.06	-10.60	0.42
51.5	48.52	3.69	13.15	-21.17	2.06	28.31	16.97	-10.69	0.41
52.0	46.65	3.55	13.15	-21.39	1.30	32.86	17.16	-10.51	0.42
52.5	48.32	3.59	13.48	-21.31	1.74	29.37	18.01	-9.68	0.48
53.0	47.97	3.66	13.11	-21.74	1.97	32.25	18.04	-9.65	0.48
53.5	47.74	3.62	13.20	-22.01	1.30	34.92	17.19	-10.47	0.43
54.0	45.76	3.51	13.04	-22.32	1.60	24.31	17.16	-10.50	0.42
54.5	48.39	3.66	13.21	-22.21	1.86	30.32	16.65	-11.00	0.39
55.0	47.48	3.63	13.08	-22.63	1.66	27.66	17.95	-9.74	0.47
55.5	46.61	3.57	13.07	-22.52	1.76	25.53	15.92	-11.71	0.35
56.0	47.89	3.53	13.55	-22.34	1.30	29.41	16.39	-11.26	0.38
56.5	49.00	3.63	13.49	-22.59	1.80	26.95	16.60	-11.05	0.39
57.0	47.02	3.53	13.31	-23.13	1.32	26.64	16.48	-11.16	0.38
57.5	47.44	3.49	13.58	-22.12	1.66	29.39	17.02	-10.64	0.41
58.0	47.64	3.59	13.27	-24.73	1.60	30.91	16.87	-10.79	0.41
58.5	49.85	3.70	13.48	-23.66	1.11	30.09	17.40	-10.27	0.44
59.0	47.97	3.57	13.44	-23.00	1.64	30.19	17.37	-10.30	0.44
59.5	47.71	3.56	13.41	-25.21	1.27	31.13	17.20	-10.46	0.43
60.0	47.21	3.50	13.49	-24.20	1.40	30.71	17.04	-10.62	0.42
60.5	47.26	3.42	13.82	-26.00	1.19	27.52	16.58	-11.06	0.39
61.0	47.50	3.48	13.65	-25.84	1.78	27.15	15.73	-11.89	0.34
61.5	47.30	3.46	13.65	-26.60	1.69	30.16	16.32	-11.32	0.37
62.0	47.57	3.49	13.64	-27.03	1.11	26.96	17.63	-10.05	0.45
62.5	49.70	3.61	13.78	-27.26	1.66	26.15	18.04	-9.65	0.48
63.0	48.07	3.47	13.83	-27.81	1.17	26.81	16.44	-11.21	0.38
63.5	48.14	3.52	13.67	-27.72	1.65	30.88	17.35	-10.31	0.44
64.0	48.42	3.50	13.83	-27.72	1.51	26.65	17.66	-10.02	0.46
64.5	46.66	3.39	13.76	-27.01	1.04	26.54	17.64	-10.04	0.45
65.0	47.76	3.44	13.88	-27.98	1.23	25.16	18.82	-8.89	0.53
65.5	49.40	3.46	14.26	-28.50	1.70	24.83	17.60	-10.08	0.45
66.0	48.10	3.45	13.95	-28.29	1.64	24.00	17.64	-10.03	0.45

66.5	46.89	3.38	13.85	-28.09	0.96	23.37	15.54	-12.08	0.33
67.0	48.88	3.45	14.17	-27.93	1.02	22.06	16.78	-10.87	0.40
67.5	50.06	3.51	14.26	-28.24	1.51	25.96	17.76	-9.92	0.46
68.0	47.49	3.36	14.12	-28.26	1.39	24.58	16.34	-11.30	0.37
68.5	49.80	3.48	14.30	-28.87	1.47	24.14	16.80	-10.85	0.40
69.0	48.71	3.40	14.34	-28.35	1.15	21.66	15.95	-11.68	0.35
69.5	50.18	3.56	14.10	-28.18	1.53	24.57	16.77	-10.88	0.40
70.0	49.03	3.35	14.64	-29.09	1.50	23.79	15.68	-11.94	0.34
70.5	46.98	3.23	14.54	-29.05	1.19	28.92	15.52	-12.10	0.33
71.0	48.04	3.26	14.74	-29.08	1.43	26.75	17.41	-10.26	0.44
71.5	47.91	3.32	14.42	-28.99	1.65	25.09	15.17	-12.44	0.31
72.0	47.37	3.24	14.63	-29.38	1.75	26.66	16.39	-11.25	0.38
72.5	47.91	3.31	14.48	-29.34	1.21	29.56	15.76	-11.87	0.34
73.0	46.79	3.22	14.51	-29.23	1.06	22.08	15.58	-12.04	0.33
73.5	47.37	3.25	14.56	-29.34	1.17	24.01	16.39	-11.25	0.38
74.0	47.38	3.27	14.48	-29.02	1.33	24.63	14.85	-12.75	0.29
74.5	47.48	3.30	14.41	-29.54	1.46	27.37	17.19	-10.47	0.43
75.0	46.96	3.26	14.40	-29.35	1.33	21.57	15.11	-12.49	0.30
75.5	45.75	3.17	14.42	-29.42	1.57	21.90	18.10	-9.59	0.48
76.0	42.88	3.01	14.23	-29.32	1.29	20.18	16.23	-11.40	0.37
76.5	44.16	3.14	14.07	-29.37	1.65	20.93	15.24	-12.38	0.31
77.0	43.29	3.04	14.22	-29.36	1.81	28.62	14.98	-12.63	0.30
77.5	44.49	3.18	13.98	-29.44	1.30	18.92	16.80	-10.85	0.40
78.0	42.30	3.02	13.98	-29.40	1.76	14.51	15.76	-11.86	0.34

Table F4. WAB 4 C3.

Top Depth (cm)	% C$_{org}$ (%)	%N (%)	C/N ratio	δ^{13}C (‰)	δ^{15}N (‰)	%O (%)	δ^{18}O$_{cell}$ (‰)	δ^{18}O$_{lw}$ (‰)	E/I ratio
0.0	28.10	2.62	10.75	-30.34	0.01	14.26	13.60	-13.97	0.23
0.5									
1.0									
1.5	28.04	2.62	10.70	-30.49	-0.57	15.12	14.24	-13.34	0.26
2.0									
2.5	28.44	2.75	10.35	-30.73	-0.50	16.72	15.27	-12.35	0.31
3.0	26.60	2.56	10.40		-0.09	14.83	14.83	-12.77	0.29
3.5	28.27	2.79	10.15	-30.66	-0.08	15.34	16.02	-11.61	0.35
4.0	27.83	2.72	10.24	-30.82	-0.19	19.75	16.52	-11.13	0.38
4.5	28.45	2.71	10.48	-30.46	-0.18	20.24	17.05	-10.61	0.42
5.0	28.56	2.75	10.37	-30.71	-0.53	16.71	16.62	-11.03	0.39
5.5	28.64	2.67	10.74	-30.49	-0.02	20.69	17.74	-9.94	0.46
6.0	28.55	2.71	10.52	-30.70	-0.49	19.33	16.21	-11.42	0.37
6.5	27.75	2.71	10.24	-30.54	-0.21	19.58	16.00	-11.63	0.35
7.0	29.78	2.92	10.21	-30.65	-0.42	17.43	16.77	-10.88	0.40
7.5	28.77	2.84	10.13	-30.68	-0.95	19.40	16.40	-11.24	0.38
8.0	29.07	2.84	10.25	-30.69	-0.67	19.24	16.45	-11.19	0.38
8.5	29.07	2.84	10.24	-30.63	-0.41	21.17	16.55	-11.10	0.39
9.0	29.13	2.80	10.39	-30.44	-0.66	18.75	16.19	-11.44	0.36
9.5	27.98	2.74	10.19	-30.46	-0.24	22.88	16.34	-11.30	0.37
10.0	28.98	2.83	10.23	-30.59	-0.63	18.64	15.60	-12.02	0.33
10.5	28.92	2.80	10.33	-30.51	-0.42	18.45	15.64	-11.98	0.33
11.0	29.34	2.82	10.41	-30.57	-0.69	18.45	15.74	-11.88	0.34
11.5	30.85	2.98	10.35	-30.45	-0.34	19.61	16.51	-11.14	0.38
12.0	28.22	2.72	10.38	-30.51	-0.02	19.30	15.87	-11.76	0.35
12.5	26.81	2.57	10.42	-30.59	-0.40	14.79	12.53	-15.01	0.18
13.0	25.47	2.42	10.53	-30.65	-0.56	13.17	12.29	-15.24	0.17
13.5	27.22	2.55	10.69	-30.64	0.28	17.34	14.94	-12.66	0.29
14.0	26.93	2.53	10.62	-30.65	-0.44	16.53	13.50	-14.06	0.22
14.5	27.17	2.51	10.84	-30.58	0.19	18.89	13.61	-13.96	0.23
15.0	26.90	2.51	10.70	-30.54	0.06	18.91	13.47	-14.10	0.22
15.5	26.74	2.43	11.01	-30.36	-0.15	16.26	14.38	-13.21	0.27
16.0	26.42	2.39	11.08	-30.36	0.26	18.94	14.49	-13.10	0.27
16.5	25.94	2.34	11.09	-30.25	0.03	19.72	14.53	-13.06	0.27
17.0	24.95	2.23	11.18	-30.09	-0.08	20.51	14.75	-12.85	0.28
17.5	26.23	2.32	11.29	-29.97	0.42	20.38	14.57	-13.02	0.28
18.0	26.52	2.33	11.37	-29.94	0.10	19.57	14.48	-13.11	0.27
18.5	25.71	2.29	11.24	-29.81	0.59	17.87	12.76	-14.78	0.19
19.0	26.26	2.33	11.28	-29.58	0.61	17.03	13.50	-14.06	0.22
19.5	26.36	2.32	11.35	-29.34	0.34	17.55	13.80	-13.77	0.24
20.0	27.11	2.40	11.30	-29.19	0.74	19.13	12.93	-14.62	0.20

20.5	28.11	2.44	11.54	-29.08	0.47	18.80	12.63	-14.91	0.18
21.0	28.32	2.45	11.55	-28.81	0.56	22.35	12.06	-15.47	0.16
21.5	27.85	2.41	11.56	-28.93	0.62	17.77	13.33	-14.23	0.21
22.0	27.32	2.34	11.68	-28.80	0.59	21.09	12.62	-14.92	0.18
22.5	26.39	2.26	11.65	-28.85	0.62	15.87	12.67	-14.88	0.18
23.0	26.26	2.27	11.56	-28.87	0.47	20.56	14.30	-13.29	0.26
23.5	26.45	2.29	11.54	-28.79	0.36				
24.0	26.61	2.32	11.45	-28.72	0.53	14.97	9.45	-18.01	0.05
24.5	26.98	2.38	11.34	-28.63	0.29	15.10	10.29	-17.19	0.08
25.0	28.30	2.46	11.49	-28.52	0.12	18.10	10.93	-16.57	0.11
25.5	28.82	2.50	11.52	-28.28	0.78	14.90	9.47	-17.98	0.05
26.0	28.35	2.46	11.51	-28.25	0.54	17.36	11.00	-16.50	0.11
26.5	29.64	2.58	11.49	-28.21	0.76	19.82	9.76	-17.71	0.06
27.0	28.17	2.46	11.47	-28.19	0.48	16.74	9.49	-17.96	0.05
27.5	28.89	2.49	11.58	-28.28	0.56	18.57	9.67	-17.79	0.06
28.0	29.24	2.54	11.51	-28.06	0.45	17.09	9.69	-17.77	0.06
28.5	29.78	2.56	11.63	-28.19	0.66	16.64	9.64	-17.82	0.06
29.0	29.22	2.48	11.79	-28.25	0.68	17.64	9.55	-17.90	0.05
29.5	29.78	2.58	11.56	-28.14	0.51	16.86	10.00	-17.47	0.07
30.0	30.20	2.47	12.24	-27.96	1.06	15.97	9.67	-17.79	0.06
30.5	29.32	2.44	11.99	-28.20	0.93	18.76	10.21	-17.27	0.08
31.0	29.14	2.47	11.82	-28.18	0.27	17.56	9.12	-18.32	0.04
31.5	28.29	2.38	11.89	-28.23	1.31	18.36	10.97	-16.52	0.11
32.0	28.79	2.46	11.72	-28.05	0.54	15.56	10.01	-17.46	0.07
32.5	29.43	2.47	11.93	-28.33	1.05	15.98	10.14	-17.34	0.08
33.0	29.21	2.49	11.74	-28.13	0.71	16.78	8.69	-18.75	0.02
33.5	28.78	2.44	11.80	-28.19	1.32	14.72	8.28	-19.14	0.01
34.0	29.17	2.45	11.89	-28.22	0.73	17.00	8.27	-19.15	0.01
34.5	28.95	2.42	11.98	-28.29	0.91	16.36	10.51	-16.97	0.09
35.0	28.34	2.39	11.83	-28.27	1.19	11.46	8.34	-19.09	0.01
35.5	27.99	2.35	11.90	-28.36	0.96	13.61	9.39	-18.07	0.05
36.0	29.26	2.45	11.96	-28.29	1.55	13.53	8.26	-19.16	0.01
36.5	29.24	2.45	11.93	-28.29	0.96	13.26	11.57	-15.94	0.13
37.0	28.47	2.36	12.05	-28.33	1.35	13.90	9.27	-18.18	0.04
37.5	28.97	2.36	12.25	-28.17	1.47	14.64	8.95	-18.49	0.03
38.0	28.37	2.30	12.35	-28.39	1.33	16.32	8.97	-18.47	0.03
38.5	27.82	2.23	12.46	-28.47	1.19	15.86	9.65	-17.82	0.06
39.0	27.06	2.14	12.65	-28.41	1.55	16.11	9.88	-17.59	0.07
39.5	26.92	2.12	12.68	-28.46	1.25	14.69	8.53	-18.90	0.02
40.0	26.93	2.17	12.42	-28.36	1.31	15.66	8.93	-18.51	0.03
40.5	27.47	2.18	12.58	-28.40	0.95	14.14	9.31	-18.14	0.05
41.0	24.43	1.98	12.35	-28.53	1.23	13.03	9.02	-18.42	0.03
41.5	25.59	2.10	12.19	-28.45	1.47	18.03	8.91	-18.53	0.03
42.0	27.34	2.20	12.40	-28.36	1.08	14.88	9.45	-18.01	0.05
42.5	25.97	2.11	12.30	-28.27	1.55	15.30	9.63	-17.83	0.06
43.0	27.49	2.25	12.22	-28.39	1.38	19.20	9.78	-17.69	0.06

|								
43.5	25.97	2.13	12.22	-28.32	1.28	17.80	9.87	-17.60	0.07
44.0	24.82	2.06	12.03	-28.40	1.63	17.78	8.64	-18.79	0.02
44.5	25.99	2.14	12.14	-28.29	1.56	17.65	9.39	-18.06	0.05
45.0	24.36	2.04	11.93	-28.33	1.43	15.42	8.14	-19.28	0.00
45.5	20.92	1.70	12.30	-28.31	1.50	15.52	7.21	-20.18	-0.03
46.0	21.78	1.78	12.26	-28.32	1.05	14.78	7.20	-20.19	-0.03
46.5	21.45	1.78	12.05	-28.28	1.73	16.69	7.50	-19.91	-0.02
47.0	21.90	1.82	12.03	-28.19	1.26	16.17	8.57	-18.86	0.02
47.5	22.50	1.91	11.81	-28.34	1.23	14.61	6.80	-20.58	-0.04
48.0	23.35	1.93	12.11	-28.31	1.36	17.36	9.40	-18.06	0.05
48.5	22.69	1.90	11.96	-28.22	1.32	16.99	8.16	-19.26	0.00
49.0	20.86	1.77	11.79	-28.15	1.68	14.28	8.62	-18.81	0.02
49.5	21.24	1.83	11.62	-28.17	1.61	14.92	7.49	-19.91	-0.02
50.0	20.46	1.78	11.50	-28.13	1.71	18.59	8.01	-19.41	0.00
50.5	21.41	1.81	11.85	-28.23	1.59	18.15	9.01	-18.44	0.03
51.0	20.10	1.72	11.69	-28.24	2.09	18.27	8.55	-18.88	0.02
51.5	20.35	1.78	11.43	-28.10	2.31	17.16	8.51	-18.92	0.02
52.0	17.23	1.66	10.37	-27.89	2.87	17.77	7.60	-19.81	-0.01
52.5	17.99	1.59	11.33	-28.05	2.16	16.21	8.89	-18.55	0.03
53.0	19.12	1.70	11.23	-28.20	2.35	19.31	8.82	-18.62	0.03
53.5	22.05	1.86	11.84	-28.31	1.31	15.82	8.67	-18.77	0.02
54.0	13.46	1.24	10.86	-28.15	2.32	14.91	6.92	-20.47	-0.04
54.5	13.25	1.20	11.04	-28.14	1.91	16.10	7.29	-20.11	-0.02
55.0	12.32	1.14	10.77	-28.28	2.49	14.54	5.49	-21.86	-0.08
55.5	8.60	0.82	10.54	-28.26	2.72	13.76	5.43	-21.92	-0.08
56.0	7.36	0.75	9.82	-28.32	3.20	13.60	2.07	-25.19	-0.17
56.5	10.32	1.05	9.83	-28.28	2.70	14.46	4.28	-23.04	-0.12
57.0	2.30	0.37	6.17	-27.93	3.92	11.75	3.41	-23.89	-0.14
57.5	4.41	0.60	7.32	-28.26	3.77	11.83	2.63	-24.64	-0.16
58.0	6.64	0.85	7.80	-28.32	3.32	13.35	2.80	-24.47	-0.16
58.5	11.12	1.07	10.43	-28.62	2.57	11.31	3.18	-24.11	-0.15
59.0	20.15	2.00	10.05	-28.70	2.52	14.26	4.70	-22.62	-0.10
59.5	28.11	2.60	10.83	-28.87	2.59	17.18	7.41	-19.99	-0.02
60.0	21.87	2.17	10.07	-28.75	2.60	13.59	6.06	-21.30	-0.06
60.5	30.72	2.75	11.18	-28.93	1.77	13.62	7.51	-19.90	-0.02
61.0	25.40	2.18	11.64	-29.09	1.88	12.96	8.53	-18.90	0.02
61.5	22.90	2.17	10.55	-28.90	2.14	10.28	8.95	-18.49	0.03
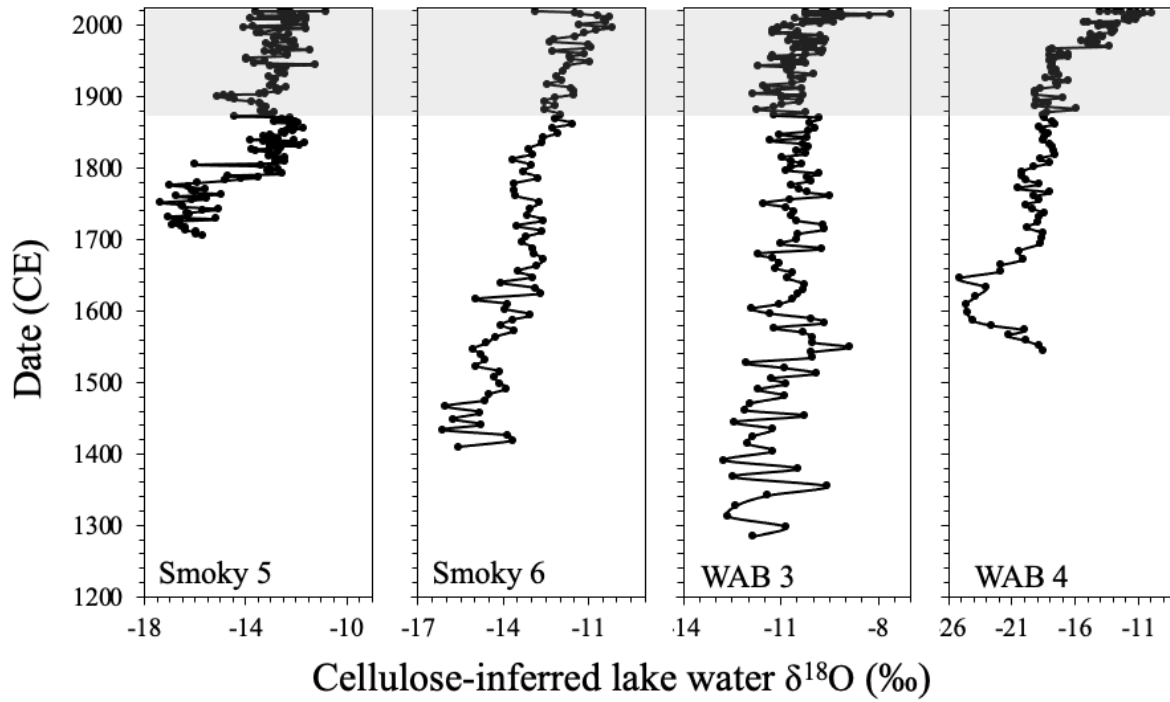
Figure F1. Graphs showing complete records of stratigraphic variation in cellulose-inferred lake water $\delta^{18}O$ from the sediment cores collected at the four upland study lakes. The grey shaded areas indicate the interval of interest since 1880 that was included in the study.